

NAVAL POSTGRADUATE SCHOOL

Monterey , California



THESIS

R26737

AN ANALYSIS OF HYDROGRAPHIC DATA
COLLECTED OFF POINT SUR, CALIFORNIA
IN NOVEMBER 1988

by

Richard H. Reece

September 1989

Thesis Advisor

C.A. Collins

Approved for public release; distribution is unlimited.

T246001

REPORT DOCUMENTATION PAGE					
1a Report Security Classification Unclassified			1b Restrictive Markings		
2a Security Classification Authority			3 Distribution/Availability of Report Approved for public release; distribution is unlimited.		
2b Declassification/Downgrading Schedule					
4 Performing Organization Report Number(s)			5 Monitoring Organization Report Number(s)		
6a Name of Performing Organization Naval Postgraduate School		6b Office Symbol (if applicable) 68co	7a Name of Monitoring Organization Naval Postgraduate School		
6c Address (city, state, and ZIP code) Monterey, CA 93943-5000			7b Address (city, state, and ZIP code) Monterey, CA 93943-5000		
8a Name of Funding Sponsoring Organization		8b Office Symbol (if applicable)	9 Procurement Instrument Identification Number		
8c Address (city, state, and ZIP code)			10 Source of Funding Numbers		
			Program Element No	Project No	Task No
11 Title (Include security classification) AN ANALYSIS OF HYDROGRAPHIC DATA COLLECTED OFF POINT SUR, CALIFORNIA IN NOVEMBER 1988					
12 Personal Author(s) Richard H. Reece					
13a Type of Report Master's Thesis		13b Time Covered From To		14 Date of Report (year, month, day) September 1989	
15 Page Count 84					
16 Supplementary Notation The views expressed in this thesis are those of the author and do not reflect the official policy or position of the Department of Defense or the U.S. Government.					
17 Cosatl Codes			18 Subject Terms (continue on reverse if necessary and identify by block number) word processing, Script, GML, text processing.		
Field	Group	Subgroup			
19 Abstract (continue on reverse if necessary and identify by block number) <p>Velocities measured by Pegasus and an Acoustic Doppler Current Profiler over a zonal section off Point Sur, California in November 1988 are compared. The inertial motion component of the total flow are determined, examined and removed from the Pegasus velocity cross sections by using casts separated by half an inertial period. Results of the processing techniques show excellent agreement between profiles measured by the instruments with correlation coefficients of 0.848 and 0.875 obtained for the U and V component velocities, respectively.</p> <p>Observations of the oceanography of the section are made by three different instruments: 1) Pegasus, an acoustically tracked float, which provides surface to bottom velocity information, 2) a ship mounted ADCP which provides continuous profiling of the upper ocean, and 3) a CTD which provides surface to bottom continuous measurements of pressure, conductivity, and temperature. From these instruments sections are constructed and conditions described. The following flows are observed: 1) A nearshore coastal trapped poleward flow which is confined to within the 100 fathom isobath, and which strengthens during relaxation events. 2) An equatorward flow occupying the outer shelf and inner continental slope, which during relaxation events widens and extends farther offshore. Between this flow and the nearshore poleward flow a strong shelf break front is observed with a shear of $1.5 \times 10^{-4} s^{-1}$ and a width of 3 km. 3) West of the equatorward flow located between 50 and 65 km offshore in the mid-continental slope region the California Undercurrent is observed. It is located farther offshore during relaxation events and weakens with distance offshore. 4) Farther offshore (approximately 100 km) and just barely resolved by the data, the California Current is observed. The core of the flow is not resolved but historically should be located more than 200 km offshore.</p>					
20 Distribution/Availability of Abstract <input checked="" type="checkbox"/> unclassified unlimited <input type="checkbox"/> same as report <input type="checkbox"/> DTIC users			21 Abstract Security Classification Unclassified		
22a Name of Responsible Individual C.A. Collins			22b Telephone (include Area code) (408) 646-2768		22c Office Symbol 68Co

Approved for public release; distribution is unlimited.

An Analysis of Hydrographic Data
Collected off Point Sur, California
in November 1988

by

Richard H. Reece
Lieutenant, United States Navy
B.S., The Citadel, 1983

Submitted in partial fulfillment of the
requirements for the degree of

MASTER OF SCIENCE IN METEOROLOGY AND PHYSICAL
OCEANOGRAPHY

from the

NAVAL POSTGRADUATE SCHOOL
September 1989

Department of Oceanography

ABSTRACT

Velocities measured by Pegasus and an Acoustic Doppler Current Profiler over a zonal section off Point Sur, California in November 1988 are compared. The inertial motion component of the total flow are determined, examined and removed from the Pegasus velocity cross sections by using casts separated by half an inertial period. Results of the processing techniques show excellent agreement between profiles measured by the instruments with correlation coefficients of 0.848 and 0.875 obtained for the U and V component velocities, respectively.

Observations of the oceanography of the section are made by three different instruments: 1) Pegasus, an acoustically tracked float, which provides surface to bottom velocity information, 2) a ship mounted ADCP which provides continuous profiling of the upper ocean, and 3) a CTD which provides surface to bottom continuous measurements of pressure, conductivity, and temperature. From these instruments sections are constructed and conditions described. The following flows are observed: 1) A nearshore coastal trapped poleward flow which is confined to within the 100 fathom isobath, and which strengthens during relaxation events. 2) An equatorward flow occupying the outer shelf and inner continental slope, which during relaxation events widens and extends farther offshore. Between this flow and the nearshore poleward flow a strong shelf break front is observed with a shear of $1.5 \times 10^{-4} s^{-1}$ and a width of 3 km. 3) West of the equatorward flow located between 50 and 65 km offshore in the mid-continental slope region the California Undercurrent is observed. It is located farther offshore during relaxation events and weakens with distance offshore. 4) Farther offshore (approximately 100 km) and just barely resolved by the data, the California Current is observed. The core of the flow is not resolved but historically should be located more than 200 km offshore.

TABLE OF CONTENTS

I. INTRODUCTION	1
II. DATA COLLECTION AND INSTRUMENTATION	3
A. CTD	6
B. ADCP	8
C. PEGASUS	10
III. DATA PROCESSING	12
A. CTD	12
B. ADCP	12
C. PEGASUS	19
IV. INTERCOMPARISON OF ADCP AND PEGASUS PROFILES	21
A. ADCP VERSUS PEGASUS FOR CASTS AT STATION THREE	21
1. Examination of the U velocity component	21
2. Examination of the V velocity component	26
B. TABLES OF RESULTS.	32
C. SUMMARY OF PROFILE ANALYSIS	36
V. OCEANOGRAPHIC CONDITIONS IN NOVEMBER 1988	38
A. OCEANOGRAPHIC CONDITIONS DURING STUDENT CRUISES ..	39
1. Velocity Sections	39
a. V Component Velocity Sections	39
b. U Component Velocity Sections	45
2. Temperature Sections	48
3. Salinity Sections	51
B. OCEANOGRAPHIC CONDITIONS DURING PEGASUS CRUISE ...	54
1. Velocity Sections	54
a. V Component Velocity Section	54
b. U Component Velocity Section	59

c. W Component Velocity Section	60
2. Temperature Sections	62
3. Salinity Sections	64
VI. SUMMARY AND RECOMMENDATIONS	66
A. DATA PROCESSING	66
B. PROFILE COMPARISONS	66
C. OCEANOGRAPHY ALONG THE POINT SUR SECTION.	67
D. RECOMMENDATIONS	69
LIST OF REFERENCES	71
INITIAL DISTRIBUTION LIST	73

LIST OF TABLES

Table 1.	1 TO 4 NOVEMBER CRUISE CTD STATIONS	6
Table 2.	5 TO 8 NOVEMBER CRUISE CTD STATIONS	7
Table 3.	14 TO 19 NOVEMBER CRUISE CTD STATIONS	8
Table 4.	14 TO 19 NOVEMBER CRUISE PEGASUS CASTS	11
Table 5.	CORRELATION COEFFICIENTS BETWEEN PEGASUS AND ADCP V VELOCITIES	32
Table 6.	CORRELATION COEFFICIENTS BETWEEN PEGASUS AND ADCP U VELOCITIES	33
Table 7.	AVERAGE CORRELATION BETWEEN PEGASUS AND ADCP VE- LOCITIES	33

LIST OF FIGURES

Figure 1.	Hydrographic Stations for 1-4 November Cruise	4
Figure 2.	Hydrographic Stations for 5-8 November Cruise	4
Figure 3.	Hydrographic Stations for 14-19 November Cruise	5
Figure 4.	Pegasus Casts for 14-19 November Cruise	5
Figure 5.	3 Minute Unfiltered Reference Layer Velocities	14
Figure 6.	5 Minute Unfiltered Reference Layer Velocities	14
Figure 7.	3 Minute Filtered Reference Layer Velocities	17
Figure 8.	5 Minute Filtered Reference Layer Velocities	17
Figure 9.	Downcast U Component Velocities for Casts 73 and 75	22
Figure 10.	Upcast U Component Velocities for Casts 73 and 75	23
Figure 11.	U Component Cast Averages for Casts 73 and 75	24
Figure 12.	U Component Station Average for Casts 73 and 75	25
Figure 13.	Downcast V Component Velocities for Casts 73 and 75	27
Figure 14.	Upcast V Component Velocities for Casts 73 and 75	28
Figure 15.	V Component Cast Averages for Casts 73 and 75	29
Figure 16.	V Component Station Average for Casts 73 and 75	30
Figure 17.	Full Depth Cast Averages for Casts 73 and 75	31
Figure 18.	ADCP Versus Pegasus U Component Velocities	35
Figure 19.	ADCP Versus Pegasus V Component Velocities	36
Figure 20.	Granite Canyon Sea Surface Temperature	39
Figure 21.	1-4 November V Component Geostrophic Velocity to 450 m	40
Figure 22.	1-4 November V Component Geostrophic Velocity to 3600 m	41
Figure 23.	1-4 November V Component ADCP Velocities to 450 m	42
Figure 24.	5-8 November V Component Geostrophic Velocity to 450 m	43
Figure 25.	5-8 November V Component Geostrophic Velocity to 3600 m	43
Figure 26.	5-8 November V Component Pegasus Velocity to 450 m	44
Figure 27.	5-8 November V Component Pegasus Velocity to 3600 m	45
Figure 28.	1-4 November U Component ADCP Velocity to 450 m	46
Figure 29.	5-8 November U Component Pegasus Velocity to 450 m	47
Figure 30.	5-8 November U Component Pegasus Velocity to 3600 m	47
Figure 31.	1-4 November Temperature to 450 m	49

Figure 32.	1-4 November Temperature to 3600 m	49
Figure 33.	5-8 November Temperature to 450 m	50
Figure 34.	5-8 November Temperature to 3600 m	50
Figure 35.	1-4 November Salinity to 450 m	52
Figure 36.	1-4 November Salinity to 3600 m	52
Figure 37.	5-8 November Salinity to 450 m	53
Figure 38.	5-8 November Salinity to 3600 m	53
Figure 39.	14-19 November V Component Geostrophic Velocity to 450 m	55
Figure 40.	14-19 November V Component Geostrophic Velocity to 3600 m	55
Figure 41.	14-19 November V Component Pegasus Velocity to 450 m	56
Figure 42.	14-19 November V Component ADCP Velocity to 450 m	57
Figure 43.	14-19 November V Component Pegasus Velocity to 3600 m	56
Figure 44.	14-19 November U Component ADCP Velocity to 450 m	59
Figure 45.	14-19 November U Component Pegasus Velocity to 450 m	60
Figure 46.	14-19 November U Component Pegasus Velocity to 3600 m	61
Figure 47.	14-19 November W Component ADCP Velocity to 450 m	61
Figure 48.	14-19 November Temperature Cross Section to 450 m	63
Figure 49.	14-19 November Temperature Cross Section to 3600 m	63
Figure 50.	14-19 November Salinity Cross Section to 450 m	65
Figure 51.	14-19 November Salinity Cross Section to 3600 m	65

I. INTRODUCTION

The California Current System is the eastern part of the North Pacific Subtropical gyre and possesses a number of common characteristics associated with other eastern boundary currents. These characteristics are a broad surface equatorward flow with a narrow poleward undercurrent located over the continental slope. The California Current System has been extensively studied by numerous investigators [Refs.1, 2, 3, 4, 5, 6, 7, and 8] who have identified a number of features of this current system. Specific features of the California Current System and their characteristics are presented below.

The most consistent and prevalent feature of the California Current System is the California Current. The California Current is a broad, weak, equatorward flow that is normally shallower than 300 m depth. Speeds are usually less than 25 cm/s but observations of speeds to 50 cm/s have been reported. The water type is Subarctic in nature and originates at the Polar front along the West Wind Drift. The signature of this water type, which decreases southward with distance as the percentage of Subtropical water increases, is characterized by low temperature and salinity, and a high dissolved oxygen content. The California Undercurrent is a narrow poleward countercurrent that is normally located just below the main pycnocline and adjacent to the continental slope. Its signature is characterized as equatorial in origin due to its traits of high temperature, salinity, and phosphate as well as a low dissolved oxygen content. These characteristics are diminished as the current flows northward due to mixing. There is speculation that the Undercurrent broadens as well as shoals in winter when it is called the Davidson Inshore Current. The Davidson Inshore Current can be thought of as a surfacing of the submerged poleward flow during the non-upwelling season from October to February. Hickey [Ref. 1] concludes from other literature that either the northward flow is enhanced in the winter season or the southward flowing current is diminished and this resulting poleward flow is the Davidson Inshore Current. In addition to these currents, the system is also characterized by an abrupt transition to the upwelling season and a gradual fall transition to the non-upwelling or "winter" season.

This study uses data collected during the Pegasus cruise conducted by the Naval Postgraduate School aboard the *RV Point Sur* during the period from 14-19 November, 1988, near Point Sur, California. In addition data from two other cruises for 1-4 November and 5-8 November in the same area are used to compare to the 14-19 November

data in order to gain a better understanding of the progression of events during November 1988. Unique features of these data sets include surface to bottom soundings of velocity and density during the fall transition.

The objective of this thesis is to describe the oceanographic conditions which occurred during November 1988. Chapter 2 provides a brief description of the instruments and collection methods used. Chapter 3 discusses the processing methods used on the raw data collected by the instruments. Chapter 4 intercompares the variations between Pegasus and ADCP profiles as well as the effects that inertial motion has on each of the profiles. Chapter 5 discusses the oceanographic features noted in each cruise and tracks their progression through the month of November. Chapter 6 is a summary of results and recommendations for future work.

II. DATA COLLECTION AND INSTRUMENTATION

The data collected by the *RV Point Sur* during November 1988 were from a section known as the "Point Sur transect" which runs along $36^{\circ} 20' \text{ N}$ from Point Sur to $123^{\circ} 02' \text{ W}$, and then turns Southwest along a rhumb line bearing 240 degrees (this is line "67" which is used for data collection efforts in this area by the California Cooperative Fisheries Investigations (CalCOFI)). The data analyzed in this study does not include the turn to the Southwest and thus ends at approximately $123^{\circ} 03' \text{ W}$. This section is approximately 100 km long and samples were collected at depths from 50 to 3500 m. The Point Sur transect is occupied at least twice a year by the Naval Postgraduate School as part of a continuing investigation of the long term variability and dynamics of the California Current System.

Observations during the three cruises in November 1988 were collected by three different instruments. These instruments were: 1) Pegasus, an acoustically tracked Lagrangian float which provides surface to bottom velocity and temperature profiles for each cast, 2) a ship mounted Acoustic Doppler current profiler (ADCP) which provides continuous measurements of currents in all three spatial directions to an effective depth of 450 m, and 3) continuous measurements of conductivity, temperature and pressure made by means of an instrument (called a 'CTD') which is lowered from the ship on a wire. The first cruise from 1-4 November, see Figure 1 on page 4, followed the Point Sur transect to $123^{\circ} 03' \text{ W}$. with approximately 10 km CTD station spacing along $36^{\circ} 20' \text{ N}$. The second cruise was from 5 to 8 November and consisted of a grid of CTD stations which are shown in Figure 2 on page 4 as well as three Pegasus casts conducted along the transect at locations near $122^{\circ} 16.3' \text{ W}$, $122^{\circ} 23.5' \text{ W}$, and $122^{\circ} 29.4' \text{ W}$. The grid is centered on the Point Sur transect directly west of Point Sur and extends from Point Pinos in the North to Point Lopez in the South. The grid spacing is uniform with approximately 10 km spacing in both the meridional and zonal directions. The third cruise, see Figure 3 on page 5, once again repeated the Point Sur transect to $123^{\circ} 02.5' \text{ West}$ after which additional stations were occupied inshore along the axis of Monterey Canyon as well as along CalCOFI line 67. Each cruise also collected ADCP data continuously. In addition, the third cruise used 17 Pegasus casts to provide additional velocity information from the surface to the bottom at the locations shown in Figure 4 on page 5 .

Student Cruise November 1988 CTD Station Positions

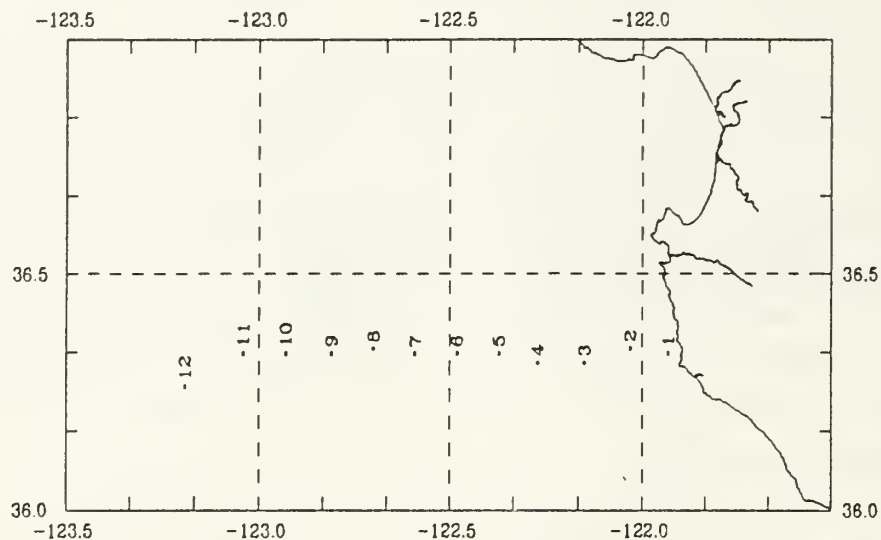


Figure 1. Hydrographic Stations for 1-4 November Cruise

Student Cruise November 1988 CTD Station Positions

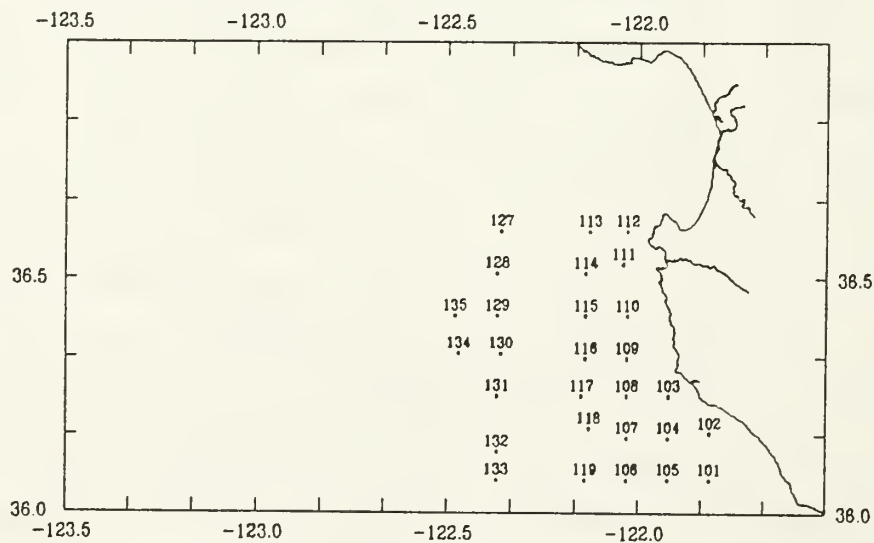


Figure 2. Hydrographic Stations for 5-8 November Cruise

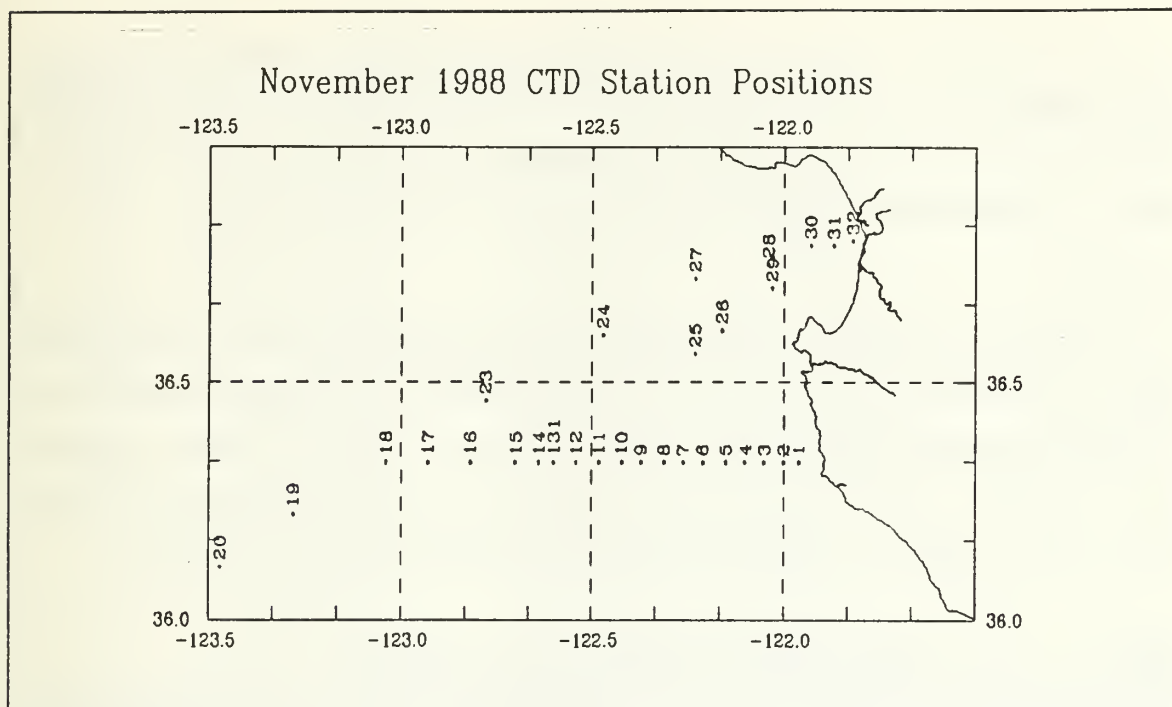


Figure 3. Hydrographic Stations for 14-19 November Cruise

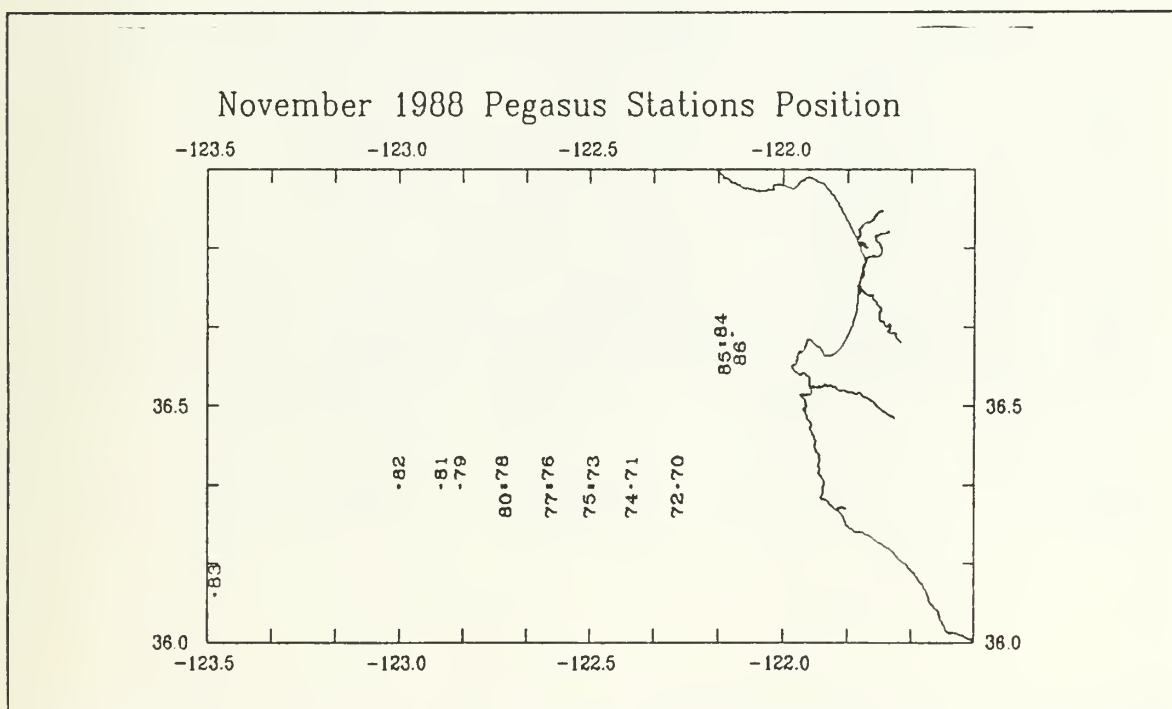


Figure 4. Pegasus Casts for 14-19 November Cruise

The bathymetry of the area is characterized by a ridge which extends West from Point Sur and narrows with increasing distance from shore. The top of the ridge roughly follows 36° 20' N. To either side of this ridge, depths increase rapidly as the Monterey Canyon is approached to the North and the Point Sur Canyon to the South.

A. CTD

CTD data was collected from the surface to near the bottom with a Neil Brown Mk III CTD System using a lowering rate of approximately 45 m/minute. Pertinent information regarding individual stations is listed in Table 1, Table 2 on page 7, and Table 3 on page 8. The CTD data was collected as one meter averages during the downcast only, with bottle samples being taken during the upcast for calibration.

Table 1. 1 TO 4 NOVEMBER CRUISE CTD STATIONS

CTD cast #	Date Time	Location	Depth(m)
1	11/1 21:21	36° 19.95' N. 121° 55.74' W.	40
2	11/1 22:17	36° 20.14' N. 122° 01.85' W.	132
3	11/1 23:47	36° 18.59' N. 122° 09.11' W.	650
4	11/2 01:18	36° 18.75' N. 122° 16.04' W.	920
5	11/2 02:45	36° 19.67' N. 122° 22.46' W.	1120
6	11/2 04:14	36° 20.04' N. 122° 28.93' W.	1797
7	11/2 06:04	36° 20.08' N. 122° 35.41' W.	2530
8	11/2 08:18	36° 20.12' N. 122° 42.19' W.	2907
9	11/2 11:03	36° 20.04' N. 122° 48.75' W.	2850
10	11/2 13:36	36° 19.89' N. 122° 55.60' W.	2500
11	11/2 15:42	36° 19.94' N. 123° 02.50' W.	3400

Table 2. 5 TO 8 NOVEMBER CRUISE CTD STATIONS

CTD cast #	Date Time	Location	Depth(m)
101	11/5 21:36	36° 03.96' N. 121° 48.65' W.	900
102	11/5 23:18	36° 10.34' N. 121° 48.67' W.	500
103	11/6 00:38	36° 14.75' N. 121° 55.35' W.	300
104	11/6 01:40	36° 09.44' N. 121° 55.32' W.	813
105	11/6 03:03	36° 04.07' N. 121° 55.26' W.	1098
106	11/6 04:40	36° 04.09' N. 122° 01.68' W.	1400
107	11/6 06:19	36° 09.53' N. 122° 02.08' W.	950
108	11/6 07:36	36° 14.93' N. 122° 02.08' W.	428
109	11/6 08:36	36° 20.05' N. 122° 02.04' W.	133
110	11/6 09:27	36° 25.28' N. 122° 02.05' W.	670
111	11/6 10:38	36° 31.80' N. 122° 02.16' W.	740
112	11/6 11:48	36° 35.73' N. 122° 02.06' W.	500
113	11/6 12:46	36° 35.97' N. 122° 08.08' W.	1604
114	11/6 14:32	36° 30.81' N. 122° 08.61' W.	980
115	11/6 16:04	36° 25.22' N. 122° 08.56' W.	800
116	11/6 17:20	36° 20.04' N. 122° 08.60' W.	800
117	11/6 18:23	36° 14.77' N. 122° 09.05' W.	840
118	11/6 19:38	36° 10.61' N. 122° 07.75' W.	1200
119	11/6 21:02	36° 04.00' N. 122° 08.56' W.	1600
127	11/7 14:28	36° 30.01' N. 122° 21.70' W.	2000
128	11/7 16:05	36° 30.73' N. 122° 22.09' W.	1610
129	11/7 17:56	36° 25.23' N. 122° 22.00' W.	1610
130	11/7 19:33	36° 20.17' N. 122° 21.63' W.	1200
131	11/7 20:48	36° 14.91' N. 122° 22.12' W.	1334
132	11/7 22:14	36° 07.57' N. 122° 22.12' W.	1662
133	11/8 00:00	36° 03.96' N. 122° 22.04' W.	2001
134	11/8 14:20	36° 20.03' N. 122° 28.78' W.	1850
135	11/8 15:56	36° 25.18' N. 122° 28.77' W.	2500

Table 3. 14 TO 19 NOVEMBER CRUISE CTD STATIONS

CTD cast #	Date Time	Location	Depth(m)
1	11/14 20:51	36° 20.20' N. 121° 57.30' W.	64
2	11/14 15:56	36° 20.28' N. 121° 59.90' W.	113
3	11/14 21:49	36° 20.20' N. 122° 02.80' W.	143
4	11/14 22:26	36° 20.20' N. 122° 05.70' W.	334
5	11/14 23:02	36° 20.20' N. 122° 08.70' W.	665
6	11/14 23:51	36° 19.60' N. 122° 12.70' W.	885
7	11/15 00:38	36° 20.20' N. 122° 15.30' W.	986
8	11/15 03:45	36° 20.10' N. 122° 18.80' W.	894
9	11/15 04:46	36° 20.10' N. 122° 22.30' W.	1183
10	11/15 08:27	36° 20.50' N. 122° 25.20' W.	1650
11	11/15 09:27	36° 20.20' N. 122° 29.00' W.	1886
12	11/15 20:33	36° 20.20' N. 122° 32.40' W.	2198
131	11/15 21:49	36° 20.00' N. 122° 35.70' W.	2625
14	11/16 06:16	36° 20.20' N. 122° 38.50' W.	3076
15	11/16 08:15	36° 20.10' N. 122° 42.10' W.	3150
16	11/16 18:32	36° 19.90' N. 122° 48.90' W.	3401
17	11/17 06:44	36° 20.30' N. 122° 55.70' W.	3565
18	11/17 16:55	36° 20.00' N. 123° 02.50' W.	3600

B. ADCP

The acoustic Doppler profiler (ADCP) data has the advantage of continuously measuring ocean currents in all three spatial directions. With the advent of this instrument upper ocean current fields can be mapped with the only restraint being the rate at which the instrument can accurately determine velocities. In this study, data was collected continuously with a RD Instrument RD-DR0300 with a four beam JANUS configuration operating at a frequency of 307.2 KHz. For the 14-19 November cruise the data was collected in three minute averages while for the other two cruises the data was collected in five minute averages. In all cases the velocity data was stored at 4 m vertical intervals.

The ADCP provides vertical profiles of velocity from two meters beneath the ship's keel to a maximum depth of about 450 m. At the frequency used in this study vertical

resolution is 4 m. The ADCP measures velocities relative to the ship by measuring the Doppler shift between the outgoing acoustic signal and the returning signal for each of the four beams which are declined 30 degrees from the vertical. The ADCP assumes that the velocity of the targets (zooplankton, air bubbles, fish, ocean bottom, etc.) is random such that averaging yields a Gaussian spectrum centered at the Doppler shifted frequency corresponding to the relative velocity of the water. This relative velocity is recorded as U, V, and W components relative to the platform and averaged over 3 to 5 minutes of observations. The component velocities are defined with U being positive eastward, V being positive northward and W being positive upward. The accuracy to which the shifted frequency can be determined is inversely proportional to the range. The accuracy in determining the shifted frequency can also be improved by decreasing the depth resolution which allows for a longer time segment to be analyzed for each individual ping. The system also assumes straight line acoustic propagation and thus ignores refractive effects. The data near the surface is distorted by refractive effects and surface interference while the data at greater depths is less accurate due to a lower percentage of good returns; as a result, it is important to use the data between these two regions to correct the profile for an absolute velocity. Another error source is the speed of sound that the instrument uses which does not take into account subsurface sound speed variations, which will effect the range.

Of prime importance is the measurement of the ship's motion. Since the ship usually moves at speeds which are at least an order of magnitude greater than ocean currents, a small error in measuring ship's motion (roll, pitch, and speed) results in a large error in calculating the absolute current measured. These errors can be due to either the surface wave field or navigation errors. Previous investigators have estimated error due to navigation by using a current meter comparison to the ADCP velocities at a fixed location. Joyce [Ref. 5] found the error due to navigation data to be 5-10 cm/s. Kosro [Ref. 9] obtained standard deviations of 4.1-5.4 cm/s in the cross-shore direction and 3.6 to 4.4 cm/s in the alongshore direction. He also pointed out that the ADCP consistently showed larger magnitude velocities in the V direction in relation to the current meter. Barth and Brink [Ref. 3] found standard deviations using a smaller data set to be 8.1 cm/s in the east-west direction and 12.3 cm/s in the north-south direction. They attributed the larger standard deviations to reduced navigational accuracy for their study. Inaccurate velocity calculations can result from navigation errors which cause inaccurate determination of ship velocity over ground. These errors appear as spikes which when averaged over the averaging interval spread the error over the raw time band. A more

detailed discussion of ADCP errors is given by Kosro [Ref. 9]. One can see that extreme care must be taken with ADCP data if low velocity ocean currents are to be accurately resolved.

C. PEGASUS

Pegasus is a float which is acoustically tracked during both ascent and descent. It emits a 10 KHz acoustic signal every 16 seconds which is received by previously surveyed bottom transponders which send a response signal of 12.0 and 12.5 KHz. The fall rate of the device is controlled by the amount of weight attached whereas the ascent rate is controlled by the buoyancy. For this study fall and ascent rates were approximately 38 m/minute. Pegasus has an internal memory which stores the round trip travel time for both the 12.0 and 12.5 KHz signals along with a measurement of temperature and pressure. Data is collected during both the up and downcast and is retrieved from the instrument's memory between casts. A more complete discussion of this instrument is given by Spain [Ref. 10]. When more than one cast was done at a station, the casts were separated by approximately one-half an inertial period, 10 hours, in an attempt to avoid aliasing by inertial frequencies. Due to heavy weather, only one cast (82) was done at the offshore station near 123° W. Pertinent information regarding the Pegasus casts is listed in Table 4 on page 11.

Table 4. 14 TO 19 NOVEMBER CRUISE PEGASUS CASTS

Pegasus #	Date Time	Location	Depth(m)
70	11/15 02:18	36° 20.30' N. 122° 16.40' W.	1004
71	11/15 06:42	36° 20.10' N. 122° 23.50' W.	1380
72	11/15 12:54	36° 20.30' N. 122° 16.30' W.	1021
73	11/15 15:28	36° 20.10' N. 122° 29.40' W.	1856
74	11/15 18:16	36° 20.10' N. 122° 23.50' W.	1369
75	11/16 00:32	36° 20.00' N. 122° 29.80' W.	1882
76	11/16 03:15	36° 20.20' N. 122° 36.50' W.	2763
77	11/16 11:11	36° 20.20' N. 122° 36.20' W.	2698
78	11/16 14:39	36° 20.50' N. 122° 43.80' W.	3331
79	11/16 21:21	36° 20.60' N. 122° 50.20' W.	2991
80	11/17 00:55	36° 20.20' N. 122° 43.40' W.	3270
81	11/17 09:04	36° 19.80' N. 122° 53.50' W.	3458
82	11/17 13:19	36° 19.10' N. 122° 59.90' W.	3349
84	11/19 01:50	36° 37.80' N. 122° 09.00' W.	2253
85	11/19 12:44	36° 37.70' N. 122° 09.00' W.	2264
86	11/19 15:45	36° 38.70' N. 122° 07.50' W.	2170

III. DATA PROCESSING

A. CTD

Processing of CTD data included editing the raw one meter averages using a computer program to remove salinity spikes and instabilities. These points were replaced by linearly interpolating values from adjacent data points. The edited CTD data was then transferred to nine track tape and subsequently put in mass storage on the IBM mainframe computer at the Naval Postgraduate School. The data was then corrected using calibration coefficients for temperature, pressure, and conductivity as determined by in situ bottle samples and pre-cruise and post cruise instrument calibration. The final edited data was then stored as two meter averages and is believed to be accurate to within ± 3.5 dbar, $\pm 0.003^\circ$ C and ± 0.003 psu, with a precision of ± 1.75 dbar, $\pm 0.0005^\circ$ C, and ± 0.002 psu.

Density and geopotential were calculated from this data using the 1980 equation of state, EOS 80, as presented by Fofonoff [Ref. 11]. Geostrophic velocity between adjacent stations was determined using a level of no motion of the deepest common data point. This is well supported where Pegasus bottom velocities were available. For the 1-4 November and 14-19 November cruises the orientation of the cross sections are along a line of latitude so that all geostrophic velocities are V velocities with positive defined as northward. In the case of the 5-8 November cruise meridional sections are defined with east being positive.

B. ADCP

As pointed out previously, extreme care must be taken with ADCP data if small magnitude currents of interest are to be resolved. For this reason, various processing techniques were examined.

The data for the 14-19 November cruise was collected in three minute averages while that of the other two cruises was collected in five minute averages. Although the ADCP has been in use for a decade, no standard has been determined for the data collection and averaging frequency. Examination of the literature shows a wide variability in the collection averaging intervals used by various investigators. The initial collection averaging interval plays a major role in post processing and the eventual determination of accuracy of the data. If short collection intervals are used, the temporal resolution of the data is increased due to more frequent recording, the quality of the stored relative

velocity profiles is reduced due to fewer profiles being averaged, and the raw data storage requirements are increased. In the case of longer collection intervals, temporal resolution of the data is reduced, the quality of the stored relative velocity profiles is increased, and raw data storage requirements are decreased.

Principle causes of spikes in the calculated velocities are due to inaccurate navigation data, inherent noise in the ADCP profiles, and gyro lag. Examples of spikes in the three and five minute collection averages are shown in Figure 5 on page 14, and Figure 6 on page 14. The error in accuracy of the navigation data is a first order error source in determining absolute velocities using the ADCP. The navigation data is used to calculate the ship's velocity which is subsequently used to convert the relative velocity profiles to absolute velocities. As a result it is highly desirable to have good quality resolution so that ship's motion can be determined precisely. Errors in navigation accuracy can only be improved by improving the navigation system used (the GPS navigation system when fully deployed will certainly bring a needed improvement in this area). While we are not able to eliminate errors due to bad navigation data, we are able to reduce their effects through use of a longer collection interval. The use of a longer collection interval causes a given position error to be spread over time resulting in smaller deviations from the true ship's velocity over ground from that which would be obtained from a shorter collection interval. As a result the absolute velocities calculated are closer to the true values. This is evident in the 5 minute unfiltered collection interval which shows data variations that are at a lower frequency and have smaller magnitude peaks. Little can be done to eliminate the inherent noise present in the ADCP profile at this stage of the processing; however both vertical filtering and time averaging can be employed later in the processing to reduce the noise. Gyro lag is a concern because it can cause inaccurate conversion of velocities from ship coordinates to geographical coordinates. The *Point Sur* uses a Sperry Mk-37 gyrocompass which has an inherent 0.4° lag as determined in tests conducted by Kosro [Ref. 9]. Thus for such a lag, errors of 3.5 cm/s could be obtained for a ship changing course at 10 knots. Due to this effect accelerations caused by erratic course changes result in errors that appear as spikes in the calculated absolute velocities. As can be seen from the time series of the unfiltered absolute velocities, filtering is needed to reduce the noise present in the signal due to the above errors.

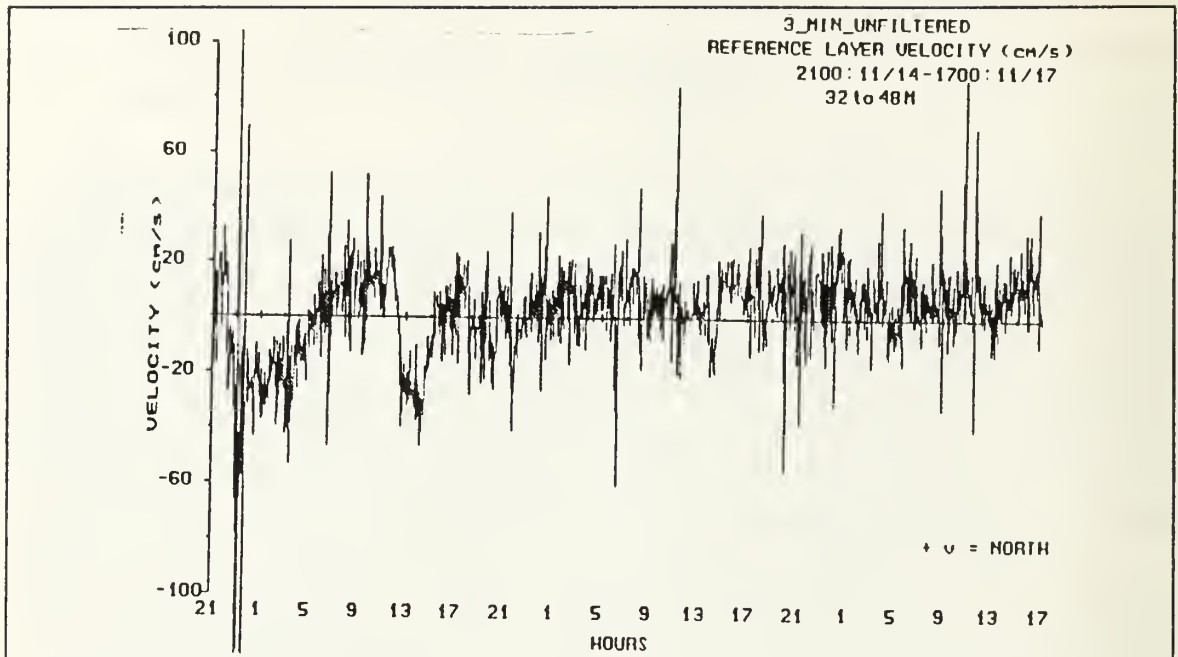


Figure 5. 3 Minute Unfiltered Reference Layer Velocities

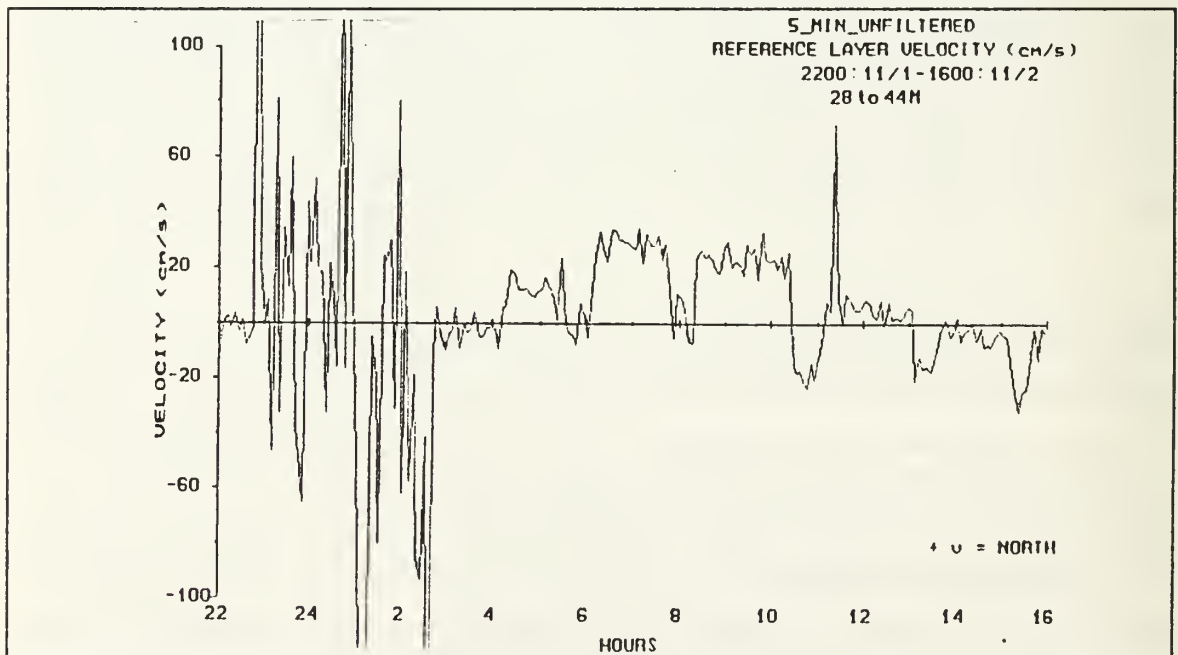


Figure 6. 5 Minute Unfiltered Reference Layer Velocities

The ADCP assumes that the velocity of the targets, zooplankton, air bubbles, fish, etc., is random such that averaging yields a Gaussian spectrum centered at the Doppler shifted frequency corresponding to the relative velocity of the water. The relative velocity profile for each ping is vector averaged over the collection time interval in order to increase the confidence in the recorded profile. The use of a longer collection interval increases the degrees of freedom and thus the resulting profile has a reduced variance with respect to the actual velocity profile. The three and five minute collection intervals average 285 and 476 profiles respectively. As a result we can assume from the Central Limit Theorem that the quality of the stored profile is good for both intervals. Since both collection intervals average at least thirty minutes of profiles in the processing phase, any advantage of the five minute collection interval with respect to the error of the relative velocity profile recorded is negligible.

The storage requirements and processing time for ADCP data are a function of the amount of raw data collected. Using a longer collection interval reduces the amount of data stored and results in reduced processing time required to compute the absolute velocities. Although this may be a concern on a long research cruise, it should not be a prime factor in deciding the collection interval for short cruises.

Having examined the data, I conclude that the advantages of the shorter collection interval outweigh those of the longer collection interval. In making this conclusion, my major concern is that, since the longer collection interval requires a lower frequency filter, it is possible that subsequent filtering could result in suppression of the true signal. A test of this hypothesis was not possible with the data sets used because the time separation between cruises prevented any direct comparisons of three versus five minute averages. Examination of the literature shows that several investigators have compared ADCP data to moored current meter data using different collection intervals. Korso [Ref. 9] using one minute average collection intervals obtained standard deviations of 4.1 to 5.4 cm/s in the cross-shore direction and 3.6 to 4.4 cm/s in the alongshore direction. Barth and Brink [Ref. 3] found standard deviations using a ten minute collection interval to be 8.1 cm/s in the meridional and 12.3 cm/s in the zonal direction. In making such a comparison, one must keep in mind that many other factors were also involved in the resulting standard deviations noted by these investigators, such as navigation accuracy, area of measurement, and surface wave field present at the time of data collection.

Initial processing of the data was done using programs written by Paul Jessen of the Oceanography Department of the Naval Postgraduate School. The first step in the

processing of the raw data was the extraction of the navigation information stored with each averaged relative velocity profile. From this position information, a record of ship's course and speed are determined based upon the navigation information stored in each 3 or 5 minute record. The resulting calculations yield an average velocity over the recording interval.

The second step in processing the raw data is the extraction of a reference layer as well as its conversion to an absolute velocity. A reference layer consists of the relative velocities at several depth intervals. A reference layer is needed because the average velocity of several depth intervals is much more characteristic of the true profile than the relative velocity at any particular depth. In making the choice of the reference layer, consideration should be given to the following. The near surface depth intervals are subject to influence by the surface wave field as well as near surface refractive effects and thus should be avoided. The reference layer should also be shallow enough that the shallowest bottom depths encountered will be deeper than the reference layer chosen. Lastly the depth chosen should not be so deep that there is an unnecessary reduction in the percent of good Doppler shift data stored. This study utilized a reference layer of 24-40 m. This depth band maximized the number of profiles deeper than the reference layer while remaining clear of both the near surface and bottom depth intervals which adversely effect the velocities. The percent of good ping returns in this depth interval averaged 99 percent. The relative velocities of the reference layer are then converted to absolute velocities by subtracting out the ship's velocity as determined previously from the navigation data.

The third step is the filtering of the reference layer velocities. Filtering of the reference layer is necessary in order to eliminate the high frequency variability due to both the noisy nature of the ADCP data as well as the spikes caused by poor navigation data and gyro lag. Examples of unfiltered reference layer velocities versus filtered reference layer velocities are shown in Figure 5 on page 14, Figure 7 on page 17, Figure 6 on page 14, and Figure 8 on page 17. The filtered examples employ a low pass filter with a cutoff frequency of 0.04 cpm, corresponding to a 25 minute period.

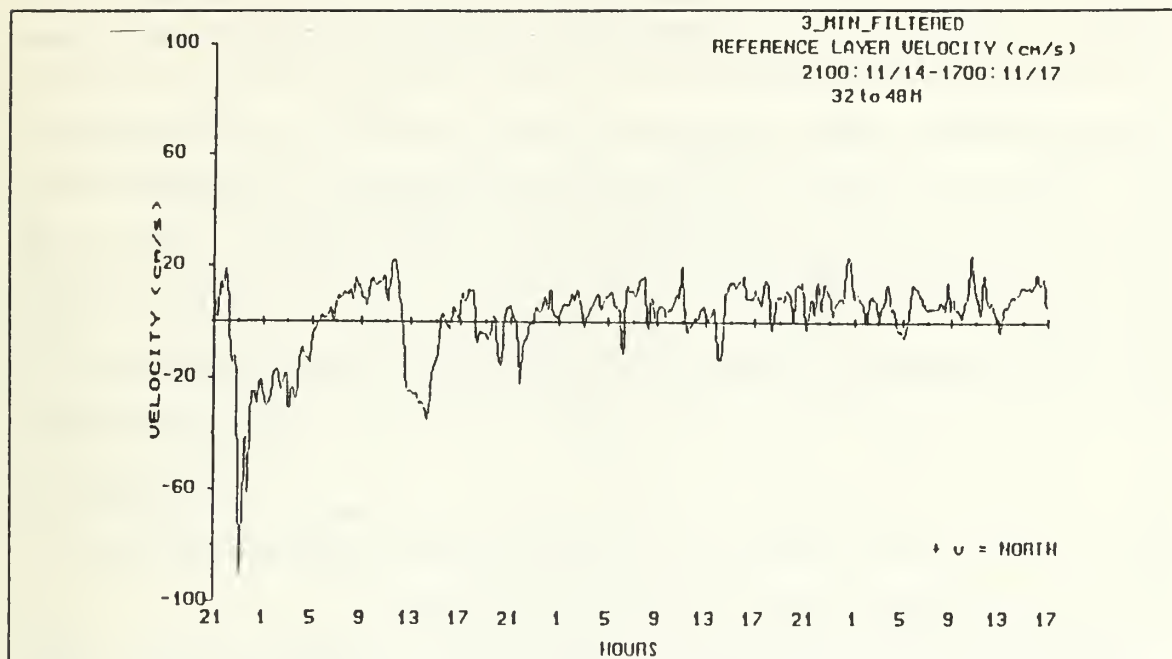


Figure 7. 3 Minute Filtered Reference Layer Velocities

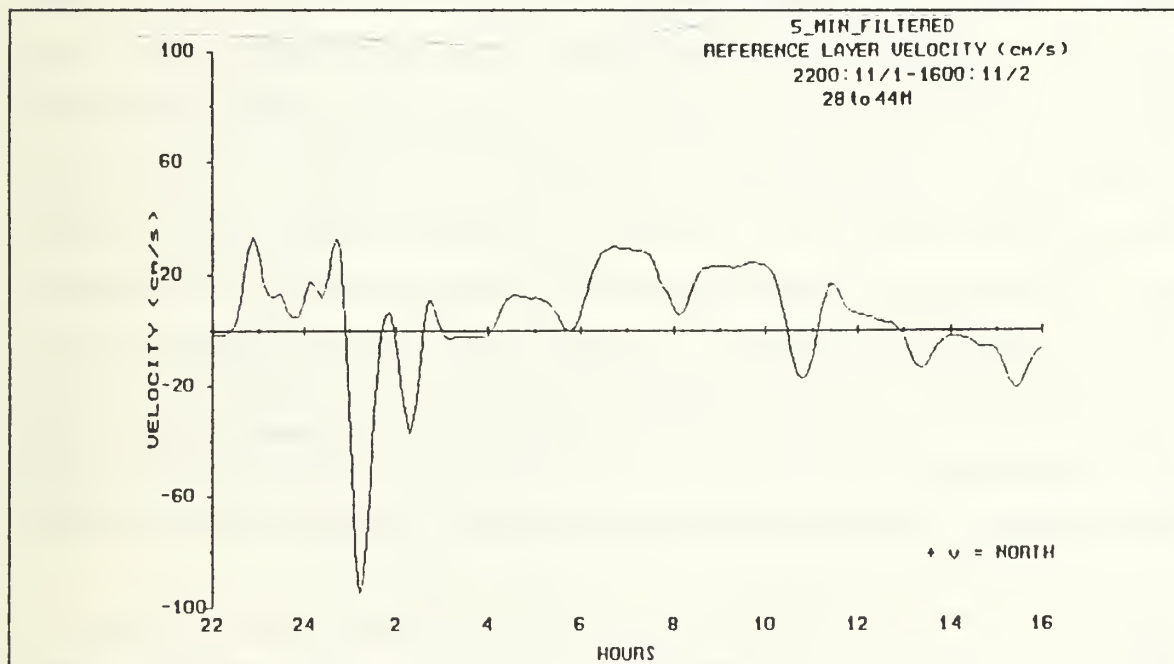


Figure 8. 5 Minute Filtered Reference Layer Velocities

Several different cutoff frequencies were tried from periods of 6 to 50 minutes. An attempt to determine the optimum filter cutoff frequency by means of the least square error between Pegasus and ADCP data at a common location was inconclusive. The test showed that filtering the data did reduce the error; however, since the data sets were taken at Pegasus stations while the ship was drifting, few spikes were present in the test. The results showed that all cutoff frequencies tested achieved about a 30% reduction in the least square error between Pegasus and ADCP data in relation to unfiltered ADCP data. In order to determine how the filter handled large spikes in the data, a data set containing severe spikes was extracted. The variance was then calculated between successive profiles to determine the variance reduction achieved between successive profiles. The results showed that cutoff frequencies with a period greater than 20 minutes provided little additional smoothing of the peak. On the basis of these results, a cutoff frequency of 0.04 cpm was chosen; it should not suffer from underfiltering of the navigation noise since its suppression of true velocities would be minimal.

In the fourth step the reference layer absolute velocities are used to compute a total profile velocity correction. This velocity correction is the difference between the absolute reference layer velocity and the relative velocity of the reference layer. The velocity correction is then applied to all depth intervals to determine an absolute velocity profile. Subsequently these absolute velocity profiles are subjectively edited to remove questionable profiles as well as profiles which are unusually shallow. Usually these profiles could be initially detected as a spike in a time series of the filtered reference velocities.

When this is completed, the basic data set has been formed which is used to create the data subsets for analysis. We wanted to compare ADCP and Pegasus data so we created ADCP data sets which corresponded both in time and location to Pegasus observations. Pegasus covers the upper 400 m of the water column in approximately 10 minutes. Kosro's [Ref. 9] study comparing moored current meter velocities with ADCP velocities showed that thirty minutes of ADCP profiles were required to obtain good measures of absolute velocity. On this basis, thirty minutes of ADCP data surrounding the ten minute time span required for Pegasus to transit the upper water column for each of the up and downcasts was extracted from the basic ADCP data set.

The final step in the ADCP processing was to vertically filter and time average the ADCP data in order to obtain a good representation of the absolute velocity profiles. The vertical filter helps to smooth the noisy nature of the ADCP profile with respect to the vertical while the time averaging helps to smooth the horizontal velocities between successive profiles. A Hanning window filter was used to vertically filter the profile, with

filter halfwidths of 8 to 28 m being examined subjectively to determine the optimum filter length. A filter halfwidth of eight meters was chosen based on visual inspection and prior work by King [Ref. 12] which showed that a filter halfwidth of 2 to 5 bins (8 to 20 m) provided the maximum variance reduction in successive profiles. A time averaging interval of 30 minutes was chosen based on the work of Kosro [Ref. 9]. In the case of the data subsets, all data was averaged to obtain a single profile, but in no instance was less than thirty minutes of data used to obtain an average profile. In the case of station averages, equal amounts of data separated by half an inertial period were averaged in an attempt to eliminate the inertial component, thus obtaining a good representation of the mean velocity profile.

C. PEGASUS

The raw Pegasus data consists of round trip travel times to each bottom mounted transponder along with a measurement of temperature and pressure every 16 seconds. Initial processing of the data was done using programs written by Tarry Rago of the Oceanography Department of the Naval Postgraduate School. These programs are based on the work of Lillibridge and Rossby [Ref. 13]. This processing entails multiplying the round trip travel times by an average speed of sound to obtain distances to each of the bottom mounted transponders. The distance from the surface is determined from the recorded pressure information. Using these distances, triangulation is used to determine the position of Pegasus in the water column and therefore the shape of its trajectory while it was deployed. The derivative with respect to time of the trajectory path then yields velocities. These velocities are then broken down into their horizontal components relative to the transponders as a function of depth. The transponders in the Naval Postgraduate School Pegasus transect are meridionally aligned and thus the component velocities are defined with V being positive northward and U being positive eastward. The resulting profiles were then despiked with interpolated values used to replace missing or bad data. These profiles were then filtered vertically using a filter halfwidth of three depth increments as recommended by Lillibridge and Rossby [Ref. 13].

The descent and ascent rates of Pegasus used in this study were about 38 m/minute resulting in a data point approximately every 10 m. Since the profiles were to be compared to data collected by the ADCP, linear interpolation was used to obtain data points corresponding to the depths of ADCP data points. After processing, each cast was then split into an up and downcast. At this point the basic data set was then averaged and

grouped as follows to obtain three different data sets. The first data set consisted 32 separate up and downcasts associated with the 16 separate Pegasus casts. The second data set consisted of each up and down cast for a individual Pegasus cast being averaged together to obtain a mean profile for that cast which yielded 16 profiles. The third data set contained averages of Pegasus casts made at a station which were separated in time by approximately one-half of an inertial period, about 10 hours at 36° N. This was done to average inertial motion.

IV. INTERCOMPARISON OF ADCP AND PEGASUS PROFILES

A number of studies have dealt with the comparison of data collected by each of these instruments with data from moored current meters; however, little has been done on comparing results obtained between these instruments. King [Ref. 12] compared Pegasus to ADCP velocity profiles and examined different processing techniques, but the correlation coefficients obtained were far from ideal (ranging in values from -0.48 to 0.93 for the U component and from -0.7 to 0.94 for the V component). This chapter provides a comparison of data obtained using Pegasus and the ADCP aboard the *RV Point Sur* between 14 and 19 November 1988. The methods build upon those used by King's study but employ a larger data set, as well as different filtering and averaging considerations (as described in the processing section) with the end result showing an overall improvement in correlation coefficients. Correlation coefficients for a profile are calculated between 24 m depth to a depth 24 m shallower than the deepest point of the ADCP profile for data resolved at four meter vertical intervals. This avoids the near surface region where neither Pegasus nor ADCP velocities are accurate. Pegasus velocities may be in error due to the momentum and acceleration imparted to it at the moment of release as well as refractive effects, while ADCP velocities are distorted in the near surface zone due to refraction and reverberation. The last 24 m of the ADCP profile were not used due to the method of vertical filtering as well as a steep decline in the percent of good return pings at depth.

A. ADCP VERSUS PEGASUS FOR CASTS AT STATION THREE

The third Pegasus station is located at approximately $36^{\circ} 20.1' \text{ N}$ and $122^{\circ} 29.6' \text{ W}$ in water 1882 m deep. Pegasus casts 73 and 75 were collected at this station 9 hours apart. The ADCP data consisted of 30 minute average profiles for the beginning and end of each Pegasus cast. Cast averages were obtained by averaging the up and downcast for both Pegasus and the associated two 30 minute ADCP profiles. A station average consists of an average of both cast averages which are separated by approximately one-half of an inertial period (thus averaging inertial-period currents).

1. Examination of the U velocity component

Figure 9 on page 22 shows the U component velocities for the downcasts for casts 73 and 75, while Figure 10 on page 23 shows the upcast U component velocity for

these same casts. Figure 11 on page 24 shows the cast averages for casts 73 and 75. The station U component velocity average is shown in Figure 12 on page 25.

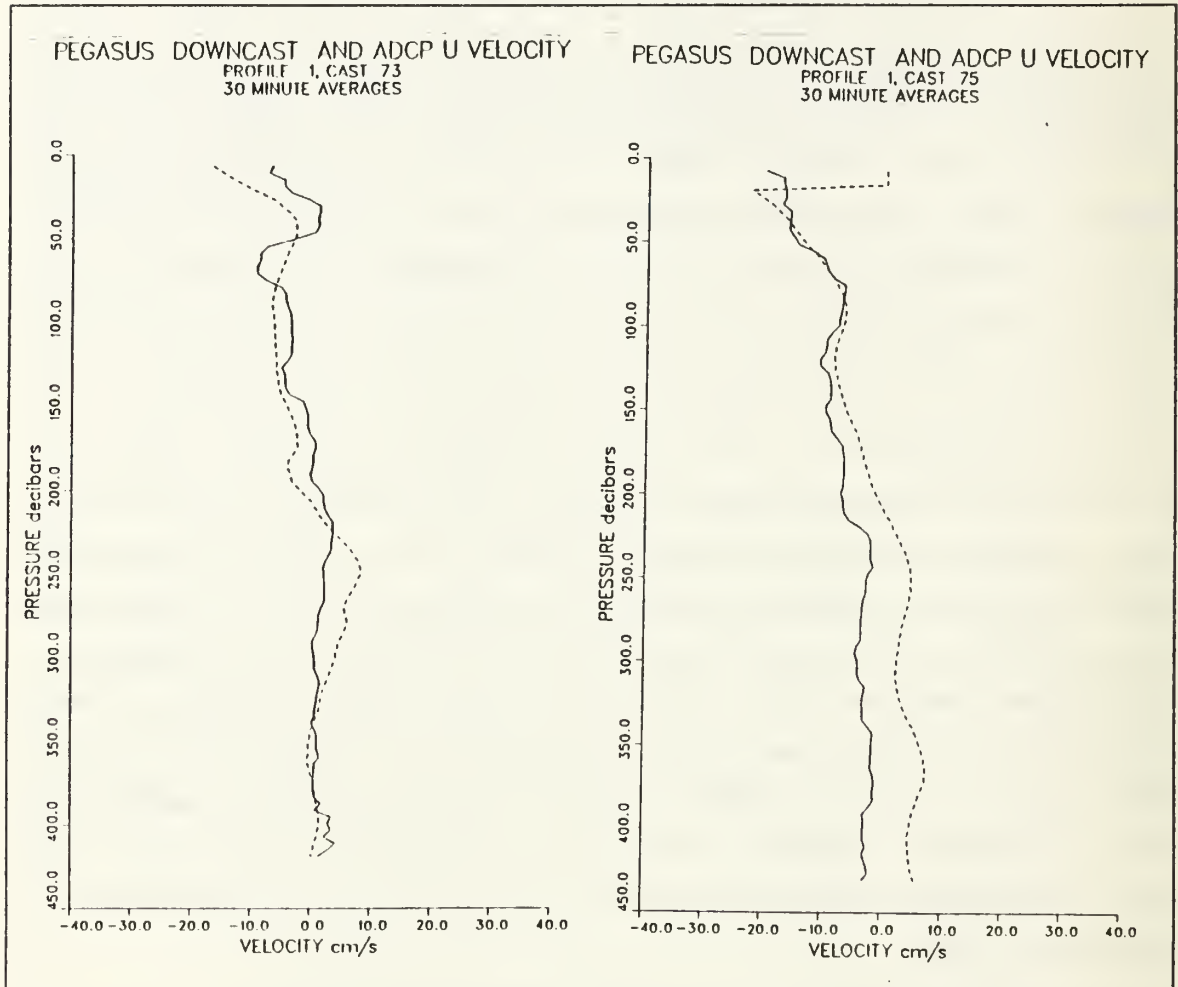


Figure 9. Downcast U Component Velocities for Casts 73 and 75: Dashed line represents Pegasus velocities while solid line represents ADCP velocities.

Several features that recur throughout the data sets are demonstrated in these figures. For example, if we examine the up and downcast for Pegasus cast 75 we notice an opposing vertical offset in the relative minimum velocity located at approximately 80 m. The downcast indicates a velocity of 8 cm/s at 87 m while the upcast indicates a velocity of 4 cm/s at 78 m. The offset is easiest seen in areas of high shear. This offset can be corrected by averaging the up and downcast in order to obtain an average profile. For this example, the correlation coefficients of the up and downcast for cast 75 are

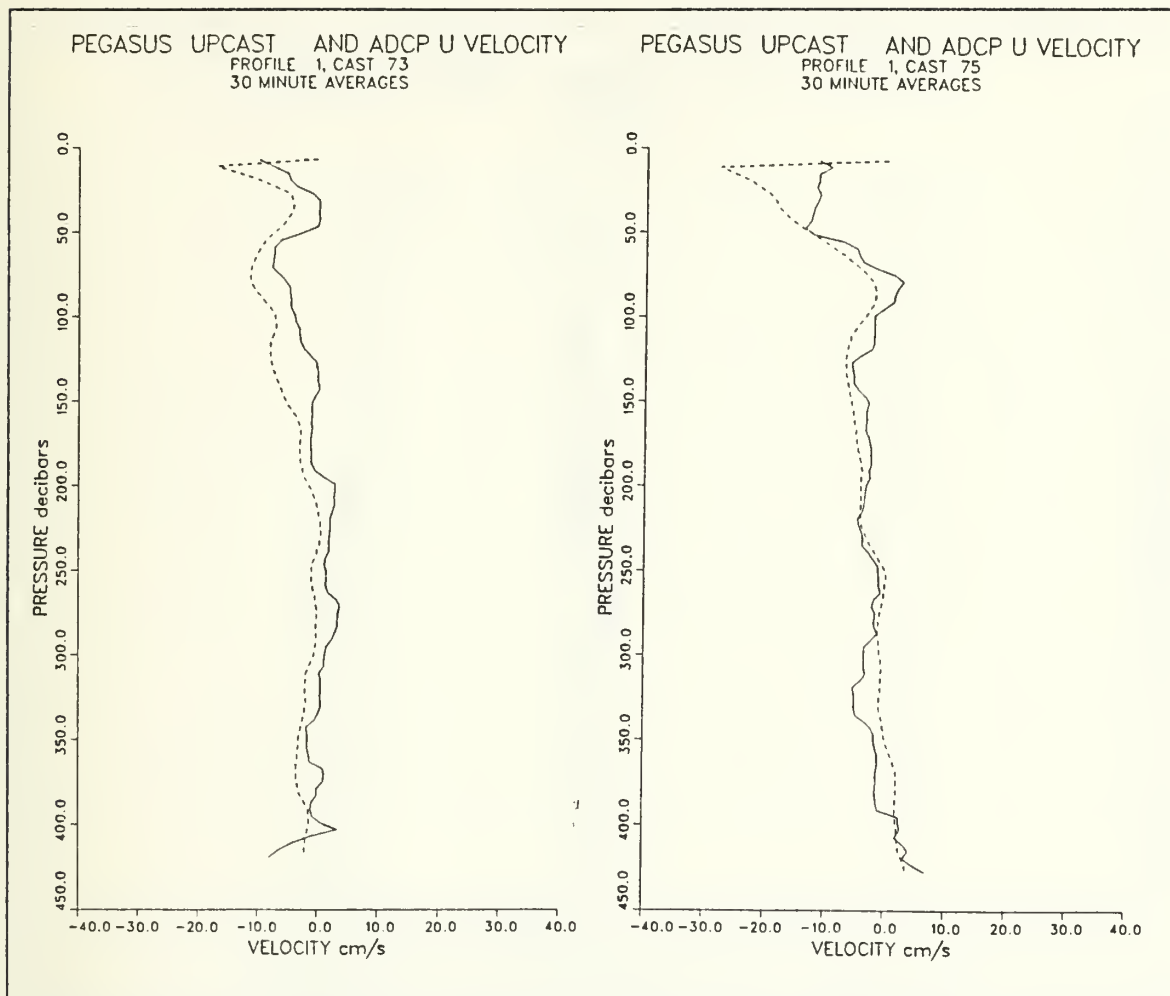


Figure 10. Upcast U Component Velocities for Casts 73 and 75: Dashed line represents Pegasus velocities while solid line represents ADCP velocities.

0.725 and 0.963 respectively. The cast average correlation coefficient is 0.866 due to the averaging of these opposing vertical offsets.

Also of note is that the Pegasus velocities for our data sets usually have a larger magnitude than the velocities recorded by the ADCP. For cast 75 the downcast Pegasus velocities are on average 4.7 cm/s higher than the ADCP velocities, while for the upcast the ADCP velocities are 0.06 cm/s higher. The reason for this is unclear since one would expect that Pegasus velocities would be an underestimate of ADCP velocities due to the inability of achieving a perfect coupling between Pegasus and an ocean current. Since this characteristic is present in both the U and V components, any alignment error of the

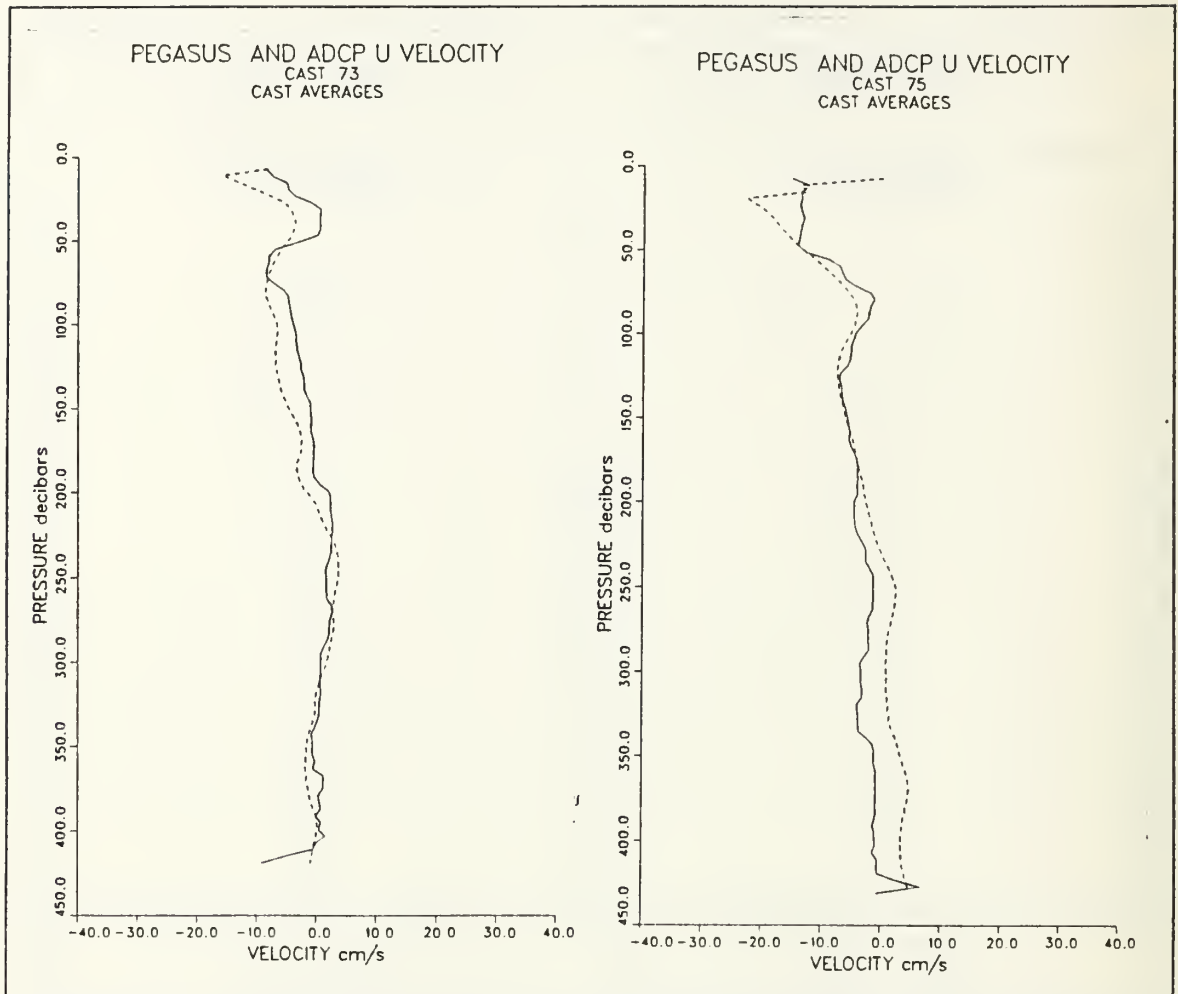


Figure 11. U Component Cast Averages for Casts 73 and 75: Cast averages consist of up and downcasts being averaged together to form a single profile. Pegasus velocities are indicated by the dashed line and ADCP velocities by the solid line.

ADCP is ruled out. The effects of roll and pitch due to the surface wave field are also ruled out since, although they would introduce an error, it would not be consistent in both directions. Although Pegasus velocities were usually larger, calculation of confidence limits on the probability of our Pegasus and ADCP data sets being significantly different were not statistically significant at the 95% confidence level. The 95% confidence limits for the probability of Pegasus being an overestimate of ADCP velocities was $0.53 < p > 0.75$, while the 95% confidence limits that Pegasus and ADCP velocities

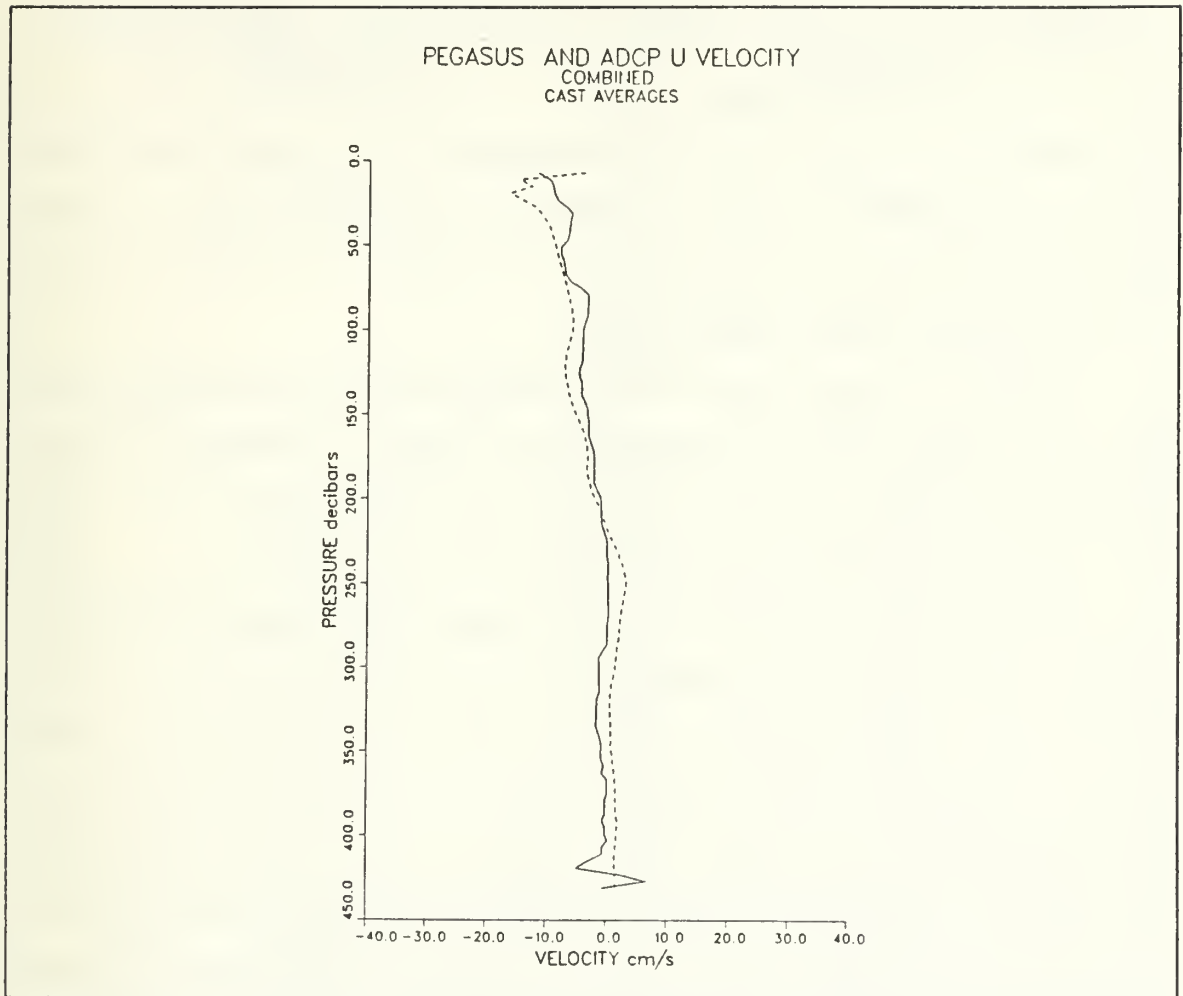


Figure 12. U Component Station Average for Casts 73 and 75: A station average is the averaging of casts conducted half an inertial period apart in order to remove inertial-period flow. Pegasus velocities are shown by the dashed line and ADCP velocities by the solid line.

are not significantly different was $0.39 < p > 0.61$. On the basis of these results, we must reserve judgment until a larger data set is collected such that the degrees of freedom will be increased and the 95% confidence intervals reduced. If we reduce the confidence limits to 76%, the probabilities diverge with the current data set, indicating a systematic error between the two instruments velocity profiles.

Another characteristic portrayed by these samples is the strength of inertial motion relative to the mean flow. In examining cast averages for cast 73 and 75 which

are separated by 9.07 hours, one notes the degree of change in the profiles that has occurred in this time. Variations of 7 cm/s can be seen in Pegasus velocities at 370 m while the ADCP velocity variation is only 2 cm/s. The correlation coefficients for cast 73 and 75 cast averages are 0.874 and 0.886 respectively. In examining the station average one can see the mean flow profile. The correlation coefficient for this profile is 0.943 which indicates a good comparison between the results of the ADCP and Pegasus. This illustration shows that for the U component velocity, the effects of inertial flow are at least the same order of magnitude as the mean flow.

2. Examination of the V velocity component

Figure 13 on page 27 shows the V component velocities for the downcasts for casts 73 and 75, while Figure 14 on page 28 shows the upcast V component velocity for these same casts. Figure 15 on page 29 shows the cast averages for casts 73 and 75. The station V component velocity average is shown in Figure 16 on page 30.

Once again we see the opposing vertical offset between upcasts and downcasts. The up and downcast for cast 73 show an 11 m vertical offset between the maximum velocities of 30 cm/s and 26 cm/s respectively at approximately 125 m. In cast 75 the downcast shows a maximum velocity of 30 cm/s at 110 m while the upcast shows a value of 31 cm/s at 130 m. The reason for the upcast maximum velocity to be deeper than the downcast maximum is believed to be due to a change in the actual profile during the two hours of elapsed time between profiles. This is supported to some extent as observations show a reduction in shear above 130 m for the upcast. Nevertheless cast averages reduce the effects of these opposing vertical offsets. The correlation coefficients are improved from 0.868 and 0.908 for the up and downcast respectively to 0.890 for the cast average due to better vertical alignment with the ADCP profiles.

As observed in the U velocity profiles, profiles of the V velocity component show Pegasus velocities with greater magnitudes than those estimated by the ADCP. For casts 73 and 75, Pegasus velocities are greater than ADCP velocities by 2.9 cm/s and 3.7 cm/s respectively, for the upcasts while the downcasts show 2.9 cm/s and 0.8 cm/s, respectively. These profiles are dominated by a maximum poleward (26 cm/s) flow centered at approximately 125 m. This is very illustrative of the oceanography in the area and would indicate a depth of approximately 125 m for the core of the California Undercurrent. The variability of cast averages at this depth is only about 2 cm/s for both the ADCP and Pegasus. At 225 m the variation in velocities has increased to 12 cm/s for Pegasus and 7 cm/s for the ADCP. In examination of the full depth Pegasus cast for casts 73 and 75 shown in Figure 17 on page 31, it can be seen that at depths where

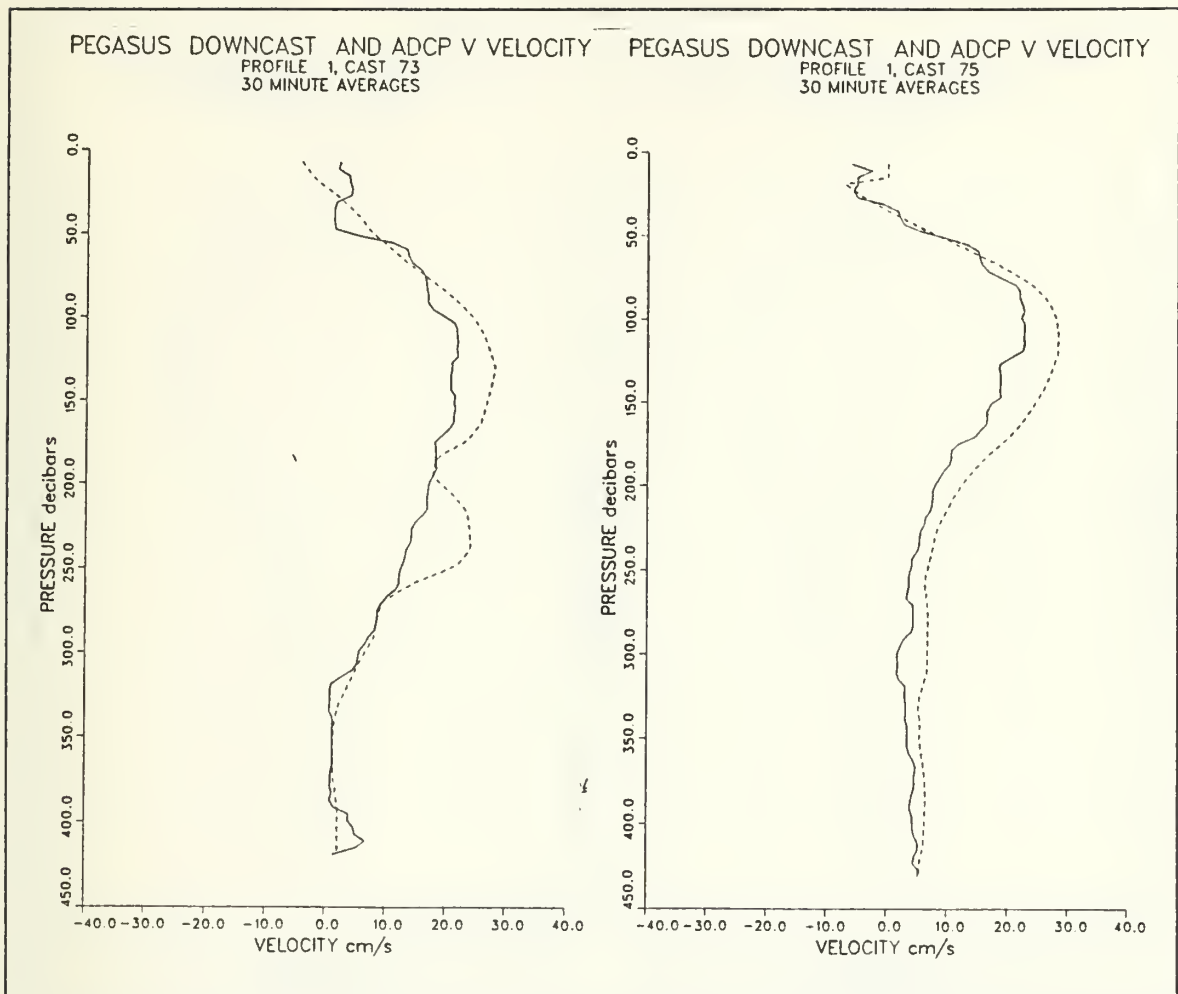


Figure 13. Downcast V Component Velocities for Casts 73 and 75: Dashed line represents Pegasus velocities while solid line represents ADCP velocities.

opposing curvatures are present, the vertical wavelength appears to be 100 to 300 m. For example, in the U velocity profile there is a node at 1100 m with the next deeper node occurring at 1300 m.

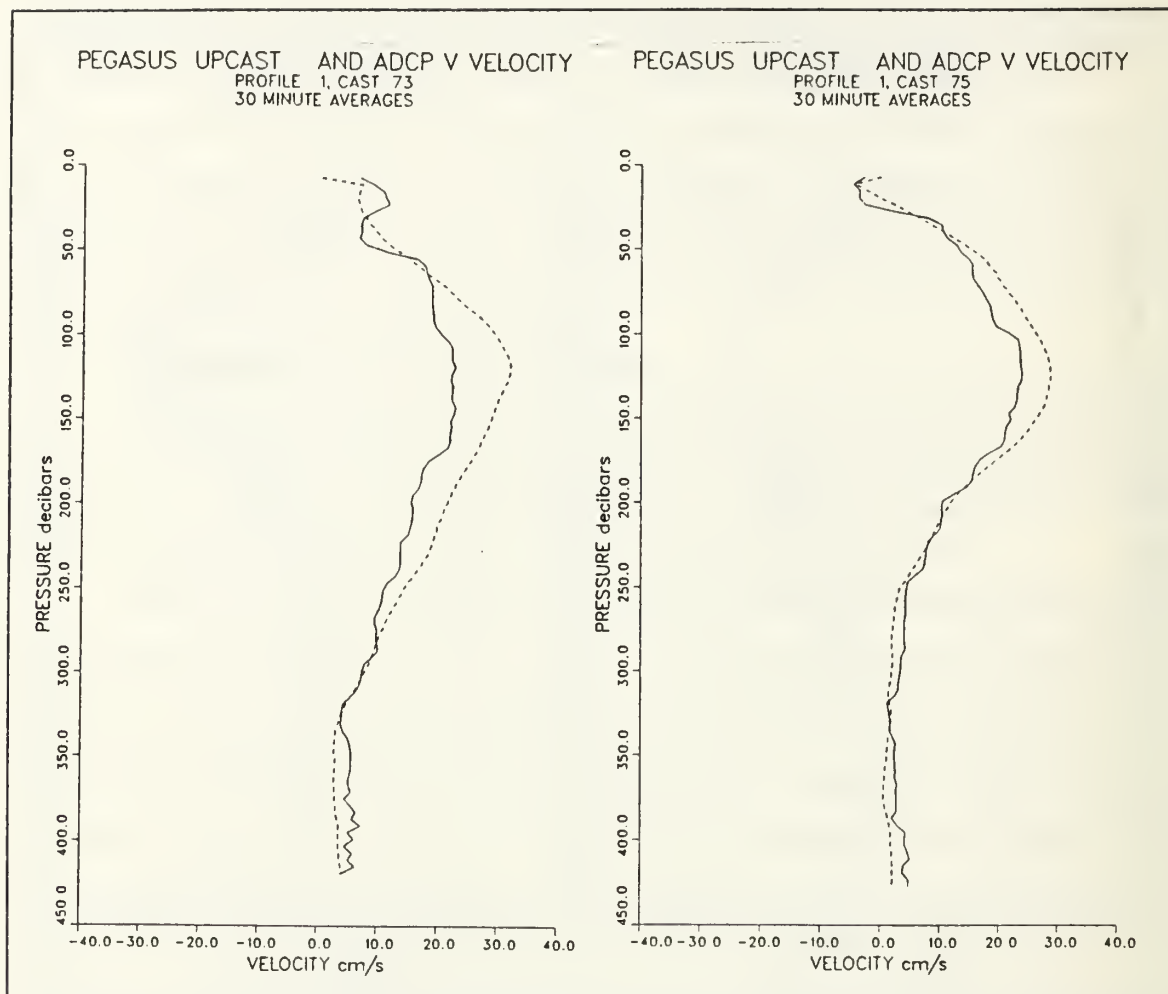


Figure 14. Upcast V Component Velocities for Casts 73 and 75: Dashed line represents Pegasus velocities while solid line represents ADCP velocities.

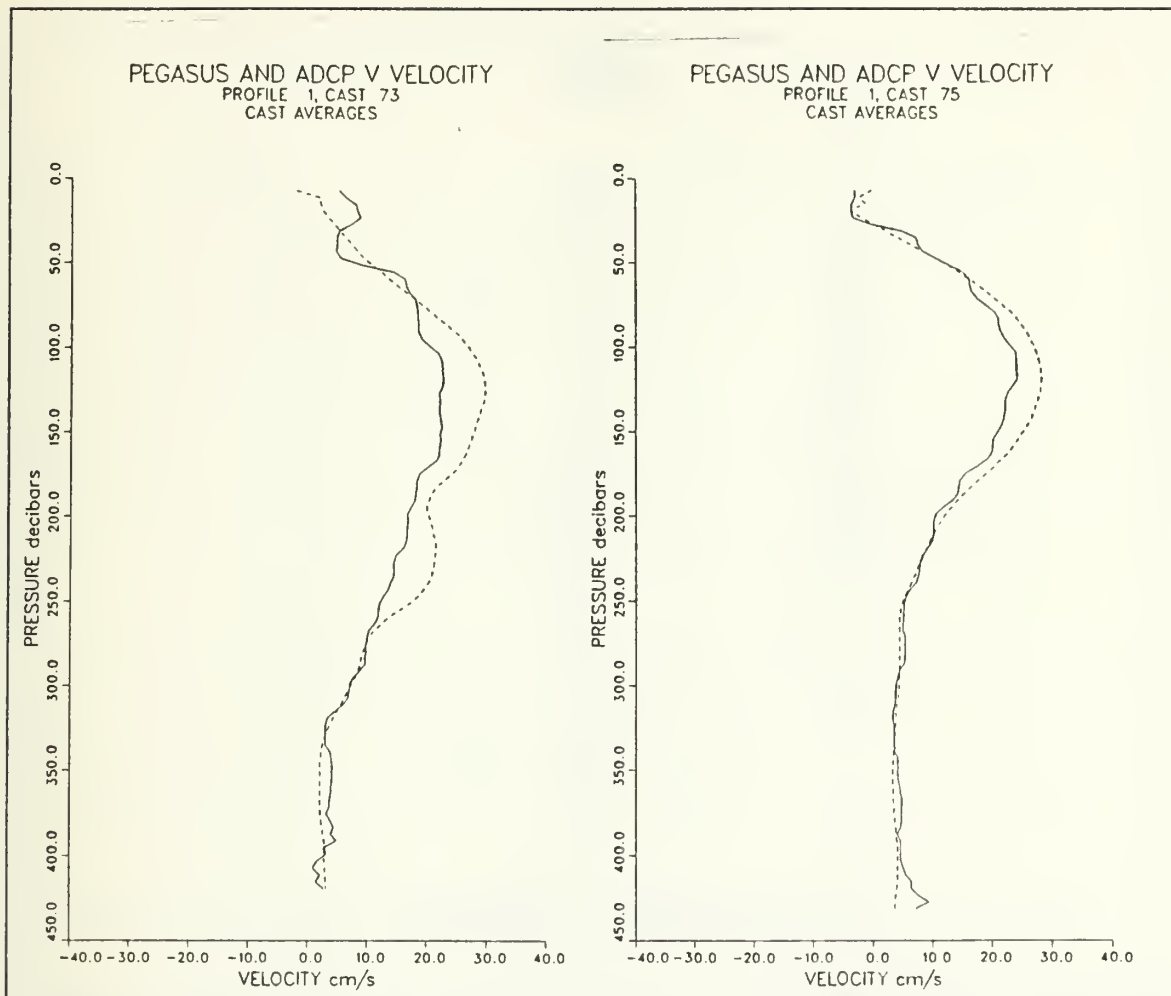


Figure 15. V Component Cast Averages for Casts 73 and 75: Cast averages consist of up and downcasts being averaged together to form a single profile. Pegasus velocities are indicated by the dashed line and ADCP velocities by the solid line.

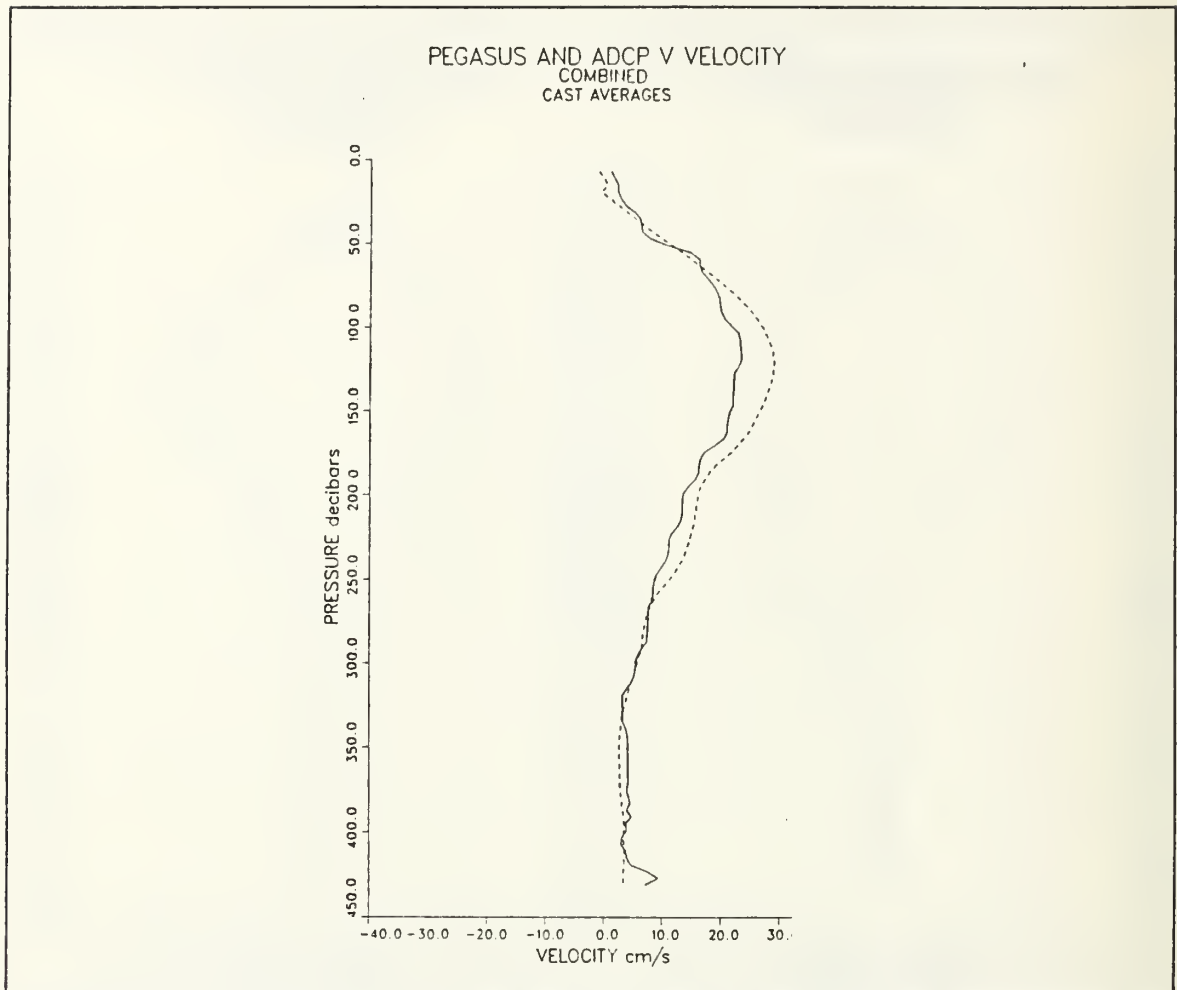


Figure 16. V Component Station Average for Casts 73 and 75: A station average is the averaging of casts conducted half an inertial period apart in order to remove inertial-period flow. Pegasus velocities are shown by the dashed line and ADCP velocities by the solid line.

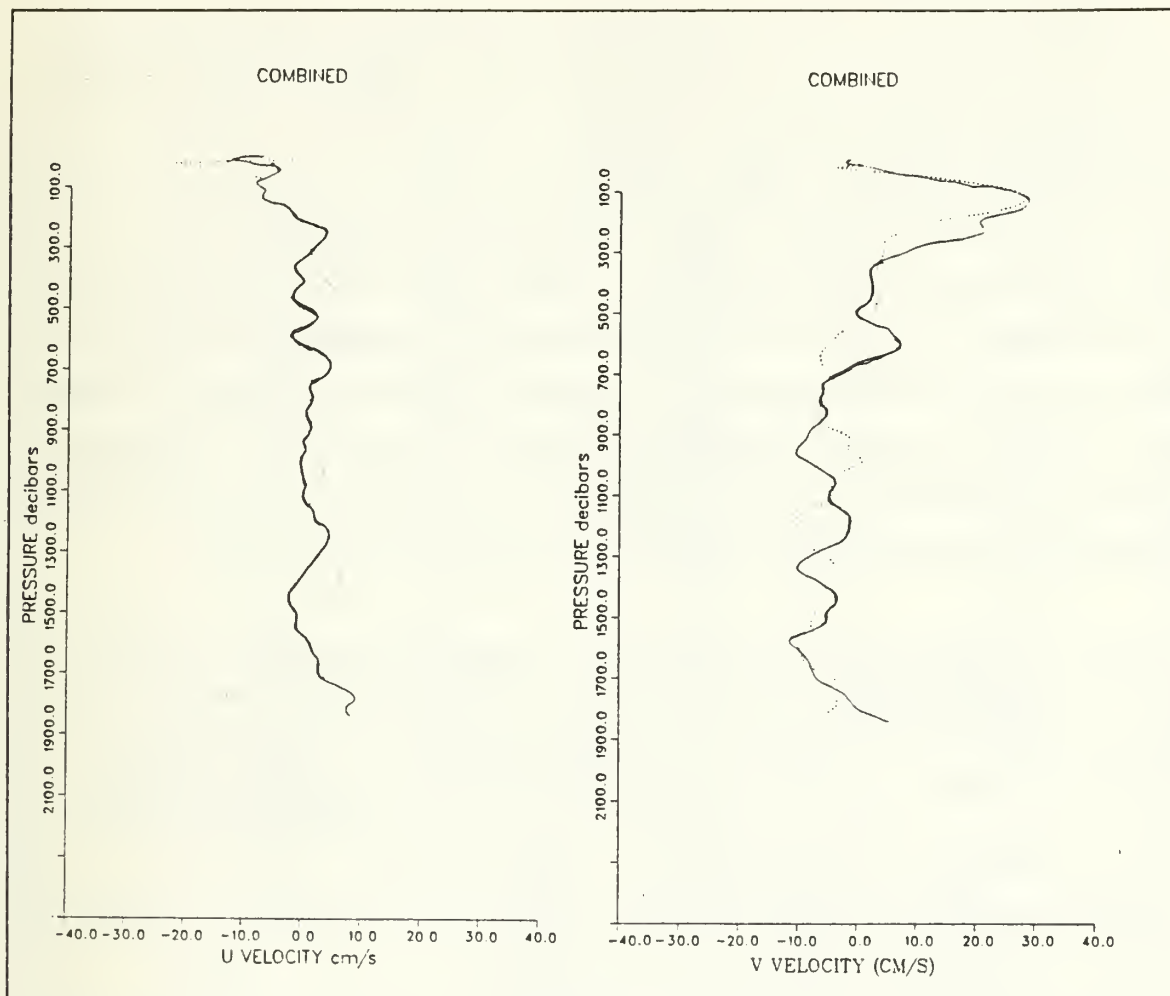


Figure 17. Full Depth Cast Averages for Casts 73 and 75: Dashed line represents Pegasus velocities for cast 75 while the solid line represents the Pegasus velocities for cast 73

B. TABLES OF RESULTS.

Correlations similar to those in section A were computed for each Pegasus station and are listed in Table 5 for the V component, Table 6 on page 33 for the U component, and Table 7 on page 33 for the averages. The averages listed in Table 7 are the mean values calculated from Tables 6 and 7. In examining the tables, it can be seen that the combined up and downcast averages show improved correlation over that of the mean of the individual up and downcasts. In addition when combined casts separated by approximately half an inertial period were averaged, a notable improvement in correlation over the mean combined casts was obtained. The results in Table 7 are interesting in that the U component velocities are better correlated than the V component velocities for individual up and downcasts, but the V component velocities are better correlated than the U component velocities for the cast and station averages.

Table 5. CORRELATION COEFFICIENTS BETWEEN PEGASUS AND ADCP V VELOCITIES

Cast #	Upcast	Down-cast	Combined up and downcast average	Station average of casts separated by half a inertial period
70	0.757	0.830	0.799	0.862
72	0.587	0.949	0.789	
71	0.823	0.827	0.880	0.865
74	0.863	0.897	0.903	
73	0.792	0.867	0.841	0.870
75	0.868	0.908	0.890	
76	0.843	0.913	0.880	0.862
77	0.865	0.921	0.885	
78	0.866	0.873	0.895	0.821
80	0.636	0.825	0.746	
79	0.746	0.476	0.702	0.874
81	0.541	0.571	0.893	
82	0.924	0.688	0.961	0.961
84	0.719	0.801	0.790	0.892
85	0.609	0.957	0.997	
86	0.911	0.832	0.890	

Table 6. CORRELATION COEFFICIENTS BETWEEN PEGASUS AND ADCP U VELOCITIES

Cast #	Upcast	Down-cast	Combined up and downcast average	Station average of casts separated by half a inertial period
70	0.892	0.865	0.909	0.979
72	0.973	0.990	0.988	
71	0.969	0.814	0.932	0.974
74	0.908	0.966	0.951	
73	0.875	0.742	0.874	0.943
75	0.725	0.963	0.886	
76	0.730	0.472	0.673	0.760
77	0.752	0.877	0.851	
78	0.755	0.830	0.797	0.851
80	0.592	0.889	0.694	
79	0.976	0.937	0.972	0.851
81	0.873	0.654	0.719	
82	0.764	0.845	0.531	0.531
84	0.850	0.779	0.765	0.833
85	0.491	0.897	0.787	
86	0.898	0.692	0.814	

Table 7. AVERAGE CORRELATION BETWEEN PEGASUS AND ADCP VELOCITIES

Component	Upcast	Down-cast	Combined up and downcast average	Station average of casts separated by half a inertial period
u	0.813	0.827	0.820	0.848
v	0.771	0.820	0.858	0.875

Some inconsistencies and details of these tables require further explanation. Cast 82 was the only cast taken at this location due to bad weather, thus its station averaged profile contains one cast and does not average inertial period flow. Casts 84, 85, and 86 were all conducted at the same station. In order to provide equal weighting to casts

separated by half an inertial period, casts 85 and 86 were averaged together to form one profile which was then averaged with cast 84 separated by half an inertial period.

Casts 76 and 77 were separated in time by 7 hours which was the shortest separation for casts taken at the same station. As a result the effects of inertial motion with a half-period of 10 hours were not completely removed. This may be the cause of lower correlation coefficients experienced at this station. This is particularly obvious in the U component velocity due to the smaller value of the mean flow relative to inertial flow.

For the V component, cast 81 stands out as having low correlation coefficients in both the up and downcast but is normal with respect to the cast and station averages. Inspection reveals that the ADCP profile for this cast has velocities close to zero for both the up and downcast, while Pegasus shifts between larger positive and negative velocities. As a result the cast average profile shows a large improvement as these opposing flows are averaged together.

The V component for the downcast of cast 79, the U component for the upcast of cast 80, and the V component for the upcast of cast 72 all show low correlation coefficients. Examination of these profiles showed Pegasus velocities that were significantly different from the ADCP data. For example in the upcast of cast 72, Pegasus velocities were -3 cm/s at 325 m; below this depth they increased rapidly to -36 cm/s at 360 m and then declined to -4 cm/s at 420 m. This would suggest the presence of a submerged equatorward jet at 360 m and is thus highly questionable. Examination of the downcast Pegasus and ADCP velocities as well as both ADCP and Pegasus velocities from cast 70, which were in the same area, show no support for such a feature. Examination of the raw Pegasus data show that a number of bad data points were present in this depth band thus increasing the doubt of the feature. Based on this information it was decided that the data in this depth band was invalid, and linear interpolation was used to connect the regions of good data. Afterwards the corrected profile was processed again and the V component correlation coefficient was increased from 0.587 to 0.798. A similar analysis was conducted on the other two profiles but due to fewer bad data points in the depth band questioned, as well as smaller differences between these profiles and other profiles, it was judged that the profiles were possible. As a result the data was not altered. Conversely the U component for the downcast of cast 76 shows ADCP velocities not supported by the Pegasus profile. A similar approach as described above was undertaken to determine the validity of the questioned profile. Due to inconclusive data to the contrary, the profile was judged to be correct and data were not modified. The reasons for these discrepancies in the ADCP and Pegasus are not known.

A scatter diagram for both the U and V components is shown for the stationed averaged profiles of ADCP and Pegasus data in Figure 18 on page 35 and Figure 19 on page 36. The calculated slope and intercept of the U and V data for ADCP versus Pegasus velocities are 0.9037 and -0.4728 for the U component and 0.9389 and 1.884 for the V component. From this information we can see that the Pegasus V component velocities are an overestimate of the ADCP velocities for velocities less than 27 cm/s. The amount of this overestimate decreases with increasing speed. In contrast the U component Pegasus velocities are an underestimate of the ADCP velocities at all speeds with the least difference being observed at smaller velocities. This type of result could be due to an alignment error in the ADCP versus the ship's gyro since it would appear that some of the ADCP V component velocity has been rotated into the ADCP U component velocity. Although this is possible it is not believed to be the cause since ADCP velocities were an underestimate of Pegasus velocities in both the U and V component for individual up and downcasts.

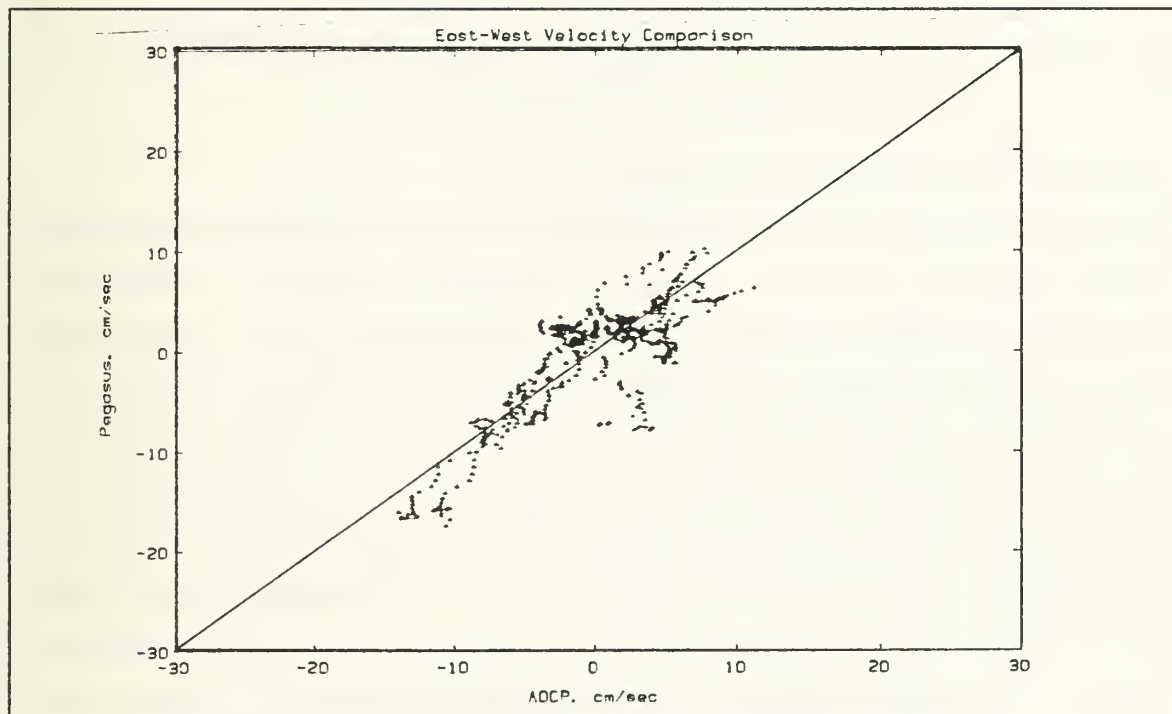


Figure 18. ADCP Versus Pegasus U Component Velocities

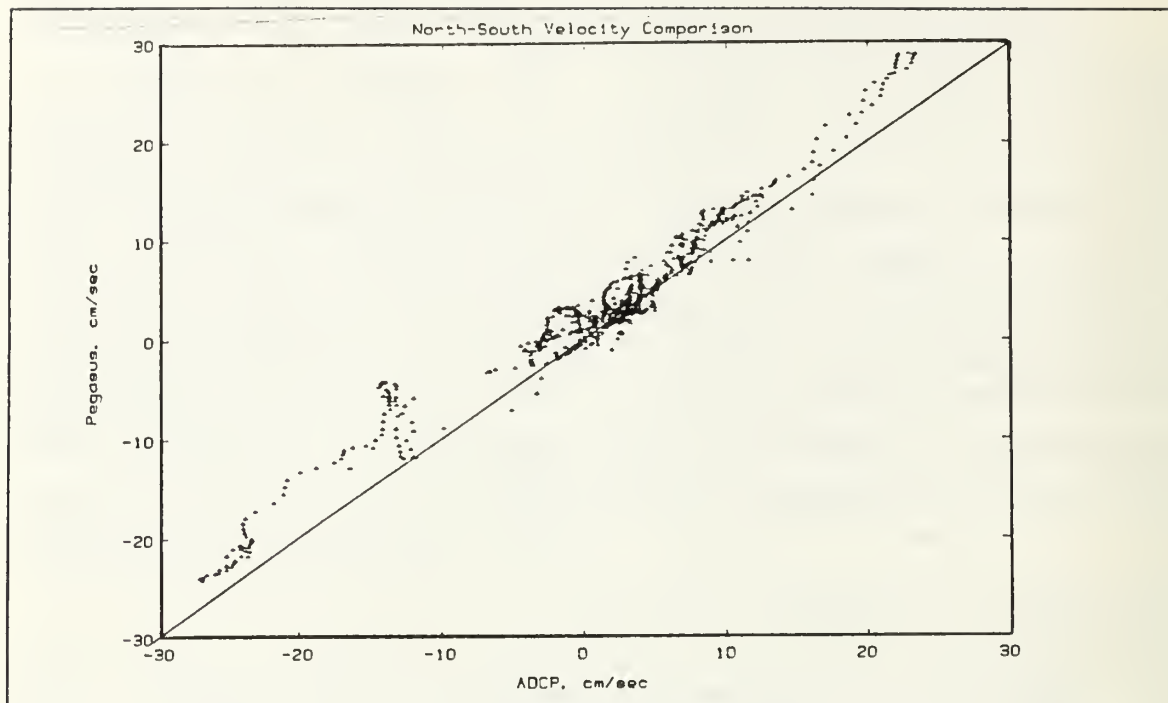


Figure 19. ADCP Versus Pegasus V Component Velocities

C. SUMMARY OF PROFILE ANALYSIS

Several generalizations can be made from the results of the profiles from this data set. Having looked at all the plots, I noted that the Pegasus profiles seem to experience a vertical offset in the direction of travel. The cause of the opposing vertical offsets could be caused by hysteresis effects in the pressure sensor, sensitivity changes in circuitry due to the temperature changes, or the moment of inertia of Pegasus. The effect of the offset on correlation coefficients was negated by averaging upcasts and downcasts together which increased correlation with the ADCP profiles. This improvement can be seen in the averaged data set results presented in the last section. The percent of improvement in the V component for cast averaged correlation coefficients is greater than in the U component. This could be explained by the inertia argument but not by the other possible causes. If the Inertia of Pegasus is causing a response lag, we would expect the offset to be a function of vertical shear. These data support this hypothesis as demonstrated in our station averaged example presented earlier. Since the V profiles contain a greater amount of shear, the offsets should have a more pronounced effect. Decreasing the fall rate of Pegasus would help correct this effect.

Pegasus velocities usually have a larger magnitude than the velocities recorded by the ADCP. This conclusion is only statistically significant if a 76% confidence interval is used, but as more data is collected, this statement can be tested with an increased number of degrees of freedom. The greater sensitivity of Pegasus to ocean currents was also noted in examination of fluctuations due to inertial motion in which the range of values recorded by Pegasus was consistently greater than those of the ADCP. The reason for the greater sensitivity of Pegasus in comparison to the ADCP is not understood but was observed consistently in these data.

A slight tendency for the correlation coefficients to become smaller as the station locations were moved offshore was noted. This same tendency was noted by King [Ref. 12]. This could be due to increased noise in the ADCP profiles due to a larger surface wave field, reduction in the benefits of averaging up and downcasts due to increased time separation, or the effect of weaker and more variable currents. The surface wave field would degrade the quality of the relative velocities determined, while the longer time separation due to increased water depth allows a greater change brought about by acceleration between the up and downcasts to occur. However the most probable explanation would be the presence of weaker and more variable currents.

The strength of the inertial motion in this area relative to the mean flow is considerable. Velocity fluctuations at a constant depth often exceeded 15 cm/s as recorded by Pegasus casts separated by half an inertial period. As noted above, Pegasus seems to be more sensitive to these flows in comparison to ADCP profiles which show a lower range of variance. As a result of these sensitivity differences, correlation between Pegasus and ADCP profiles was improved when data separated by half an inertial period was averaged together. Examination of the full depth Pegasus profiles separated by half an inertial period showed a variation in vertical wavelengths of 100 to 300 m. This is in general agreement with the 200 m vertical wavelengths for near inertial flow determined by Pinkel, et al. [Ref. 14] in the Mixed Layer Dynamics Experiment. The standard deviation noted between Pegasus and ADCP velocities was about 4 cm/s for individual up and downcasts. These values were reduced to 3.3 cm/s for cast averages and 2.7 cm/s for station averages. These values are extremely good and little improvement is believed possible due to the noise inherent in the ADCP.

V. OCEANOGRAPHIC CONDITIONS IN NOVEMBER 1988

This chapter describes the oceanography observed in November 1988 along $36^{\circ} 20'$ N off Point Sur, California. Cross sections of velocity, temperature, and salinity are used. The temperature and salinity sections were derived exclusively from CTD casts, while the velocity cross sections employed Pegasus and ADCP data. Geostrophic velocity sections are also shown and these were derived from the CTD data using the dynamic method. The Pegasus cross sections for the Pegasus cruise utilized station averaged profiles. As described in the previous chapter, these station averages, with the exception of cast 82, averaged Pegasus casts separated in time by half an inertial period. The Pegasus cross sections for the 5 to 8 November cruise are composed of only one cast per station. As a result the effects of inertial motion are not removed. The ADCP cross sections for the 1-4 November cruise are composed of averaged profiles. The processed data set was separated into 30 minute intervals with all profiles within an interval being averaged together to form an average profile representative of the water column. These 30 minute profile averages were then averaged using a 1 km distance average, with the resulting averaged profiles used to produce a cross section. The Pegasus cruise did not use the 1 km distance average in an attempt to obtain better horizontal resolution. The geostrophic cross sections were calculated using a level of no motion of the deepest point common to both stations.

All three cruises were conducted in the first half of November 1988 and thus allowed observation of movement and development of common features shared by each cruise. The fall transition marks the end of the season dominated by coastal upwelling and a gradual transition to the non-upwelling or "winter" season. The fall transition is marked by a temperature maximum in surface waters, and by shorter (and warmer) upwelling events. For our study area, a 14 year time series of sea surface temperature which illustrates this transition is available from Granite Point at $36^{\circ} 25.5'$ N, see Figure 20 on page 39. The 14 year average clearly shows warmest temperatures at the coast from mid September to early November. The 1988 data show the onset of the fall transition by a sharp rise in sea surface temperature which occurred in late August with maximum temperatures reaching 15.4° C. The last strong coastal upwelling event occurred in early September with SST dropping to 10.4° C. During early November, SST at Granite Point ranged from 12.5° C on 1 November to a minimum of 10.9° C on 6 November and then

warmed again to 12.6° C on 11 November. A second upwelling event in November began on 12 November cooling the SST to 10.8° C by 16 November, after which the temperature warmed to 11.8° C by 19 November. In terms of the Granite Point record, 1988 then seems anomalous in terms of the early onset of the fall transition so that in October and November temperatures were typically 1° C lower than normal, except in late October when SST was closer to normal.

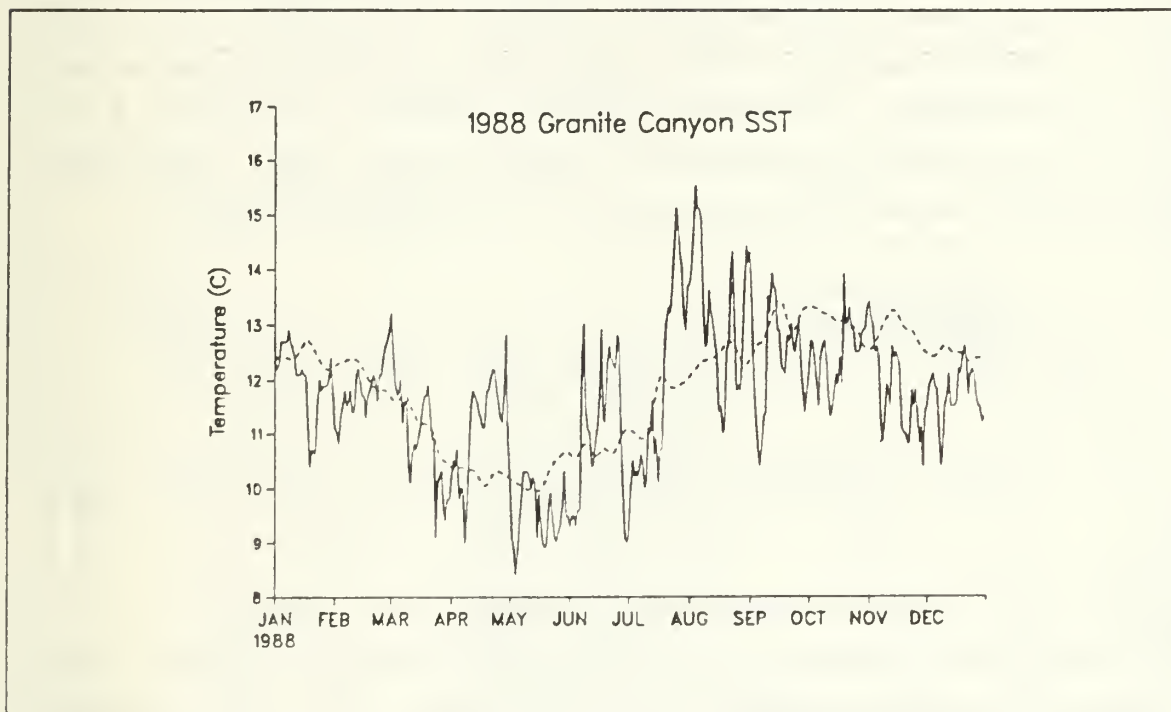


Figure 20. Granite Canyon Sea Surface Temperature: The dashed line represents a 14 year mean while the solid line represents the SST recorded for 1988.

A. OCEANOGRAPHIC CONDITIONS DURING STUDENT CRUISES

1. Velocity Sections

a. *V* Component Velocity Sections

The 1-4 November geostrophic cross section of *V* component velocities, see Figure 21 on page 40 and Figure 22 on page 41, show several distinct features. A shallow equatorward flow extending to 28 km offshore is seen over the continental shelf. The strongest flow in the region is a 20 cm/s equatorward surface flow at 18 km offshore. This relative velocity maximum corresponds to the break between the shelf and the continental slope. This is a shallow feature with the 10 cm/s isopleth lying above 75 m.

The next easily identified feature is a 30 cm/s poleward jet centered at 225 m deep, 52 km offshore corresponding to the mid-continental slope region. The 20 cm/s contour extends to the surface while the 10 cm/s contour reaches to 1000 m deep. West of 65 km offshore is a predominantly equatorward flow. At 105 km offshore a 20 cm/s equatorward flow to 60 m is indicated. The above description agrees well with the known features of the California Current System off Point Sur. The section shows the broad equatorward California Current west of 65 km offshore. The core was not resolved but a 20 cm/s maximum equatorward velocity which could be associated with the core was noted at 102 km offshore. The maximum poleward undercurrent was centered at 225 m deep, 52 km offshore with poleward flow extending to the surface. The inshore equatorward flow was also observed over the shelf as noted by Chelton [Ref. 6].

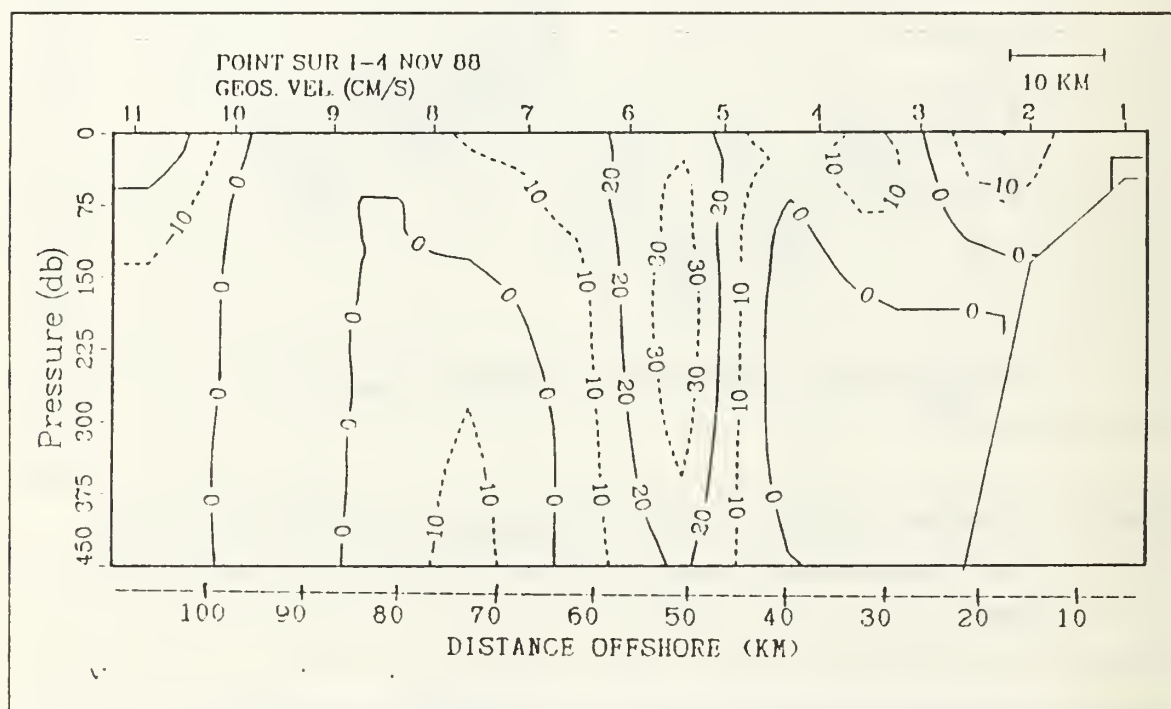


Figure 21. 1-4 November V Component Geostrophic Velocity to 450 m

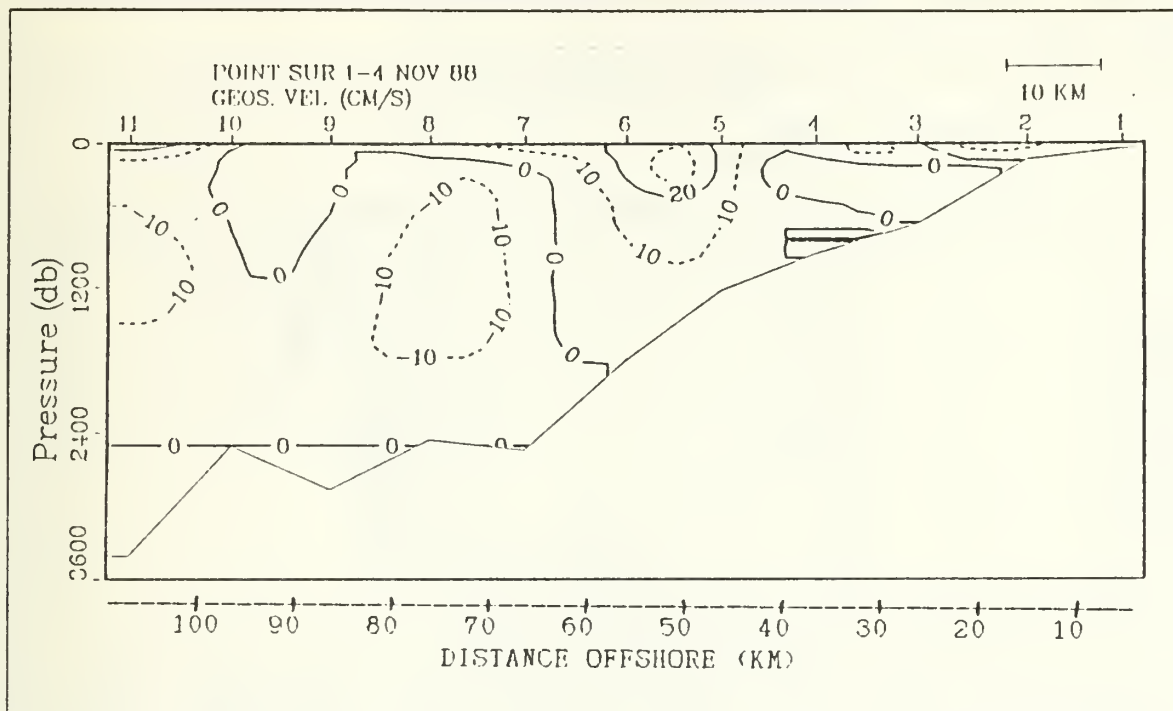


Figure 22. 1-4 November V Component Geostrophic Velocity to 3600 m

The corresponding ADCP V component velocity section for this period is shown in Figure 23 on page 42. This section has poor agreement with the geostrophic velocity cross section. This poor agreement may be due to the presence of small scale time dependent motion such as ageostrophic internal waves and inertial motion. The section shows predominately equatorward flow inshore of 45 km. An exception to this is between 10 and 20 km offshore which shows a 20 cm/s poleward flow. This poleward flow is in disagreement with the geostrophic cross section but is based upon 1.5 hours of ADCP data that is believed to be of good quality. The ADCP section also shows a large shear between 25 and 30 km offshore. The maximum velocity noted is 70 cm/s at 28 km offshore, which is significantly higher than the near zero velocity seen in the geostrophic velocity section. This shear maximum has a value of $1.5 \times 10^{-4} s^{-1}$. The location of this shear does correspond to the location of a relative maximum shear of $3 \times 10^{-5} s^{-1}$ noted in the geostrophic cross section. This strong horizontal shear and velocity between 25 and 35 km offshore depicted in the ADCP section is not normally expected. The region between 45 km and 85 km shows predominately poleward flow with a 20 cm/s maximum noted from the surface to 60 m between 65 and 80 km. West of 85 km

the flow is once again equatorward. ADCP data for the 5-8 November cruise was not available for the cross section due to power supply problems.

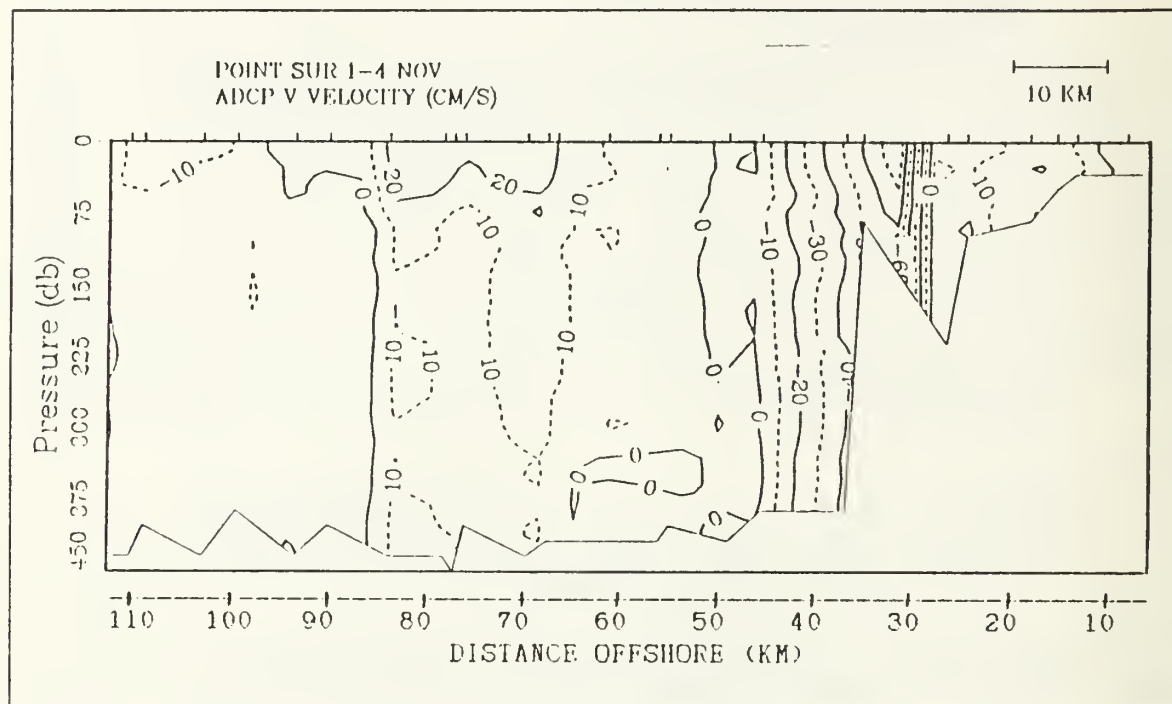


Figure 23. 1-4 November V Component ADCP Velocities to 450 m

The geostrophic velocity section for the 5-8 November cruise is shown in Figure 24 on page 43 and Figure 25 on page 43. This section does not have the horizontal resolution or extent of the 1-4 November section but nevertheless shows the same features. This section shows an equatorward surface flow to exist inshore of 35 km. The equatorward 10 cm/s contour extends to a depth of approximately 100 m. The poleward undercurrent of 30 cm/s is also just barely resolved. The depth of the core of the poleward jet is 125 m located 55 km offshore which indicates a shoaling from the 1-4 November cruise of 100 m. In comparing the geostrophic V velocities observed between the two student cruises, one observes a westward propagation on the order of 1 km/day for features common to both cruises. The westward propagation and rapid shoaling of the poleward jet are interesting properties that could be tied to the end of the downwelling on 6 November and warming of temperatures during the second student cruise. Wickham [Ref. 4] noted, in a study conducted 60 km to the South of Point Sur at Cape San Martin, that current meter data indicated a deepening and seaward spreading of the poleward jet during upwelling events.

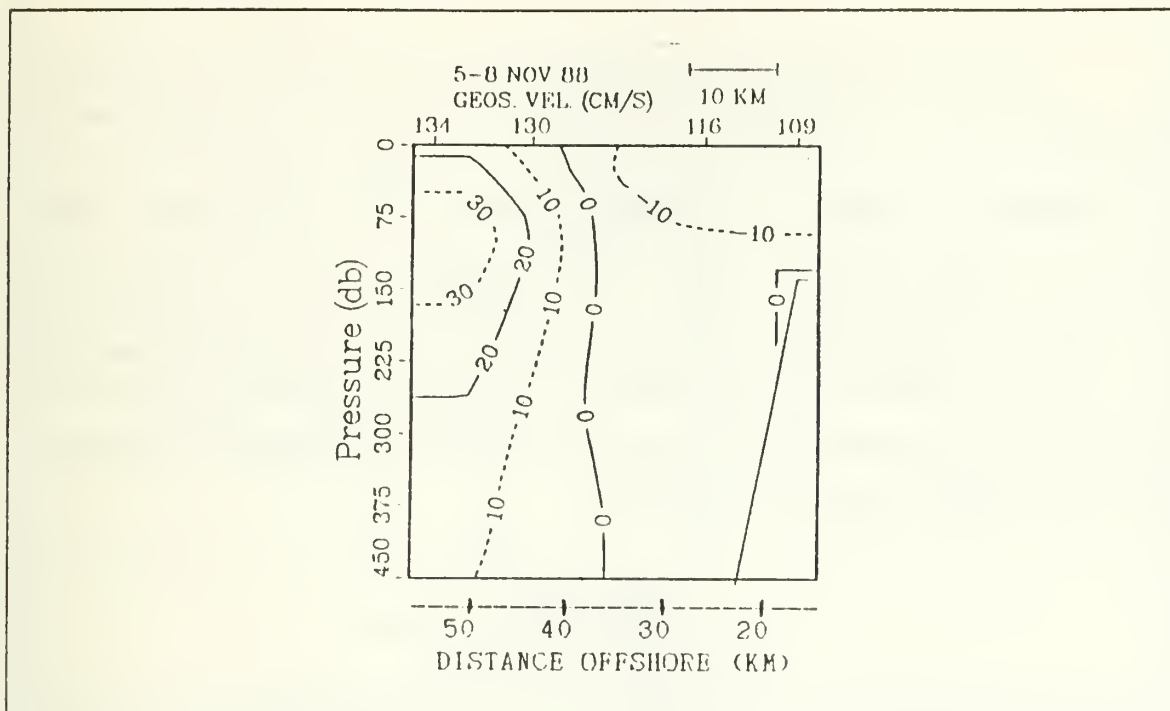


Figure 24. 5-8 November V Component Geostrophic Velocity to 450 m

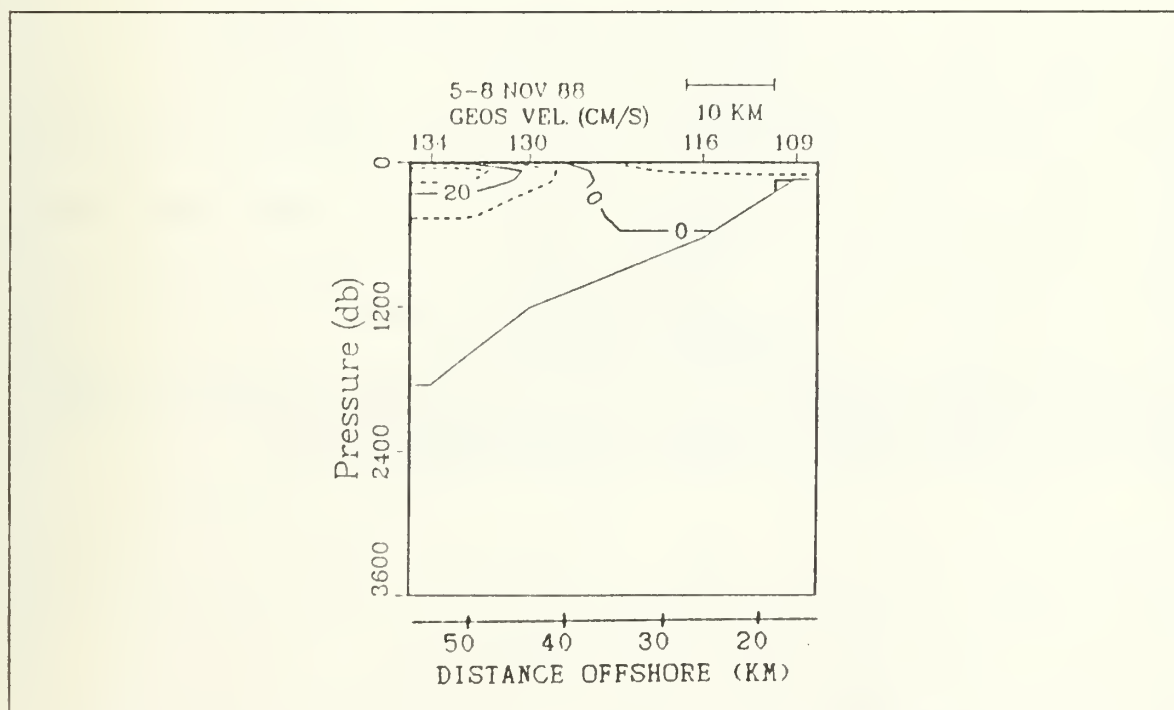


Figure 25. 5-8 November V Component Geostrophic Velocity to 3600 m

The Pegasus section of the V component velocities for the 5-8 November cruise shown in Figure 26 and Figure 27 on page 45 includes only one cast per station and consists of three casts. Despite the small amount of data, the absolute velocity section obtained by Pegasus is in excellent agreement with the geostrophic cross sections. The section shows the poleward undercurrent located at 125 m deep, 50 km offshore with a velocity maximum of 20 cm/s. Due to the nature of Pegasus it can only detect a feature if it passes directly through it. Thus the difference in velocity and location of the core between the Pegasus velocity cross section and geostrophic section can be explained by the fact that the Pegasus cast is located east of the actual core and thus did not pass through the center of the feature.

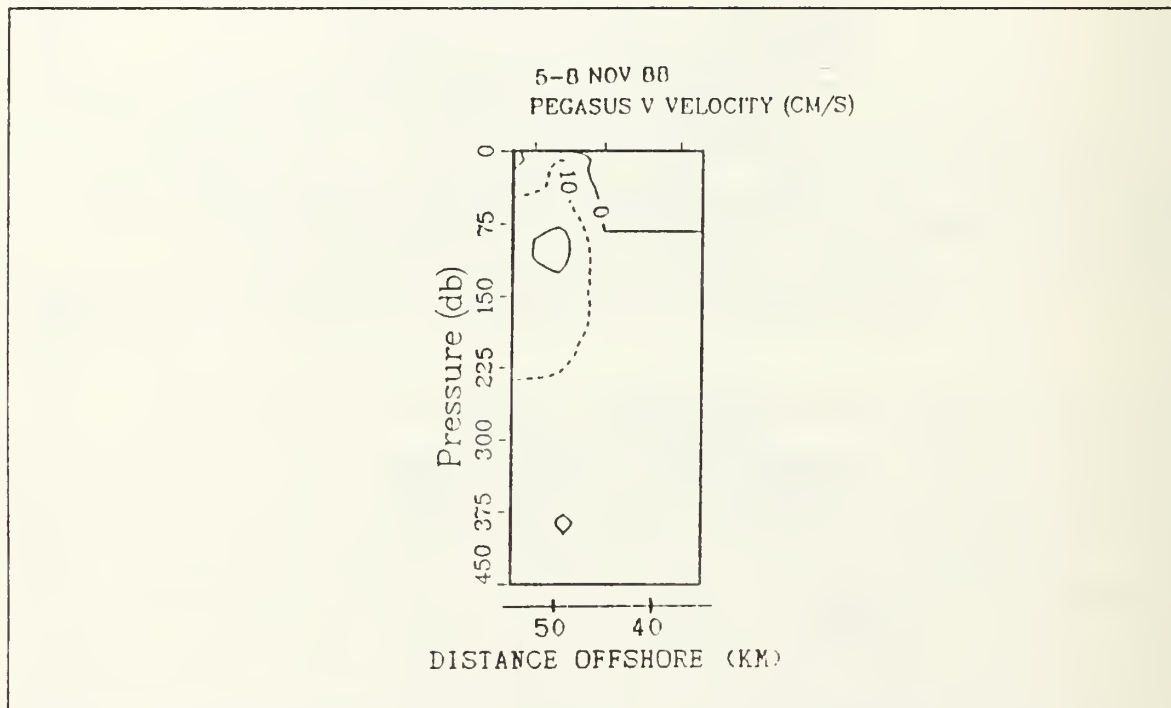


Figure 26. 5-8 November V Component Pegasus Velocity to 450 m

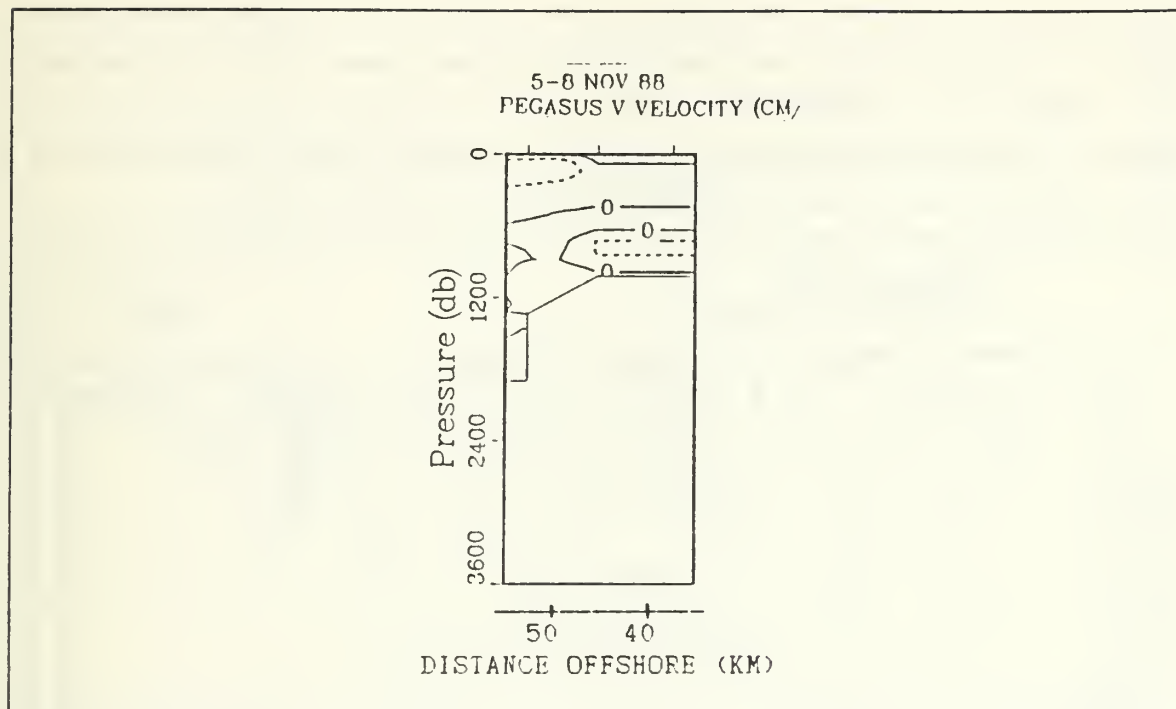


Figure 27. 5-8 November V Component Pegasus Velocity to 3600 m

b. U Component Velocity Sections

The U component velocity data for the two student cruises consist of a ADCP cross section for the 1-4 November cruise and a Pegasus cross section for the 5-8 November cruise. The ADCP U component velocity section, shown in Figure 28 on page 46, shows offshore flow out to approximately 10 km. Between 10 and 30 km offshore is a region of onshore flow followed by offshore flow between 30 and 55 km offshore. Between 55 and 90 km offshore the flow is slightly eastward, while beyond 90 km the flow is once again offshore. This depiction would indicate the presence of weak upwelling along the coast, which is in agreement with the upwelling indicated at Granite Point. The section shows a coastal convergence between 50 and 60 km offshore as well as near 10 km offshore. Divergence is noted between 80 and 90 km as well as at approximately 30 km offshore. The convergence region in the vicinity of 55 km offshore agrees well with the location of the poleward undercurrent, while the convergence region near 10 km indicates the westward extent of the nearshore poleward flow. As in the V component velocity, a maximum in horizontal shear is seen between 25 and 30 km offshore. This region of high shear is not understood but it is noted that the location is in

common with a maximum bottom slope between 200 and 300 fathoms of 0.1. The Pegasus U component velocity sections for 5-8 November, shown in Figure 29 on page 47 and Figure 30 on page 47, agree well with the ADCP section showing westward flow inshore of 50 km and onshore flow west of 50 km from shore. Below 500 m the flow is onshore, with a maximum eastward velocity of 10 cm/s located at 600 m.

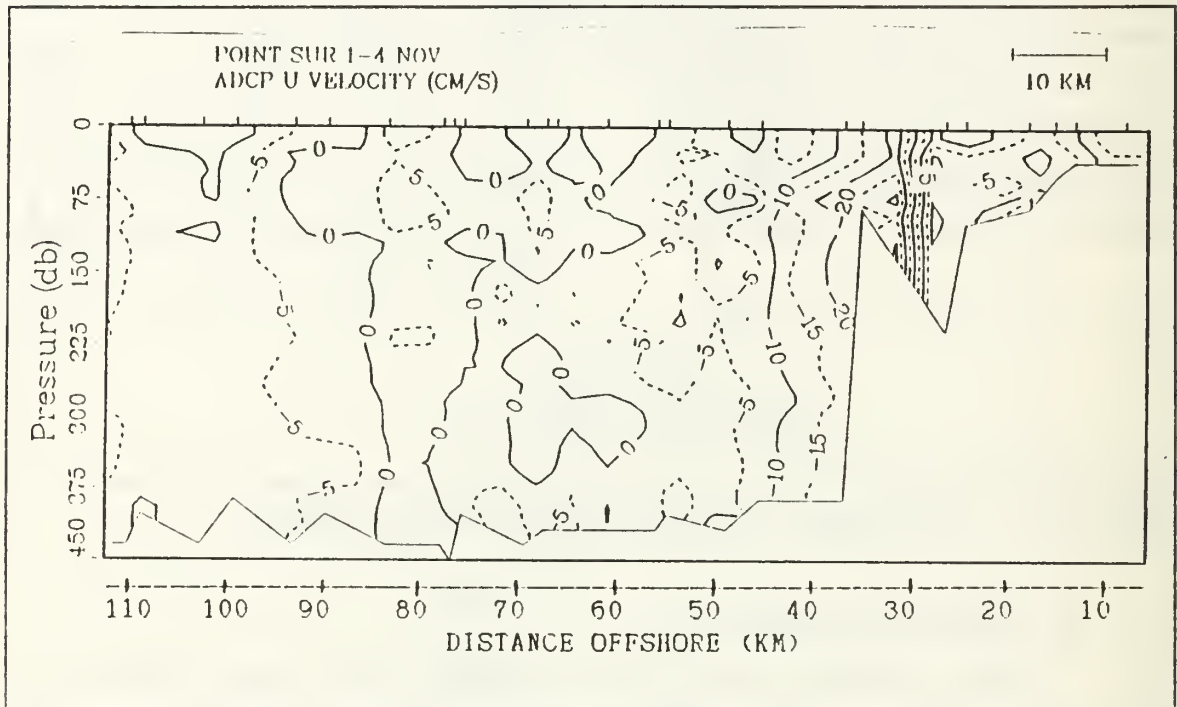


Figure 28. 1-4 November U Component ADCP Velocity to 450 m

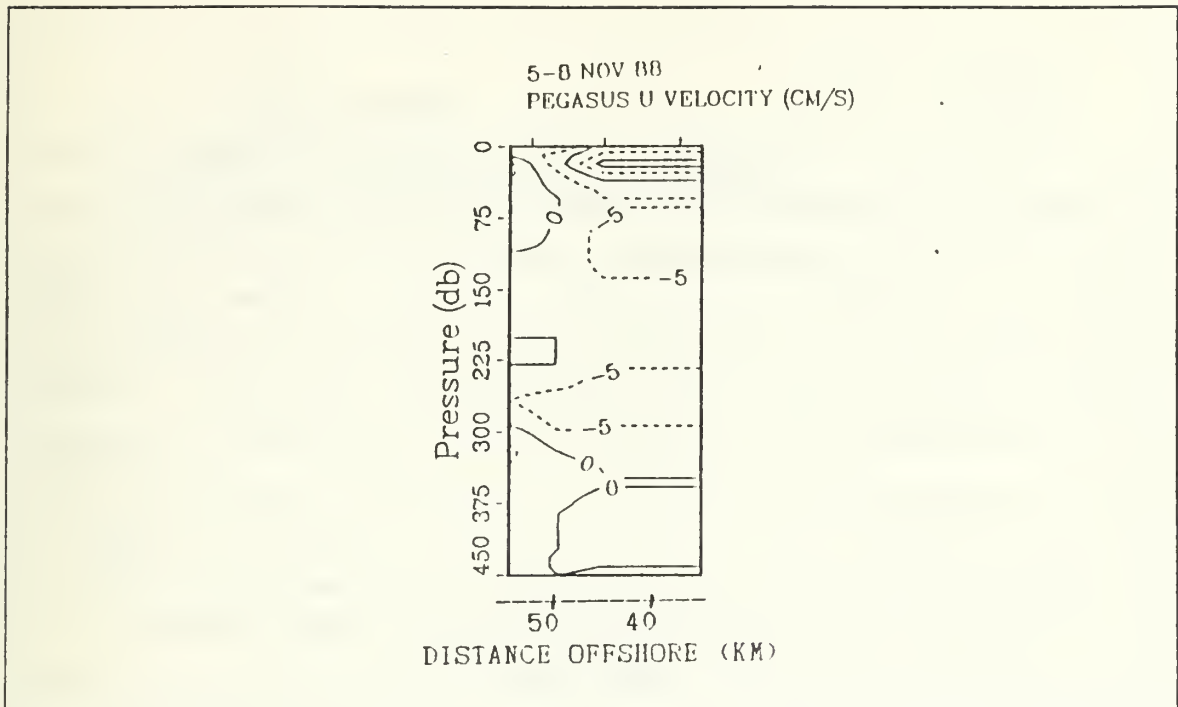


Figure 29. 5-8 November U Component Pegasus Velocity to 450 m

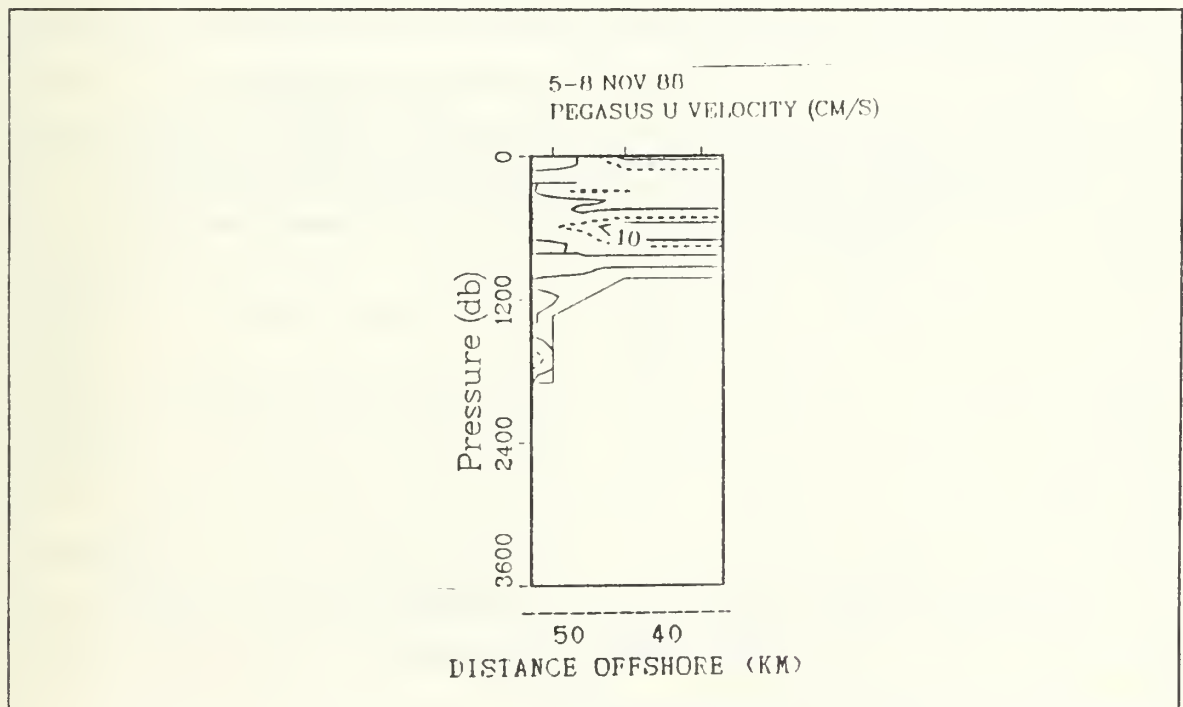


Figure 30. 5-8 November U Component Pegasus Velocity to 3600 m

2. Temperature Sections

The temperature sections for 1-4 November are shown in Figure 32 on page 49 and Figure 31 on page 49. The nearshore isotherm slope does not indicate strong upwelling although waters warmer than 10°C and shallower than 75 m appear to be colder at the coast. The Granite Point sea surface temperature (SST) shows surface cooling beginning at the start of November and continuing through 6 November when SST reaches a minimum of 10.9°C . In Fig. 32 the 12 degree isotherm does not reach the surface while the 13 degree isotherm surfaces at approximately 10 km offshore. In contrast the 5-8 November section, shown in Figure 33 on page 50 and Figure 34 on page 50, shows the 13 degree isotherm at the surface 45 km offshore with a lens of water warmer than 13 degrees located at the surface between 20 and 30 km offshore. In addition the 5-8 November section shows the 9 degree isotherm to slope upward above 150 m. The presence at corresponding depths of cooler water compared to that observed in the 1-4 November section in the upper water column indicates the effects of the continued upwelling on the nearshore region over this short time period. There is a 107 hour separation between observations at stations 1 and 109. During this time, both the 9 and 10 degree isotherms shoaled by approximately 35 m. This corresponds to the 2.3°C drop in temperature noted at Granite Point during the same interval. The other isotherms show a much reduced shoaling. The lens of warm water located at the surface at approximately 55 km offshore is depicted in both sections. This warmer water corresponds to the convergence region noted in the U velocity cross sections mentioned before. In addition, the 1-4 November section shows a surfacing of the 14 degree isotherm between 80 and 90 km which agrees with the ADCP divergence in U velocities noted in this region. The 1-4 November section shows a downward slope of the 6 to 10 degree isotherms between 45 and 70 km offshore while the 5-8 November cruise shows this downslope for the 8 to 10 degree isotherms. The reason for the shorter extent of the downsloping isotherms on 5-8 November is believed to be linked with the end of the downwelling event on 6 November. The sloped isotherms are features typical of the isotherms in the vicinity of the poleward jet. Thus the shoaling of the jet noted earlier is associated with the smaller vertical extent of the downsloping isotherms. Therefore the temperature sections for the student cruises show good dynamic support and correlation with the features observed in the velocity sections.

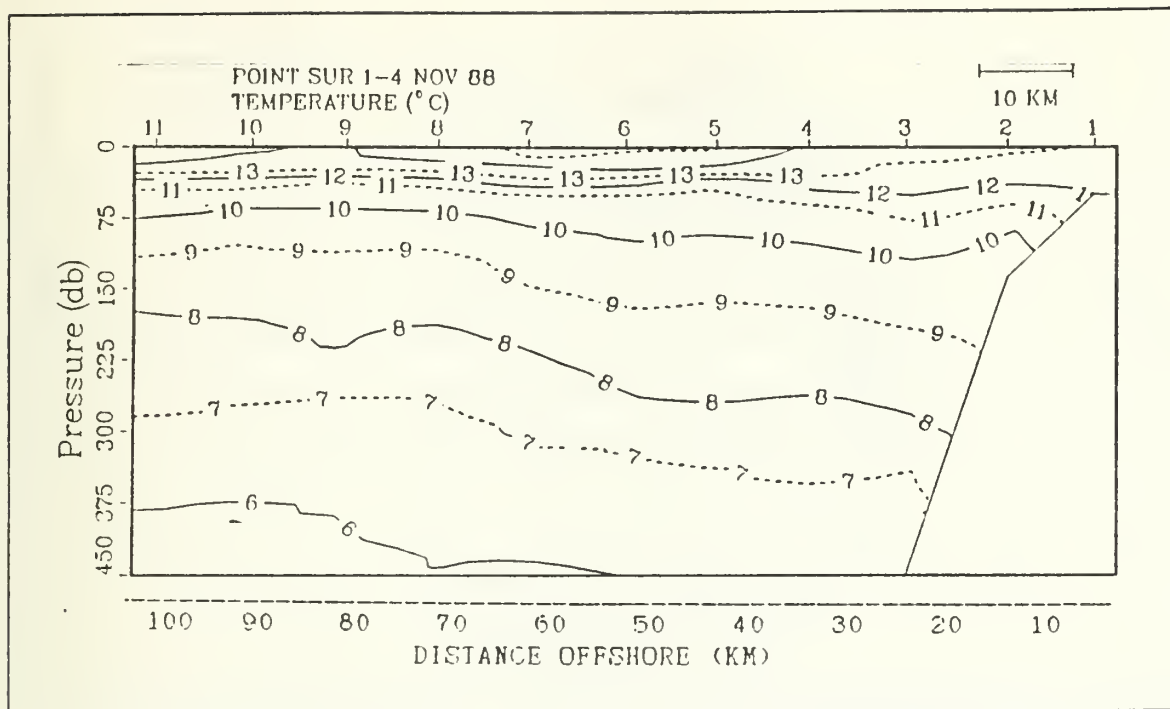


Figure 31. 1-4 November Temperature to 450 m

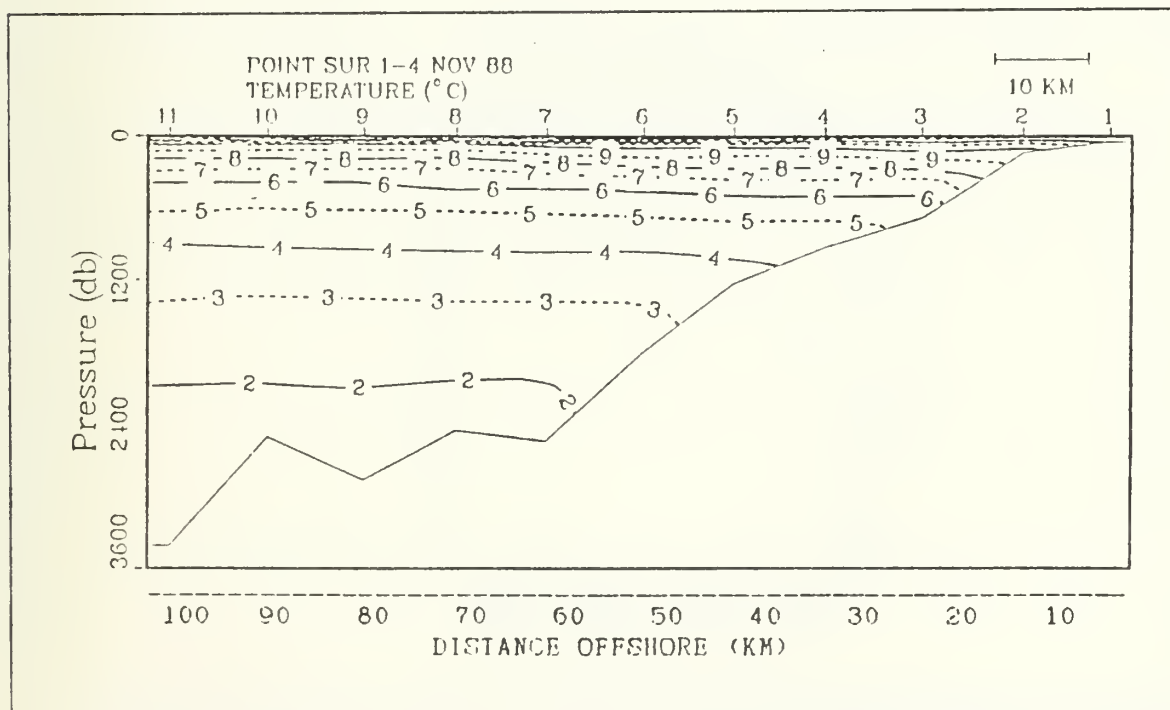


Figure 32. 1-4 November Temperature to 3600 m

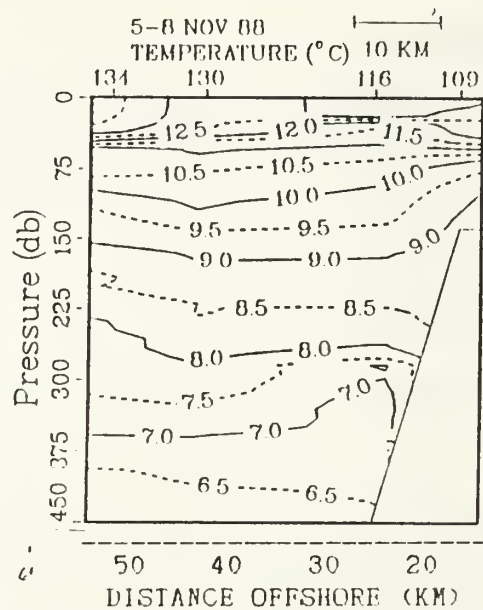


Figure 33. 5-8 November Temperature to 450 m

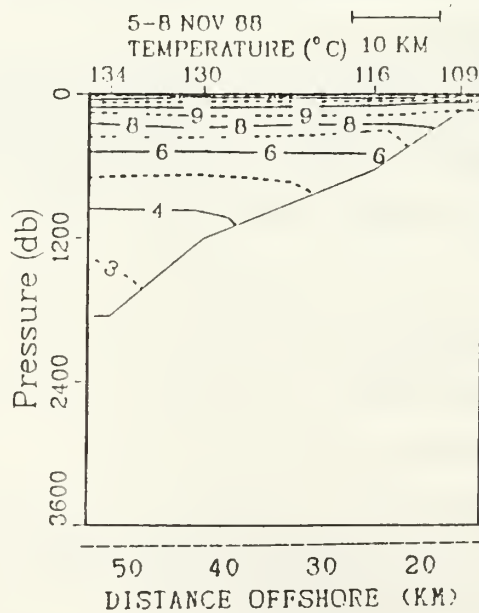


Figure 34. 5-8 November Temperature to 3600 m

3. Salinity Sections

The salinity cross sections for the 1-4 November cruise are shown in Figure 35 on page 52, and Figure 36 on page 52, while the 5-8 November cruise sections are shown in Figure 37 on page 53 and Figure 38 on page 53. Both cross sections are typical of an upwelling regime in that the nearshore isohalines less than 34 psu and above 150 m slope upward toward shore. The 5-8 November cross section shows a greater degree of upwelling with the 34.0 psu isohaline also sloping upward. The 33.875 and 34.0 psu contours show an upward displacement in time similar to that noted for the isotherms equating to approximately an 8 m/day shoaling of the isohaline surface. In examining the location of the poleward undercurrent (50 km offshore) with respect to the isohalines for the 1-4 November cruise, we note that the lowest salinity water is present at the surface at this location. The low salinity water at the surface is unusual in that one expects higher salinities in this poleward flow due to its equatorial nature. The salinities at the jet's core (225 m deep) are as expected with salinity decreasing both to the east and west of this location, which can be seen in the 34.0 psu contour. A slight doming of the isohalines is noted between 80 and 90 km offshore. This corresponds to the region of cooler temperatures at the surface in this region as well as the location of the divergence of the ADCP U component velocities. This leads to a conclusion that an upwelling regime is present at Point Sur. The low salinity values seen above 75 m at 45 km offshore in the 1-4 November cross section and at 55 km offshore in the 5-8 November cross section equate to the regions of convergence noted in the U component velocities by the ADCP and Pegasus cross sections. This low salinity surface water is also believed to be outflow from the Sacramento River.

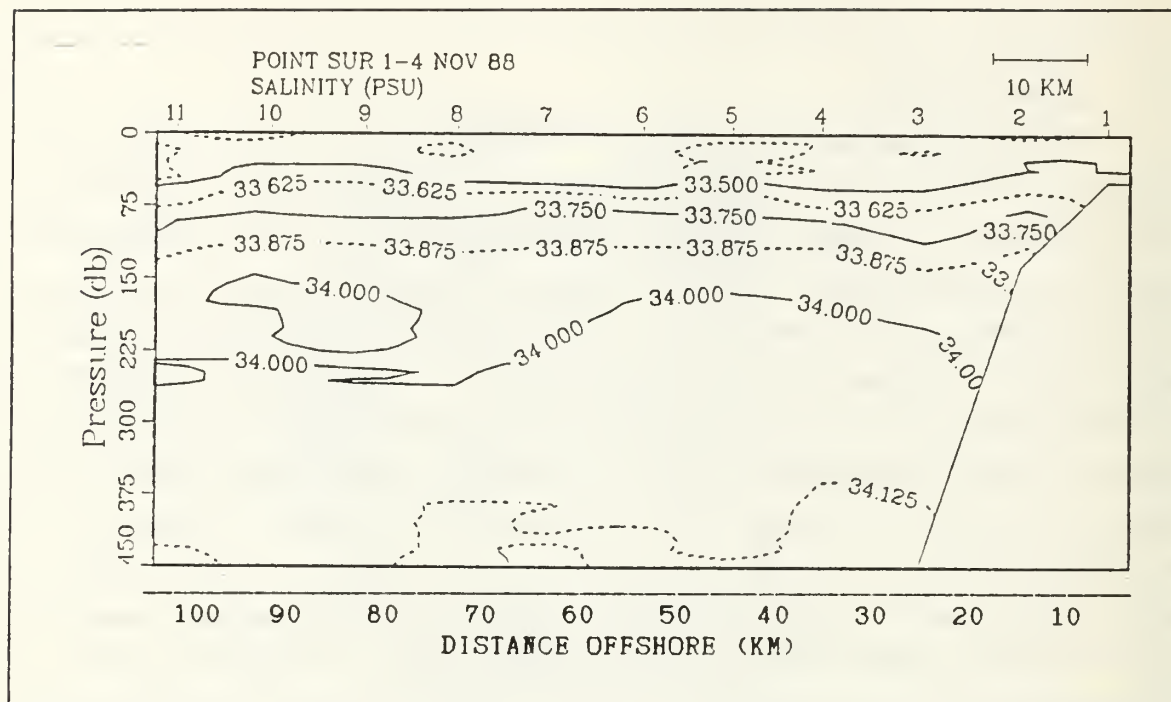


Figure 35. 1-4 November Salinity to 450 m

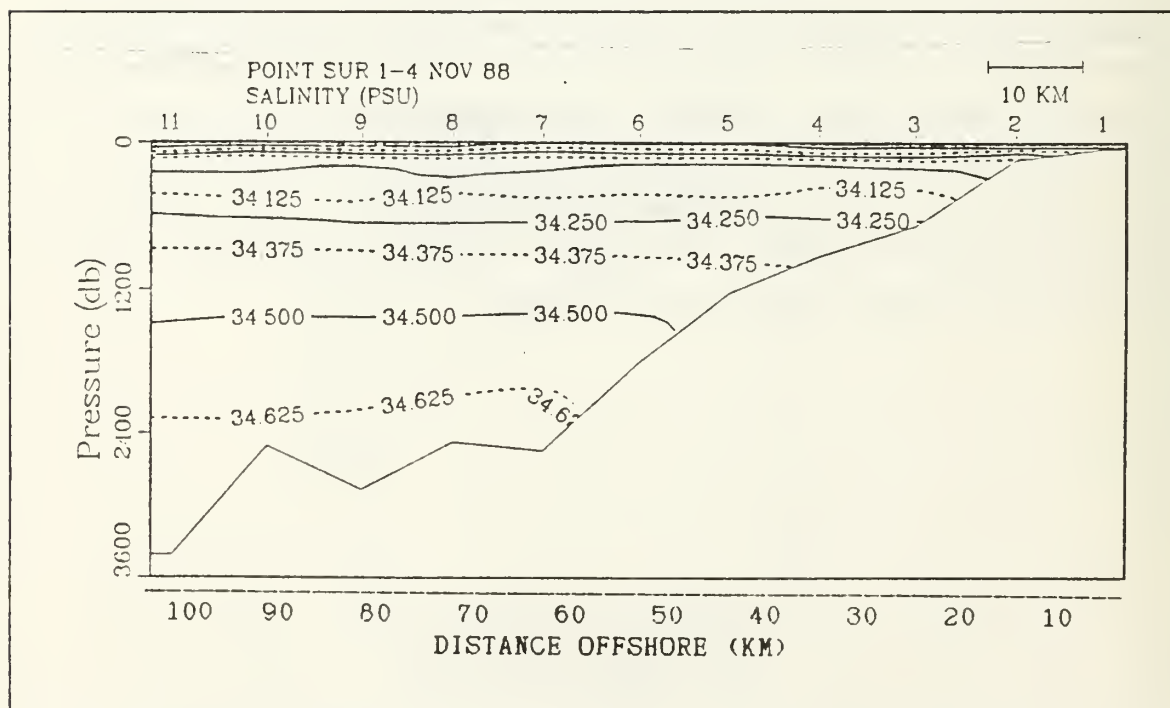


Figure 36. 1-4 November Salinity to 3600 m

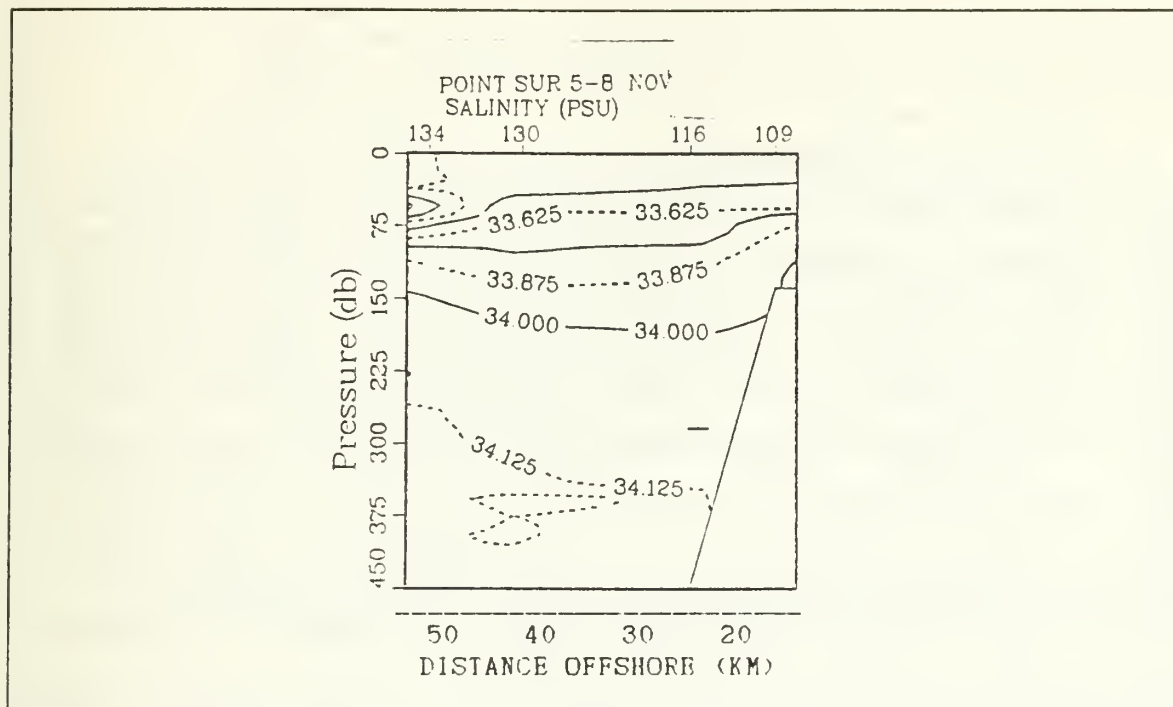


Figure 37. 5-8 November Salinity to 450 m

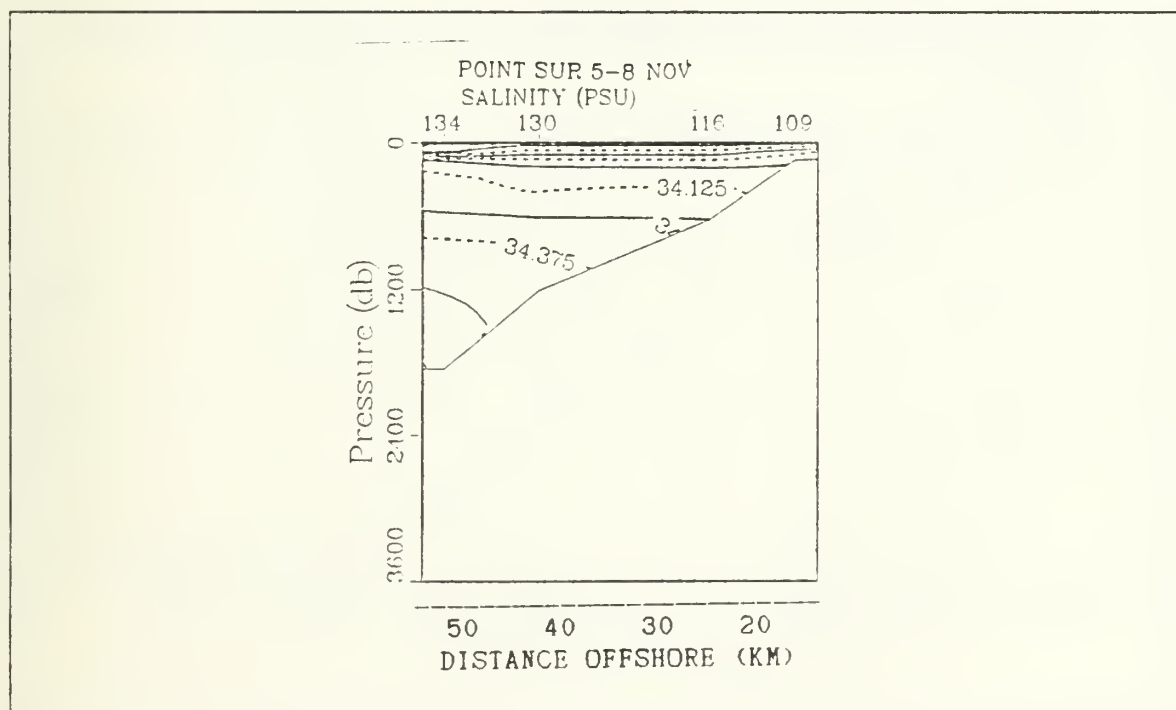


Figure 38. 5-8 November Salinity to 3600 m

B. OCEANOGRAPHIC CONDITIONS DURING PEGASUS CRUISE

1. Velocity Sections

a. *V* Component Velocity Section

The *V* component velocity information for the 14-19 November cruise consists of: 1) geostrophic velocity section, see Figure 39 on page 55 and Figure 40 on page 55. 2) a Pegasus absolute velocity section shown in Figure 41 on page 56 and Figure 43 on page 56, and 3) an ADCP velocity section shown in Figure 42 on page 57. The geostrophic velocity cross section shows a weak poleward flow inshore of 10 km. Beyond 10 km we see an equatorward flow of 30 cm/s at the surface centered 45 km offshore which decreases with depth and extends offshore to 55 km. In comparison to the previous data, we note the addition of a nearshore poleward flow. This feature was seen in the 1-4 November ADCP section but was not detected by the geostrophic velocity cross section. Although the 14-19 November cross section has a finer horizontal spacing than the student cruises, the mid point between the first two stations of each cruise, from which the geostrophic velocity is calculated, are very close in location. This would indicate that a nearshore poleward flow exists and that it has expanded offshore. The presence of a nearshore poleward flow during relaxation of upwelling events has been noted by Beardsley [Ref. 2] in the Coastal Ocean Dynamics Experiment conducted north of Point Reyes.

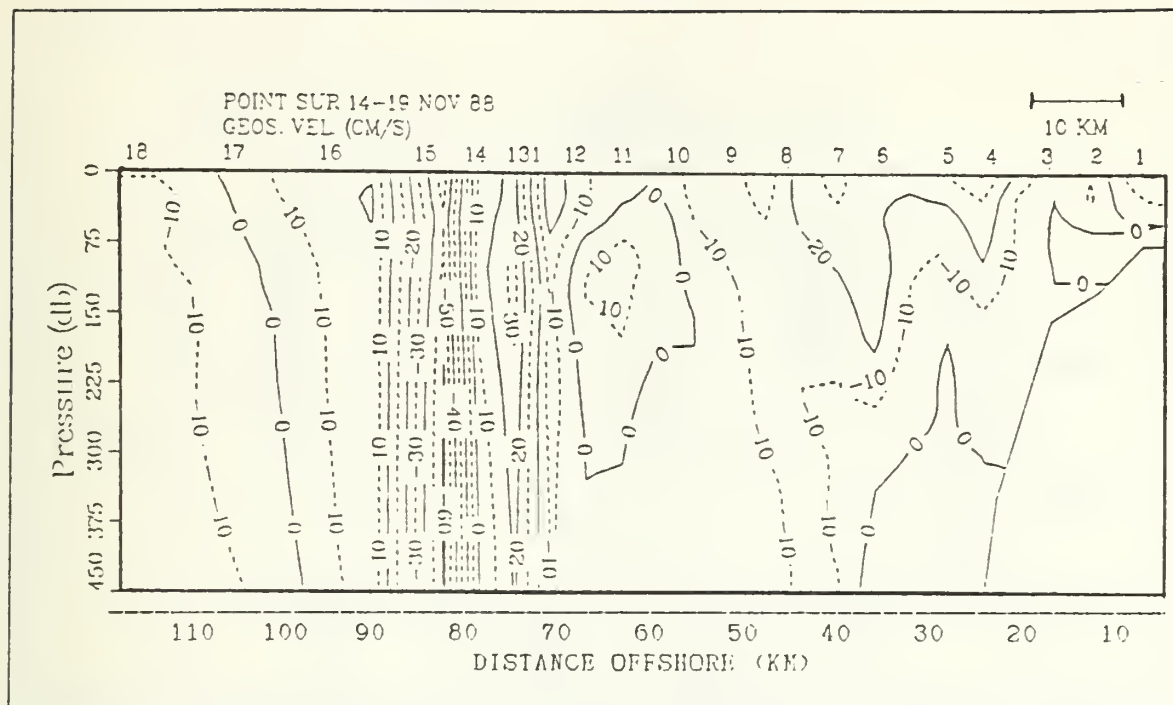


Figure 39. 14-19 November V Component Geostrophic Velocity to 450 m

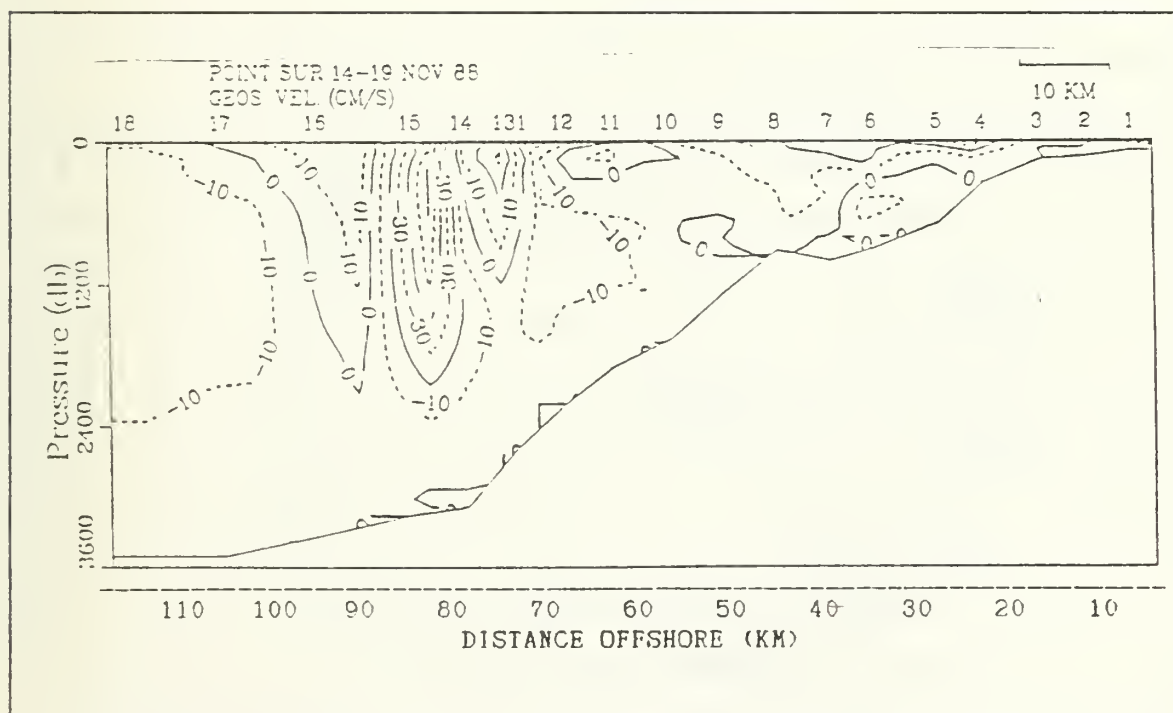


Figure 40. 14-19 November V Component Geostrophic Velocity to 3600 m

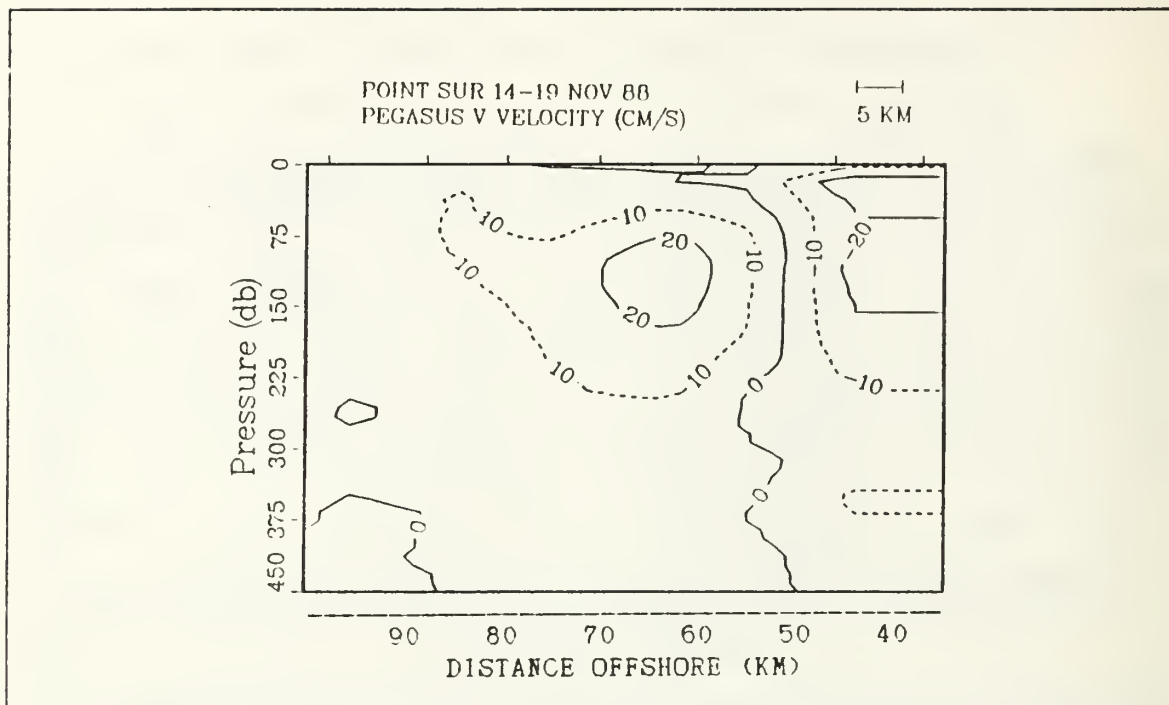


Figure 41. 14-19 November V Component Pegasus Velocity to 450 m

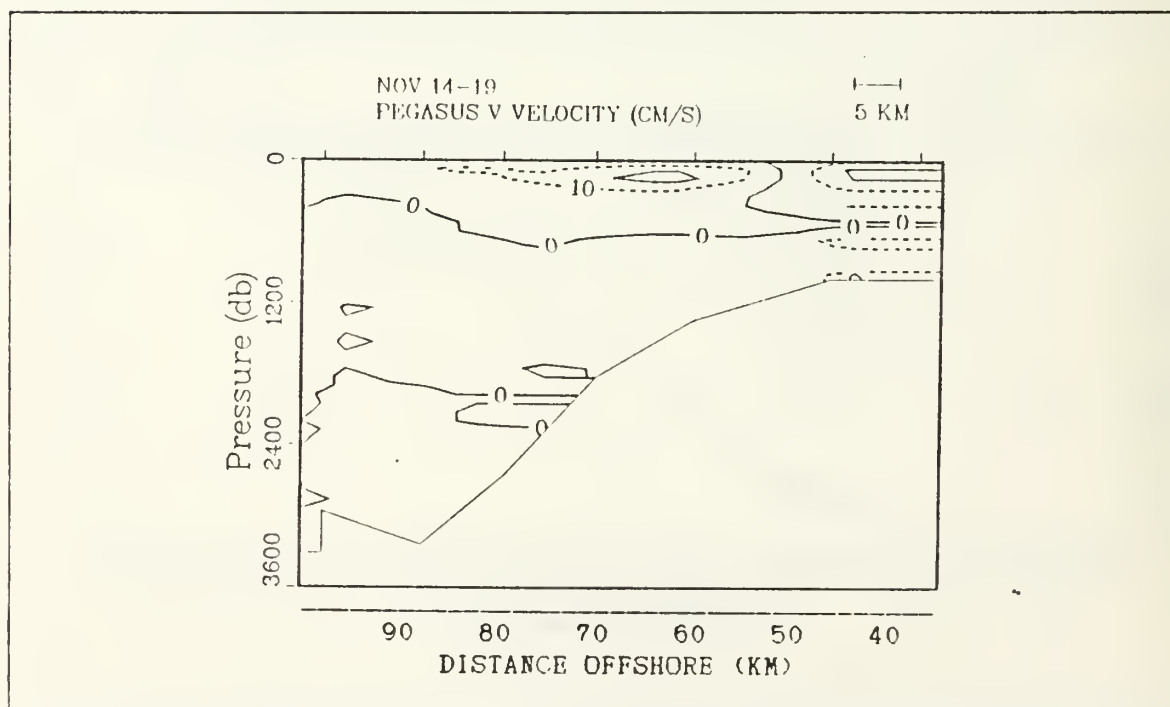


Figure 43. 14-19 November V Component Pegasus Velocity to 3600 m

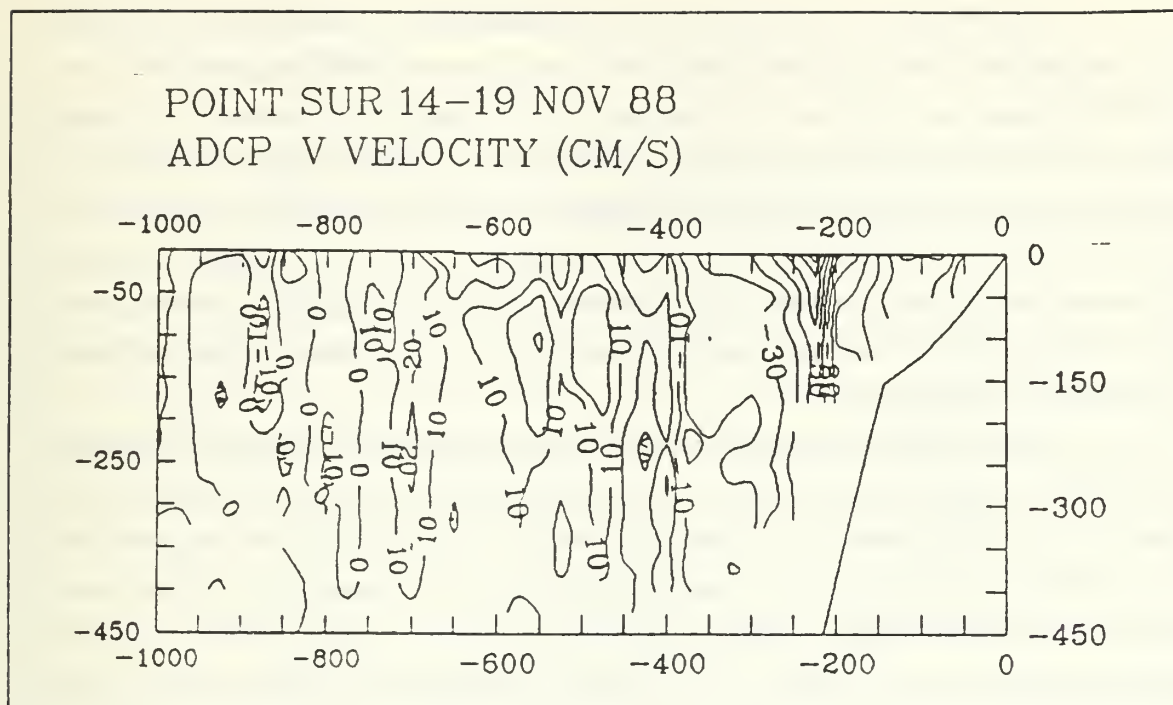


Figure 42. 14-19 November V Component ADCP Velocity to 450 m

The equatorward flow shown in the 14-19 November geostrophic velocities in comparison to the 1-4 November cross section would indicate strengthening as well as a westward propagation of the feature on the order of 2.3 km/day, while the depth of the 10 cm/s isopleth extends to nearly 1000 m. The structure depicted west of 55 km is very complex. A poleward countercurrent is located at 125 m, 65 km offshore. The poleward countercurrent does not extend to the surface and would appear to have weakened from the 5-8 November data. The weakening of the poleward current is probably associated with the upwelling noted between 12 November and 16 November. The westward propagation of the undercurrent was observed to be 1.3 km/day. Between 70 and 90 km offshore is an area of large shear and reversing currents. The relative maximums are located as follows: -10 cm/s at 72 km offshore, 30 cm/s at 75 km offshore, -60 cm/s at 84 km offshore, and 20 cm/s at 90 km offshore. This region of reversing shear is not well understood or explained although I am confident that the data collected is of good quality. Beyond 100 km offshore, the cross section indicates an equatorward flow.

The Pegasus V component velocity section shows equatorward flow inshore of 50 km, which reaches to a depth of 225 m. This agrees well with the geostrophic section. The poleward jet is shown at approximately 125 m deep, 65 km offshore with a core velocity of 20 cm s. Both the horizontal and vertical location agree well with the geostrophic section; however, the strength appears to overestimate the geostrophic velocity by 10 cm s; nevertheless, this velocity shows a deceleration from the 30 cm/s values noted in the student cruises. The Pegasus sections do not support the strong shear seen in the geostrophic cross section, but this could be due to the more coarse horizontal resolution of the Pegasus data.

Despite high correlations between individual Pegasus and ADCP profiles, the ADCP V component section has poor agreement with the Pegasus and geostrophic sections. The ADCP data shows a weak poleward flow inshore of 17 km, corresponding to the break between the shelf and the continental slope, in contrast to the geostrophic section which showed a poleward flow only to 10 km offshore. This poleward nearshore flow is confined to the shelf with water depths less than 100 fathoms. Beyond the nearshore poleward flow is a region of equatorial flow that extends to 47 km offshore. This flow is concentrated 25 km offshore at the surface with a 70 cm/s equatorward maximum. This is also a region of maximum shear that is located in the same location as the 1-4 November ADCP cross section which also showed a 70 cm/s equatorward flow. This region of high shear would appear to be anchored to a position which corresponds to the high slope of 0.1 at this location. The velocity is greater by more than a factor of 2 from the geostrophic velocity calculated using the dynamic method. The reason for this large difference in magnitude over those observed by Pegasus and CTD instruments is not known, but could be related to the finer horizontal resolution of the ADCP section and ageostrophic currents. The poleward undercurrent is located 56 km offshore. The core of the undercurrent has a flow of 30 cm/s centered at 125 m deep. Unlike the geostrophic and Pegasus sections, the ADCP measured poleward undercurrent has a weak, 10 cm/s, surface signature. The width of the 10 cm/s isopleth at the surface is only 2 km as opposed to the 25 km width present in the 1-4 November cruise ADCP data. Thus the ADCP data does support the Pegasus and geostrophic velocity data in regards to a weakening of the undercurrent. Beyond 70 km offshore, the ADCP data shows a predominantly weak poleward flow with small regions of equatorward flow. This predominantly poleward flow agrees with the weak poleward flow, 10 cm/s or less, seen in the Pegasus cross section but does not agree with the high shear observed in the geostrophic cross section.

b. U Component Velocity Section

Inshore of 20 km over the shelf the ADCP cross section, seen in Figure 44 on page 59, indicates onshore flow within 20 km of the coast which is associated with the poleward flow observed along the shelf. A large shear as seen in other ADCP cross sections is also present at 25 km offshore, again corresponding to a maximum bottom slope of 0.1. Between 20 and 65 km offshore, the flow is westward with the strongest flow located in the upper 150 m of the water column. Near 65 km offshore, there is a region of convergence due to eastward flow between 65 and 85 km offshore. This convergence location is also the westward extent of the poleward undercurrent seen in the V component. Between 85 and 95 km, the flow is once again westward while beyond 95 km the flow is eastward. The U component cross section determined by Pegasus is shown in Figure 45 on page 60 and Figure 46 on page 61. The section shows offshore flow east of 65 km offshore and onshore flow to the west of 75 km offshore. The resulting region of convergence between 65 and 75 km offshore seems to define the western boundary of the poleward undercurrent noted in the V component of the Pegasus cross section.

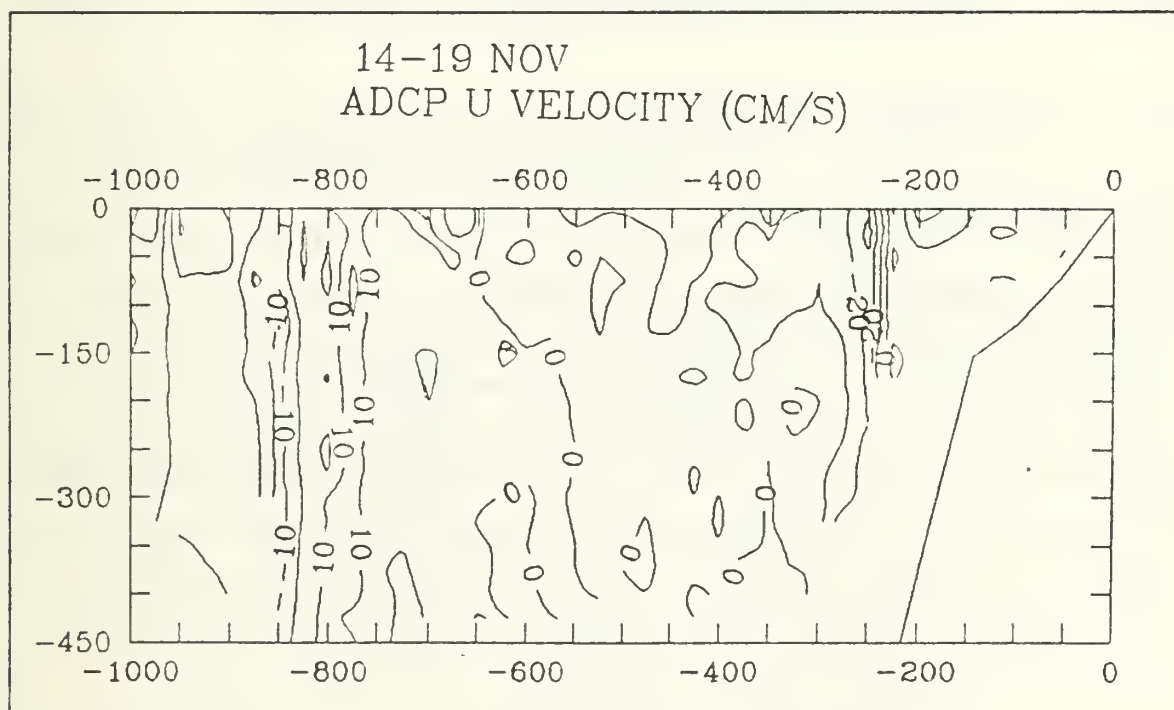


Figure 44. 14-19 November U Component ADCP Velocity to 450 m

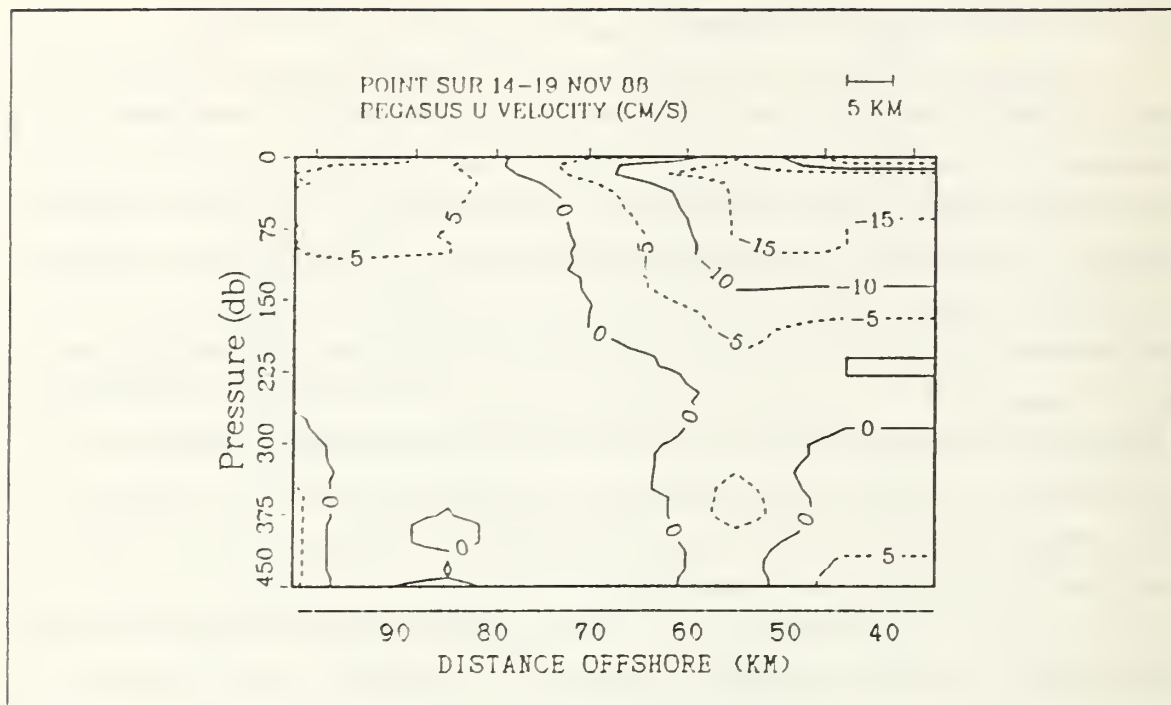


Figure 45. 14-19 November U Component Pegasus Velocity to 450 m

c. W Component Velocity Section

The W component velocity cross section was determined from ADCP data taken during the Pegasus cruise and can be seen in Figure 47 on page 61. Velocities are small, within the rms error limits, so the section should be viewed with caution. The section shows upwelling predominantly throughout the cross section. Within 30 km of shore we find a region of 3 cm/s upwelling which is at variance with the onshore flow in this area noted previously. In the U Velocity cross section we noted areas of convergence in the vicinity of 65 and 95 km offshore. These areas of convergence correspond to regions where vertical motion is near zero. The regions of strongest upwelling are; 40 km, 57 km, 70 km, 78 km, and 86 km offshore. These areas of strongest flow have a very small horizontal extent, usually less than 5 km. The location of these maximums is not understood but the maximum at 86 km offshore does correspond to a divergence in the U velocity field noted in the ADCP cross section.

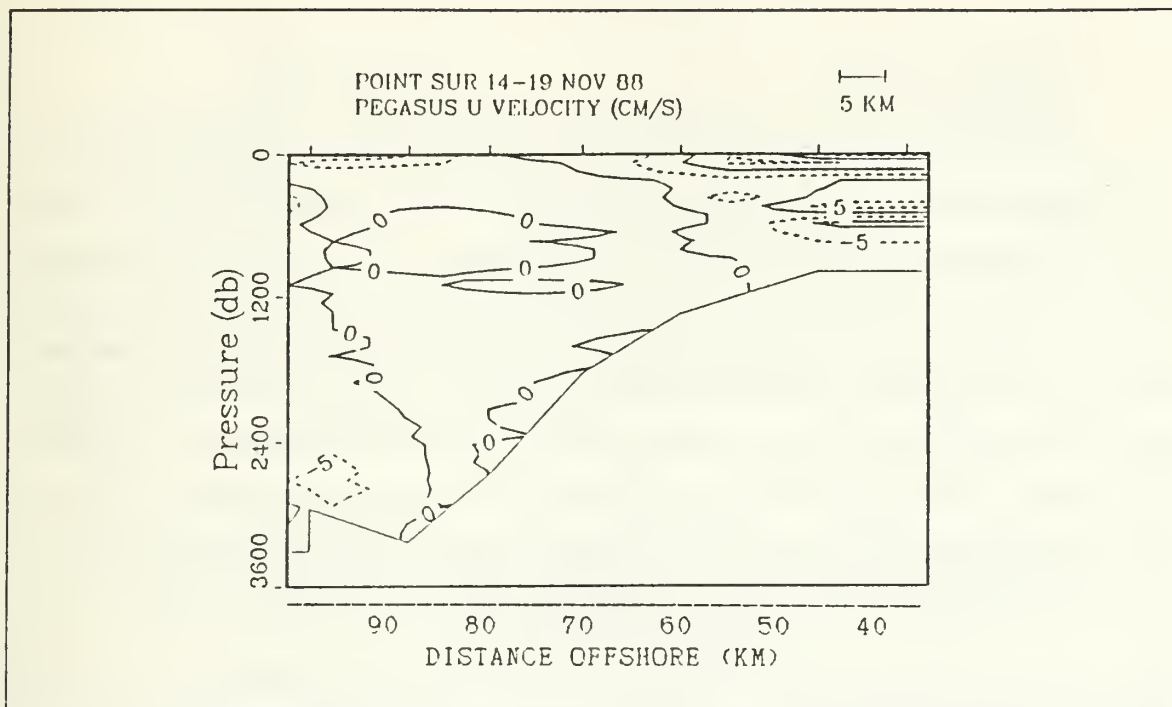


Figure 46. 14-19 November U Component Pegasus Velocity to 3600 m

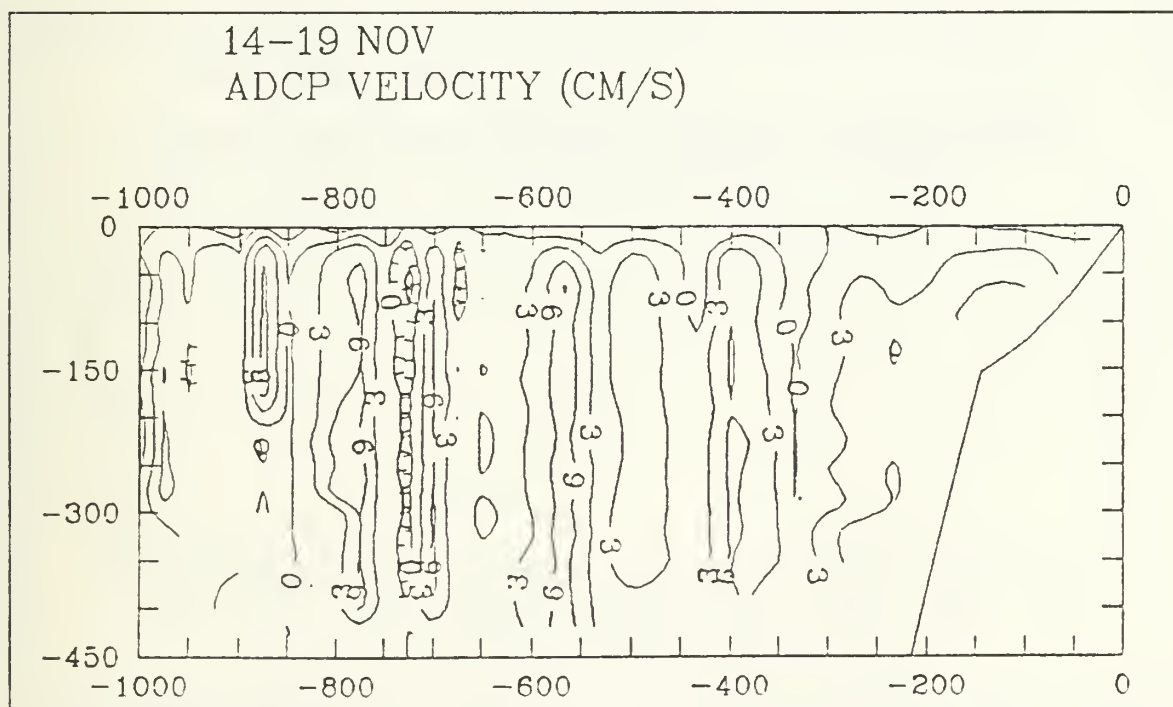


Figure 47. 14-19 November W Component ADCP Velocity to 450 m

2. Temperature Sections

The temperature section for the 14-19 November cruise is shown in Figure 48 on page 63 and Figure 49 on page 63. In this section we note the downward slope of the isotherms within 15 km of the coast. This would tend to support the onshore flow in the U component velocities observed over the coast and downwelling however the ADCP vertical velocities did not agree with this interpretation. Beardsley [Ref. 2] observed the existence of a broad band of warm water nearshore during the wind relaxation events north of Point Reyes. He noted that the isotherms sloped upward over the outer shelf and downward over the inner shelf, which is very similar to the isotherms shown in our section. The inflection point at which the isotherms shift from a upward slope to a downward slope is observed at between 20 and 15 km offshore which agrees with the divergence area noted in the U component ADCP velocities. The depth of the isotherms in this region 15 to 20 km offshore indicates upwelling from 150 m and is similar to the depth seen in the 1-4 and 5-8 November student cruises. This indicates little or no intensification of the upwelling at his location. Between 60 and 95 km offshore, we note a warm (temperatures greater than 14°C) lens of water at the surface extending to a depth of 50 m. This section also has in common with the other temperature sections a downward slope of the isotherms with the greatest slope being between 45 and 75 km offshore. This is typical of isotherms in the vicinity of the poleward undercurrent.

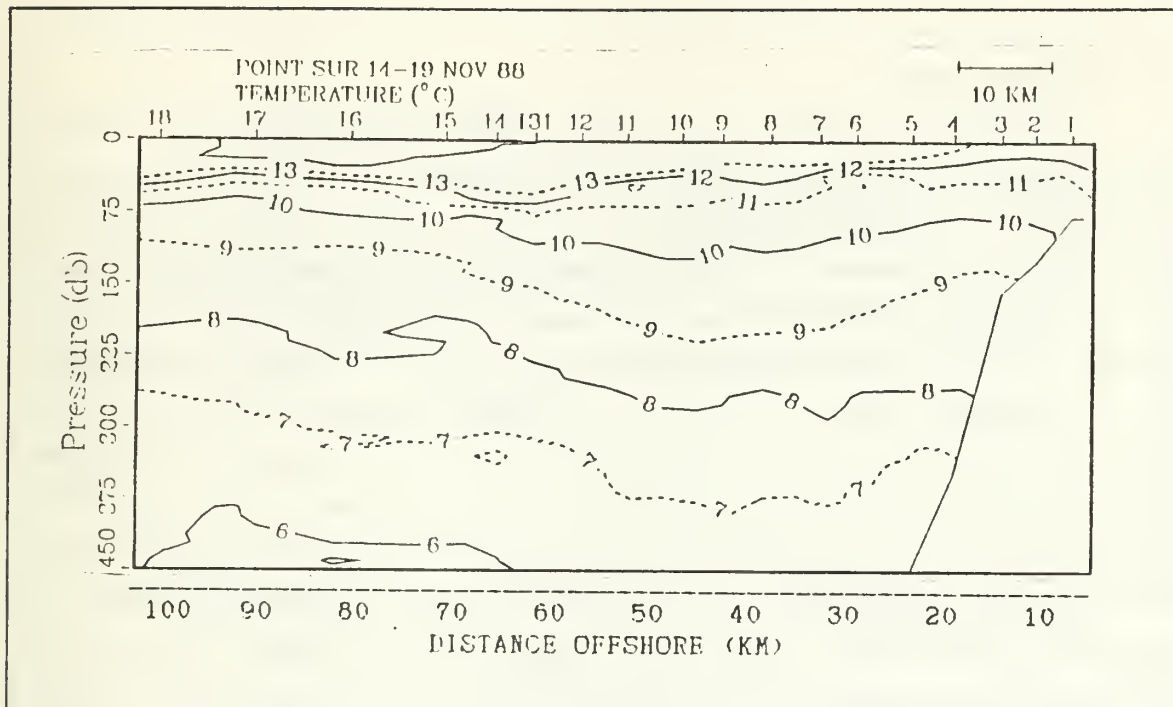


Figure 48. 14-19 November Temperature Cross Section to 450 m

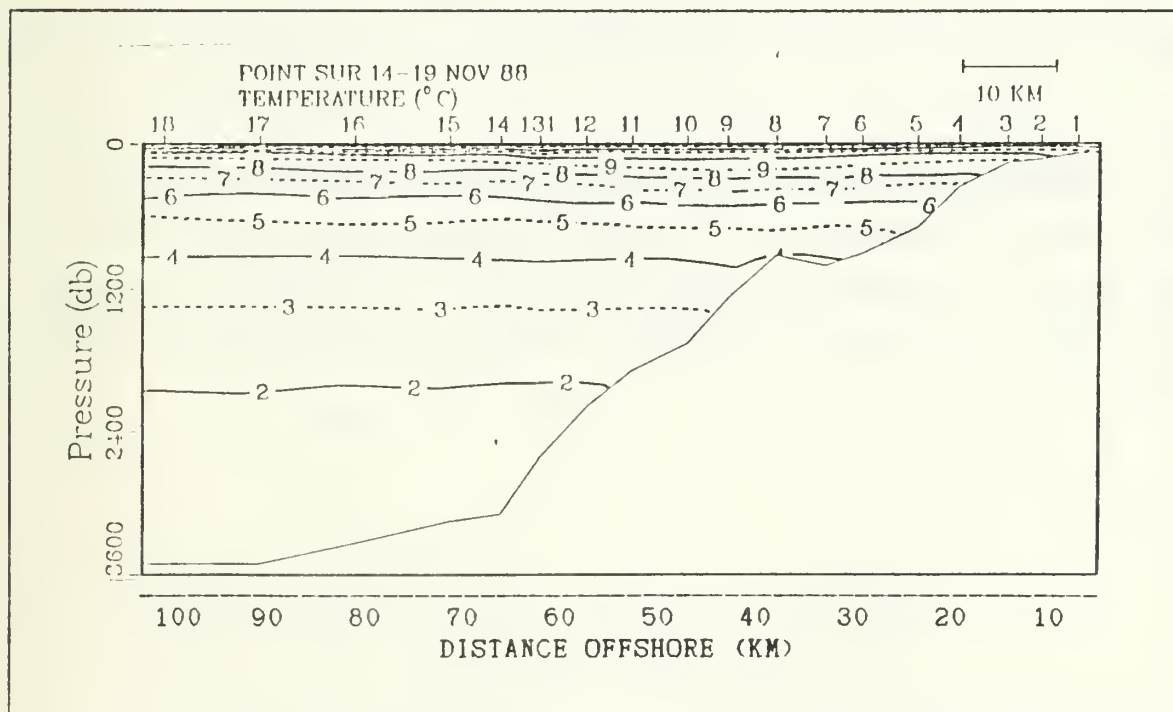


Figure 49. 14-19 November Temperature Cross Section to 3600 m

3. Salinity Sections

In examining the salinity cross section, shown in Figure 50 on page 65 and Figure 51 on page 65, one can see upward sloping isohalines within 40 km of the coast. The depth of the isohalines within 40 km of the coast is similar to the depths observed in the 5-8 November cruise. This indicates little to no strengthening of the upwelling, which is in agreement with the temperature cross section results (and would be expected since both of these cruises take place at the change from a short duration upwelling event to a relaxation period). We do notice a change taking place west of 40 km offshore. At this location the 34.0 and 33.875 psu contours show a deepening of 50 and 28 m, respectively, over the 7 day intervening period. This is believed to be due to the reduction of transport of high salinity water at these depths by the poleward undercurrent which moved from 55 km offshore to 65 km offshore during the same time interval. In examining the salinity section of the 14-19 November cruise with respect to the position of the poleward undercurrent, we see a doming of the 33.75 psu contour but no significant doming is observed below 80 m. This reduced salinity signature associated with the undercurrent is most likely related to its observed weakening from the 5-8 November strength. The low salinity water, 33.125 psu, present between 75 and 95 km offshore is believed to be outflow from the Sacramento River. The salinity cross section agrees well with the convergence and divergence areas noted in the U velocity component of the ADCP cross section. We previously noted regions of divergence at 20 and 95 km offshore. Examination of these locations on the salinity cross section reveals higher salinity values extending toward the surface. The regions of convergence at 65 and 85 km offshore agree well with salinity minimums in these areas. Thus the salinity cross section shows good dynamic support and correlation with features observed in the velocity cross section.

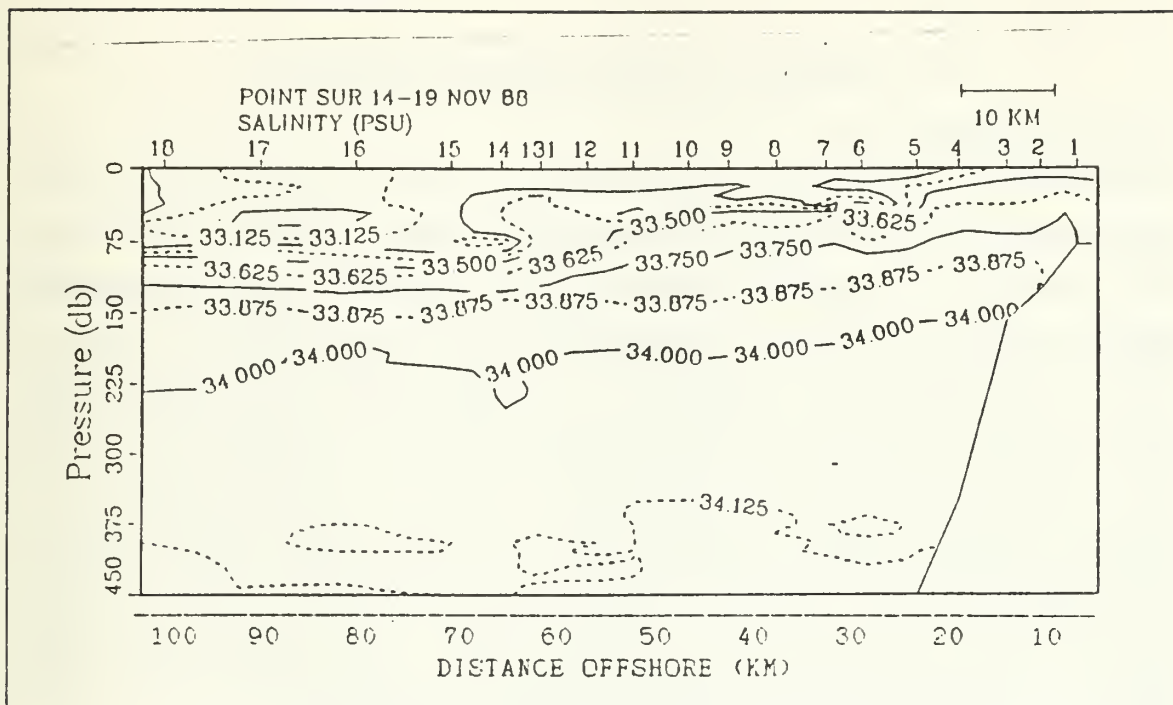


Figure 50. 14-19 November Salinity Cross Section to 450 m

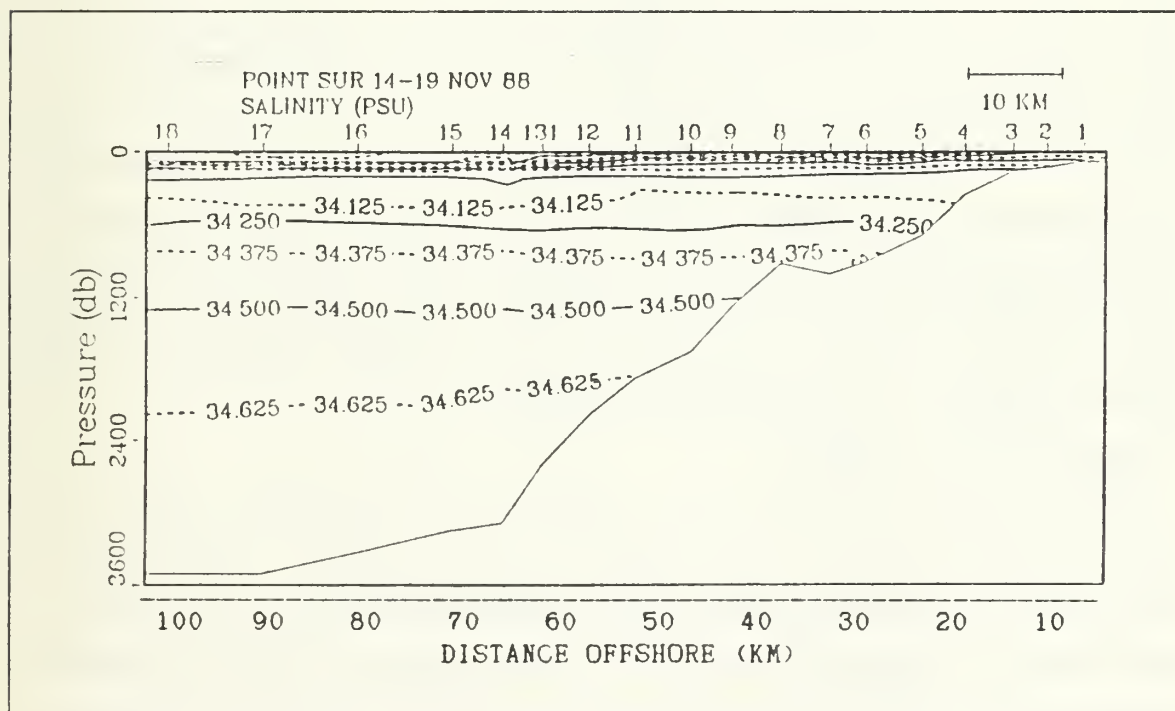


Figure 51. 14-19 November Salinity Cross Section to 3600 m

VI. SUMMARY AND RECOMMENDATIONS

A. DATA PROCESSING

ADCP data is fairly noisy and subject to a number of error sources. Thus extreme care must be taken with the data if small magnitude currents of interest are to be resolved. The initial collection averaging interval plays a major role in post processing and the eventual determination of the accuracy of the data. It is believed that a 3 minute collection averaging interval is superior to a 5 minute interval. Perhaps somewhat shorter intervals will be more advantageous when the GPS navigation system is fully deployed, due to a reduction in positioning errors. Although a 3 minute average is believed to be better in areas of good quality Loran coverage, a longer averaging interval would be required in a lower quality coverage area due to positioning errors exceeding those caused by gyro lag. The effects of bad navigation data can be seen by the high variability in Figure 5 on page 14 and Figure 6 on page 14 which cause abnormally high velocities in the ADCP data located 25 km offshore in our transect.

In regards to filtering of ADCP data, a low pass filter with a cutoff frequency of 0.4 cpm was used in combination with a Hanning window vertical filter with a half bin width of eight meters. The low pass filter is believed to be adequate in minimizing suppression of true signal while avoiding underfiltering of navigation noise. This is a slightly lower frequency filter than the 0.05 cpm cutoff frequency recommended by Kosro [Ref. 9] but is necessary due to the difference in collection averaging intervals of 3 to 5 minutes versus 1 minute. A vertical Hanning window filter with a half bin width of eight meters, as recommended by King [Ref. 12], was used to vertically smooth the profiles. This half bin width provided the best reduction in variance without excessive loss of signal. An averaging interval of 30 minutes was chosen based upon the work of Kosro [Ref. 9] and subjective comparisons to 15 and 45 minute averages.

B. PROFILE COMPARISONS

Excellent agreement was found between Pegasus and ADCP profiles. Average correlation coefficients for the U and V component velocities were found to be 0.848 and 0.875 respectively. It was found that correlation coefficients were improved by averaging up and downcasts together to obtain a cast average. In addition farther improvement was noted when combined casts separated by half an inertial period were averaged together. Interestingly, U component velocities were better correlated for individual up and

downcasts while V component velocities were better correlated for cast and station averages.

An opposing vertical offset was noted between up and downcasts for Pegasus velocities. The offset appears to be a function of vertical shear but other possible causes such as hysteresis effects in the pressure sensor or sensitivity changes in the circuitry due to temperature changes have not been ruled out. Averaging of up and downcasts together did a fair job of negating the effects of this vertical offset.

Pegasus velocities were noted to be overestimates of the ADCP velocities although more realizations are required to increase the confidence in this statement. This greater sensitivity of Pegasus to ocean currents was also noted in the inertial flow component. The strength of the inertial flow in this area relative to the mean flow was found to be considerable, with velocity fluctuations at a constant depth often exceeding 15 cm/s as reported by Pegasus casts separated by half an inertial period. A vertical wavelength of 100 to 300 m was observed for the inertial flow component. Thus with inertial flow components having the same order of magnitude as the mean flow component, it is important to average the inertial-period flow if a realistic depiction of the mean currents is to be seen.

C. OCEANOGRAPHY ALONG THE POINT SUR SECTION.

The fall transition was noted to have occurred in late August from the Granite Point SST data. The month of November was characterized by three short duration upwelling events with intervening relaxation periods in which SST rose rapidly.

In regards to the California Current System the following flows were seen in the three cruises in November 1988. An inner shelf poleward flow was noted along the coast. The strength and offshore extent of this flow are dependent upon the strength and duration of nearshore downwelling. It is hypothesized that the development and strengthening of this nearshore poleward flow results in increased shear between it and the outer shelf equatorward flow. As this shear increases a westward propagation of the offshore features develop in order to reduce the shear and increase horizontal stability. This flow is weak to nonexistent during strong upwelling but strengthens and propagates seaward during relaxation events of the upwelling. This flow seems to be confined to inshore of 100 fathoms. Examination of U velocities, temperature, and salinity data suggest an onshore flow with weak downwelling close to the coast during relaxation events.

The second flow noted is a equatorward surface flow which occupies the outer shelf and inner continental slope. The core of this flow is normally located at the break between the shelf and the continental slope but can extend offshore during relaxation events. The ADCP sections consistently show high shear with 70 cm/s equatorward velocities located 5 km west of the shelf break, 25 km offshore, where the slope has a maximum value of 0.1. This high shear region could be explained in part by the presence of a shelf break front. It is characterized by a shear of $1.5 \times 10^{-4} \text{ s}^{-1}$ with a width of 3 km. The fact that this high shear region is present in both the 1-4 November and 14-19 November sections in the same location lends more confidence to its existence. The high velocities at this location are believed to have some error present due to bad navigation data. The zonal extent of this front in respect to the coast is unknown. The confidence in the existence and strength of this high shear is not high due to bad navigation data in this region. The offshore extent of this flow was noted to propagate offshore during the relaxation events.

The California Undercurrent was seen in all three cruises. The core was seen to shoal and propagate westward at 1 km day in the presence of a relaxation in the upwelling. The strength of the core was observed to have weakened in the 14-19 November cruise although westward propagation was still noted to be 1.3 km day. The reason for the weakening is undetermined. Possible causes could be: the presence of the upwelling between 12 and 16 November; the much lower than normal SST for mid-November in relation to the 14 year mean; or the result of the westward propagation of the core toward the ridge of the downward sloping isotherms. In all three cruises the undercurrent was located in the mid-slope region offshore. This is in contrast to its normally observed position much closer inshore next to the margin. The farther offshore position is believed to be in response to the presence of a coastal poleward flow inshore. The presence of the surfaced California Undercurrent, known as the Davidson Inshore Current, is seen in all sections except the 14-19 November geostrophic velocity section. The Pegasus and ADCP 14-19 November sections did show a surface signature although it was much reduced from the early November flow, thus indicating a weakening of the flow. The location of the broad equatorward flow known as the California Current was barely resolved in this study, but was noted to be west of 100 km for the cross sections which extended this far offshore.

In summary, this study observed the following flows: 1) A nearshore coastal trapped poleward flow which was confined to inshore of 100 fathoms and which strengthens during relaxation events. 2) An equatorward flow occupying the outer shelf and inner

continental slope. During relaxation events this flow widened and extended farther offshore. Between this flow and the nearshore poleward flow a strong shelf break front was observed with a shear of $1.5 \times 10^{-4} \text{ s}^{-1}$ and a width of 3 km. 3) West of the equatorward flow located between 50 and 65 km offshore in the mid-continental slope region, the California Undercurrent was observed. It was located farther offshore during relaxation events and weakened with distance offshore. 4) Farther offshore (approximately 100 km) and just barely resolved by the data, the California Current was observed. The core of the flow was not resolved but is historically located more than 200 km offshore.

D. RECOMMENDATIONS

Although much was learned in regards to the processing of ADCP data, I do not feel an optimum processing scheme was found. Data from this study suggest that the filtering and averaging techniques used were valuable and should be part of any ADCP processing scheme; however, the best procedures in regards to collection interval and methods are still unresolved. The problem of minimizing error due to bad navigation data and gyro could possibly be solved by the creation of new software. Such software could vary the collection interval based on preset parameters. For example, the collection interval could be shortened during course changes to minimize error due to gyro lag, and conversely the collection interval could be lengthened if navigation data resulted in ship velocities that were substantially different from that indicated by an inertial navigation system, secondary navigation system, or even outside a set deviation from speeds calculated from underwater log input. Another possible way to improve the quality of the ADCP data would be to perform an in situ calibration of the ADCP during each data collection cruise. Joyce [Ref. 15] describes methods of in situ calibration using both water and bottom tracking. Joyce found that the use of bottom tracking in combination with satellite navigation position fixing offer the possibility of greatly improved calibration of the ADCP.

Secondly some thought needs to be given to ADCP utilization in the cruise planning stage. Thus if the desired horizontal resolution of the data set desired is 3 km then ship's speed needs to be limited to 6 knots to allow for a 30 minute average to be obtained in a 3 km distance.

In regards to Pegasus, a measurement of the vertical offset due to the moment of inertia, temperature sensitivity of the control circuitry, and possible hysteresis effects of the pressure sensor, needs to be determined so that a solution to the offset can be

developed. Such an experiment needs to be conducted in a water environment in which vertical shear can be controlled.

This study has shown a high correlation between individual profiles collected by Pegasus and the ADCP. Despite this agreement large differences in cross sections are observed due in part to the above problems. Although similar cross sections could be produced if one only uses a portion of the ADCP data, this negates the continuous collection capability of the ADCP. The determination of techniques to minimize the above problems should be actively sought after so that the ADCP cross sections will present a better picture of the true ocean current fields. The complete deployment of the GPS navigation system will be a valuable first step to solve this problem.

It would be desirable to combine data collected by Pegasus and the ADCP into a single full depth absolute velocity cross section. Unfortunately simply merging the two data sets would cause regions of erroneous shear due to the differences in velocity recorded by the instruments at a single point. In order to avoid this problem one of the data sets would have to be calibrated or adjusted to the other. Calibration could be accomplished using data from the station averaged profiles. Such a method would entail calculating the slope and intercept using linear regression (as done in chapter 4). The slope and intercept could then be used to adjust the ADCP data to obtain the ideal slope of one and intercept of zero. The adjusted ADCP data could then be merged with the full depth Pegasus profiles to produce a full depth absolute velocity cross section. This cross section would have the advantages of both instruments, in that high horizontal resolution would be possible in the much more variable upper water column while deeper velocities are supplied with adequate resolution for the lower water column.

Studies by the Naval Postgraduate School Point Sur Transect Program should continue to measure the nearshore oceanography and associated current regime. The nearshore flows are far less understood in comparison to the main traits of the California Current System due to a smaller data base, but are essential if modeling is to be developed that adequately predicts the California Current System. The accurate knowledge of nearshore currents has important military applications in regards to mooring mines, bottom contour navigation, and ASW operations.

LIST OF REFERENCES

1. Hickey, B.M., The California Current System - hypotheses and facts, *Prog. Oceanog.*, 8, 191-279, 1979.
2. Beardsley, R.C. and S.T. Lentz, The Coastal Ocean Dynamics Experiment Collection: An Introduction, *J. Geophys. Res.*, 92, 1455-1463, 1987.
3. Barth, J.A. and K.H. Brink, Shipboard Acoustic Doppler Profiler Velocity Observations near Point Conception: Spring 1983, *J. Geophys. Res.* 92, 3925-3943, 1987.
4. Wickham J.B., A.A. Bird, and C.N.K. Mooers, Mean and Variable flow over the central California continental margin, 1978-1980, *Continental Shelf Research*, 7, 827-849, 1987.
5. Joyce, T. M., D. S. Bitterman, Jr., and K. E. Prada, Shipboard Acoustic Profiling of Upper Ocean Currents, *Deep Sea Research*, 29, 903-913, 1982.
6. Chelton, D.B., Seasonal Variability of Alongshore Geostrophic Velocity off Central California, *J. Geophys. Res.* 89, 3473-3486, 1984.
7. Lynn, R.J. and J.J. Simpson, The California Current System: The Seasonal Variability of it's Physical Characteristics, *J. Geophys. Res.* 92, 12,947-12,966, 1987.
8. Huyer, A., Hydrographic Observations Along the CODE Central Line Off Northern California, 1981., *Journal of Physical Oceanography*, 14, 1647-1658, 1984.
9. Kosro, P.M., *Shipboard Acoustic Doppler Current Profiling During the Coastal Ocean Dynamics Experiment*, Ph.D. Dissertation, SIO Ref. 85-8, Scripps Institution of Oceanography, 1985.
10. Spain, P.F., D.L. Dorson, and H.T. Rossby, PEGASUS, a Simple Acoustically Tracked, Velocity Profiler, *Deep Sea Res.*, 1553-1567, 1981.
11. Fofonoff, N.P., Physical Properties of Seawater: A New Solution Scale and Equation of State for Seawater, *J. Geophys. Res.*, 90, 3332-3342, 1985.
12. King, C.H., *A Comparison of Pegasus and Combined CTD/ADCP Current Profiles off the California Coast*, Master's Thesis, Naval Postgraduate School, Monterey, California, March 1989.
13. University of Rhode Island, TR 87-6, *Program PEGKEY: at sea Processing of PEGASUS Data on an HP-85 Microcomputer*, by J.L. Lillibridge and H.T. Rossby, 1987.
14. Pinkel, R., A.J. Plueddemann, R.J. Williams, Internal Wave Observations from FLIP in MILDIX, 1987, *Journal of Physical Oceanography*, 17, 1737-1757, 1987.

15. Joyce, T.M., On In Situ "Calibration" of Shipboard ADCPs, *Journal of Atmospheric and Oceanic Technology*, 6, 169-172, 1987.

INITIAL DISTRIBUTION LIST

	No. Copies
1. Defense Technical Information Center Cameron Station Alexandria, VA 22304-6145	2
2. Library, Code 0142 Naval Postgraduate School Monterey, CA 93943-5002	2
3. Chairman (Code 63Rd) Department of Meteorology Naval Postgraduate School Monterey, CA 93943-5000	1
4. Chairman (Code 68Co) Department of Oceanography Naval Postgraduate School Monterey, CA 93943-5000	1
5. Professor C. A. Collins (Code 68Co) Department of Oceanography Naval Postgraduate School Monterey, CA 93943-5000	1
6. Professor Mary Batteen (Code 68Bv) Department of Oceanography Naval Postgraduate School Monterey, CA 93943-5000	1
7. Director Naval Oceanography Division Naval Observatory 34th and Massachusetts Avenue NW Washington, DC 20390	1
8. Commander Naval Oceanography Command Naval Oceanography Command Stennis Space Center, MS 39529-5000	1
9. Commanding Officer Fleet Numerical Oceanography Center Monterey, CA 93943	1
10. Commanding Officer Naval Oceanographic Office Stennis Space Center, MS 39522-5001	1

11. Commanding Officer 1
Naval Ocean Research and Development Activity
Stennis Space Center, MS 39522-5001

12. Commanding Officer 1
Naval Environmental Prediction Research Facility
Monterey, CA 93943-5006

13. Chairman, Oceanography Department 1
U. S. Naval Academy
Annapolis, MD 21402

14. Chief of Naval Research 1
800 North Quincy Street
Arlington, VA 22217

15. Office of Naval Research (Code 420) 1
Naval Ocean Research and Development Activity
800 North Quincy Street
Arlington, VA 22217

16. Paul Jessen (Code 68Js) 1
Department of Oceanography
Naval Postgraduate School
Monterey, CA 93943-5000

17. Lt. Paul Berryman 1
Box 1796
Naval Postgraduate School
Monterey, CA 93943-5000

18. Lt. Richard H. Reece 2
Naval Oceanography Command Detachment
Fleet Activities
FPO Seattle, WA 98770-0051

19. Dr Eric Firing 1
Department of Oceanography
University of Hawaii
Honolulu, HI 98622

20. Professor Steve Ramp (Code 68Ra) 1
Department of Oceanography
Naval Postgraduate School
Monterey, CA 93943-5000

21. Dr Francisco Chavez 1
Monterey Bay Aquarium Research Institute
160 Central Ave
Pacific Grove, CA 93950

- | | | |
|-----|---|---|
| 22. | Dr. Toby Garfield (Code 68Gf)
Department of Oceanography
Naval Postgraduate School
Monterey, CA 93943-5000 | 1 |
| | | |
| 22. | Mr. Tarry Rago (Code 68Rg)
Department of Oceanography
Naval Postgraduate School
Monterey, CA 93943-5000 | 1 |
| | | |
| 22. | Professor Tim Stanton (Code 68St)
Department of Oceanography
Naval Postgraduate School
Monterey, CA 93943-5000 | 1 |

Thesis
R26737 Reece
c.1

An analysis of hydro-
graphical data collected
off Point Sur, Califor-
nia in November 1988.

Thesis
R26737 Reece
c.1

An analysis of hydro-
graphical data collected
off Point Sur, Califor-
nia in November 1988.



thesR26737

An analysis of hydrographic data collect



3 2768 000 90784 4

DUDLEY KNOX LIBRARY